Refraction Crustal Models and Plate Reconstruction of the Nova Scotia and Morocco Margins

Keith Louden and Helen Lau

Department of Oceanography
Dalhousie University

Yue Wu[1] and Mladen Nedimovic

Department of Earth Sciences
Dalhousie University

30 July 2010

1 present address: Shell Canada Limited
400 4th Avenue S.W.
P.O. Box 100 Station M
Calgary, Alberta T2P 2H5

SUMMARY

The primary objective of this report is to interpret refraction crustal profiles on and across the Nova Scotia margin in order to determine:

- the maximum seaward extent of continental crust;
- the existence of regions of serpentinized mantle and post-breakup volcanic oceanic crust;
- the minimum seaward extent of original unstretched continental crust.

We begin in section 1 with a review of rifting history of the Nova Scotia margin and previous deep seismic observations. These observations indicate that the Nova Scotia margin is characterized by a transition between typically volcanic margins to the south and non-volcanic margins to the north. However, only the south-western-most region of the Scotian margin shows clear volcanic characteristics. Thus the majority of the Nova Scotia margin has a rift structure typical of a rifted margin formed without major syn-rift volcanism. This process resulted in a very wide and complex margin transition between original continental crust and fully-developed oceanic crust.

In section 2, we analyze the new refraction profile collected by Geopro GmbH in 2009 along the ION/GX NovaSPAN Line 2000 under contract to OETR. We compare this new profile with previous refraction profiles across the margin. The new profile is consistent with previous results, indicating that the central and northern sections of the margin formed by non-volcanic rifting. The continent-ocean transition (COT) is represented by very thin crust above a partially serpentinized mantle. The nature of this thin crust appears variable along the margin and is not uniquely defined by the existing models.

In section 3, the interpreted refraction structures across Nova Scotia are related to plate reconstructions of the conjugate margin with Morocco. We include an updated analysis of the SISMAR refraction profile across the Morocco margin. This analysis indicates that the two conjugate margins are highly asymmetric, with the Moroccan margin much narrower and including a sharp COT. Revised poles of rotation are determined for the maximum (at breakup) and minimum (before rift) extent of continental crust. The first-order geometry of the rifting appears relatively simple without need for major discontinuities for the central-to-northern segment of the margins.

1. INTRODUCTION

This contribution aims to provide a better characterization of the rifting mechanism and tectonic structure of the rifted Scotian margin. The data used in this study include wide-angle seismic refraction data and coincident multi-channel seismic reflection data across the central and northern Nova Scotia margin. The derived crustal structures across the central and northern Nova Scotia margin have been correlated with other existing margin transects off Morocco and Nova Scotia, from which this conjugate margin pair is reconstructed to the continental breakup and pre-rift position. The rifting geometry across the conjugate margin pair are elucidated in the breakup reconstruction.

Section 1 gives a general overview of the crustal structure and geology of the Nova Scotian margin from earlier studies. Section 2 details and compares new refraction data across the northern Nova Scotian margin collected and analyzed under contract to Geopro GmbH. Section 3 considers plate reconstructions of the Nova Scotia – Morocco conjugate margin in terms of the crustal structures previously discussed. Much of this study is taken from the PhD thesis of Wu (2007).

1.1 Rifted Continental Margins

1.1.1 Formation of Rifted Continental Margins

Rifted continental margins are formed during the extension and breakup of continents. As rifting begins, the continental crust thins and extends. A rift valley appears as the thinned continental crust subsides through faulting and stretching. As the continental crust thins, the reduced pressure allows the underlying lithosphere and hot asthenosphere to rise and partially melt to form magma. The magma may intrude into the extended crust or solidify and underplate at the base of the crust. The magma may also find its way through faults and rise to surface, forming volcanoes and basaltic lava flows. As rifting proceeds, the increasingly thinned continental crust becomes entirely brittle (Perez-Gussinye and Reston 2001) and eventually breaks up, resulting in the formation of continental margins and opening of oceans. The North Atlantic passive margins were formed during the opening of the North Atlantic Ocean between the North American, African and European continents (Figure 1.1). Recent studies of the crustal structures along this margin system have shown many complications compared to the above simple view for the formation of rifted continental margins (e.g. Louden and Chian 1999).

1.1.2 Volcanism of Rifted Continental Margins

Rifted continental margins can be divided into two major categories: volcanic and non-volcanic. Volcanic margins are those that have been extensively affected by syn-rift volcanism, which has modified or obscured the extensional fabric within the crust. The crustal structure of volcanic margins is characterized by the large quantities of volcanic rocks. Figure 1.2a shows a typical crustal structure for a volcanic margin—the southern Baltimore Canyon Trough along EDGE 801 (SB, Figure 1.1; Holbrook and Kelemen 1993; Talwani and Abreu 2000), where seaward dipping reflec-

tions (SDR), indicative of volcanic extrusives, are observed in the basement across the ocean-continent transition (OCT), and a thick high-velocity lower crustal (HVLC) layer of intrusives underplates the base of the rifted crust. The SDR sequences are produced by extensive subaerial lava flows that have since subsided and rotated seaward, giving them a characteristic appearance on seismic-reflection records as sequences of seaward-dipping reflectors. The existence of extrusive rocks has been confirmed by drilling on the Outer Vøring Plateau of the Norwegian Sea margin (Eldholm et al. 1986) and the SE Greenland margin (Fitton et al. 1995), while the presence of underplated rocks was interpreted from seismic refraction data based on the characteristic lower crustal velocity (v_p=7.2-7.5 kms^{-1}), and anomalous thickness of igneous rocks (e.g. 15-25 km; e.g. Holbrook and Kelemen 1993).

The excessive volcanism (including extrusion and intrusion) has been attributed to the rising decompressional melting of anomalously hot asthenosphere during the formation of rifted continental margins. White and McKenzie (1989) showed that the amount of observed magmatism across the Hatton Bank margin could result if the potential temperature of the asthenosphere under the rifted continental margin was raised by ~100-150°C from the normal temperature (1300°C) at the oceanic spreading center. Along the North Atlantic margin system, the southwestern-most part of the Scotian margin and the entire US East Coast margins are largely classified into this category (e.g. Holbrook and Kelemen 1993; Keen and Potter 1995a; Talwani and Abreu 2000). Holbrook and Kelemen (1993) estimated that a total volume of 3.2×10^6 km^3 of igneous rocks was produced by magmatism during the formation of the US East Coast margin. A mantle plume was proposed to have been situated off present day Florida at ~200 Ma, which may have initiated the continental rifting of the North American and African continents and widespread volcanism along the North Atlantic margin system (Sleep 1996; Ernst and Buchan 2001). Previously de Boer et al. (1988) had proposed a weak mantle plume that moved southward from New England to Florida. Non-plume models were also suggested to create voluminous volcanism, which require shallow thermal anomalies or rapid upwelling of the mantle material (e.g. Vogt 1991; Anderson et al. 1992). Mutter et al. (1988) suggested that small scale mantle convection at the continental edges, possibly due to lateral and vertical temperature gradients between colder lithosphere and warmer upwelling lithosphere could enhance magmatic activity in the absence of elevated mantle potential temperatures.

Non-volcanic margins, on the other hand, are often characterized by limited melt generation, which may be a result of slow extension rates or cold upper mantle (Sleep and Barth 1997; Reston et al. 2003). In this case, a relatively thin layer with velocity of v_p =7.2-7.6 kms^{-1} is observed across the transition zone (Figure 1.2b). Such velocity layers are associated with basement highs on the Galicia Bank/Iberia Abyssal Plain, which have been evidenced by drilling at ODP (Ocean Drilling Program) Sites 637 (Shipboard Scientific Party, 1987; Figure 1.2), 897, 899 and 1068 as peridotite ridges, indicative of exhumed upper mantle (Sawyer et al. 1994). The exhumed mantle presents *P*-wave velocity anisotropy of 5-7 % at depth of 3-7 km below the top of acoustic basement

(Cole et al. 2002). Most models of *P*-wave azimuthal seismic anisotropy suggest that the fast velocity direction is parallel to the direction of stretching, normal to the rift (e.g. Vauchez et al. 2000). This is an indicator of initial stretching direction in a region adjacent to oceanic crust where no fracture zones have been identified, as well as an indicator for exhumed mantle due to stretching instead of underplated rocks with similar velocities. In contrast to the volcanic margins, the non-volcanic margins are devoid of surface volcanic activity. Along the North Atlantic margin, margins north of Nova Scotia, from the Grand Banks/Newfoundland-Iberia Abyssal Plain conjugates (e.g. Reid 1994; Dean et al. 2000; Funck *et al.* 2003; Lau et al. 2006a) to the Labrador Sea-SW Greenland margins, also have similar crustal structures (Chian and Louden 1994; Chian et al. 1995a).

The limited melt generation for the northern North Atlantic margins may be a result of one or several of the following factors in the course of rifting. The temperature anomaly of hot asthenosphere for the volcanic US East Coast margins, which was suggested to have originated from a mantle plume located off Florida (Sleep 1996), may be diminishing toward the northern passive margins, which are thousands of kilometers away from the anomaly center. Secondly, the rifting rates for the northern North Atlantic margins should be lower than that of the southern US East Coast margins because the Mesozoic rotation poles were located north or northeast of Iceland (Klitgord and Schouten 1986; Roest et al. 1992). Reduced rifting rates will affect the thermal regime by allowing more time for vertical diffusion to reduce the thermal anomaly associated with rifting. In addition, compared to the sharp necking of the US margins, the wider zones of lithospheric thinning of the Scotian margin, the Galicia Bank margin (Whitmarsh and Miles, 1995; González *et al.*, 1999), and the Labrador Sea margin (Chian et al. 1995a; Louden and Chian 1999), may result in reduced melt production. As shown by the melt generation models of Bown and White (1995), melt production can be completely suppressed if rifting lasts 15-20 m.y., despite extreme continental thinning. Minshull et al. (2001) also suggested that melt production at the time of continental breakup may have been reduced by effects of lateral heat conduction, depth-dependent stretching or reduced mantle temperature.

1.1.3 Volcanic to Non-Volcanic Transition

Based on the above characterization, the Nova Scotia margin is located at the transition along the North Atlantic from volcanic margins to the south to non-volcanic margins to the north (Figure 1.1). The southwestern-most Scotian margin near Georges Bank is volcanic, evidenced by the SDR sequences on multi-channel seismic (MCS) reflection lines 89-3, 4 (Figure 1.3; Keen and Potter 1995a), similar to the volcanic US East Coast margins (e.g. Holbrook and Kelemen 1993). The northern Nova Scotia margin has been classified as a non-volcanic rift margin based on the absence of SDR sequences along MCS line 89-1 (Figure 1.3; Keen and Potter 1995b). Hence, the volcanic to non-volcanic transition should have occurred somewhere along the central Scotian margin.

Figure 1.3 shows the regional magnetic anomaly offshore Eastern Canada and US. Along the volcanic margin from the US Atlantic coast to the southwest-

ern-most margin of Nova Scotia near Georges Bank, a strong, linear magnetic anomaly, referred to as the East Coast Magnetic Anomaly (ECMA), is well developed and coincident with a ~100 km wide zone of thick igneous wedge (e.g. Holbrook and Kelemen 1993; Keen and Potter 1995a). Magnetic models showed that the high-amplitude ECMA is attributed to the extrusive rocks or the entire igneous wedge (Alsop and Talwani 1984; Talwani and Abreu 2000; Dehler et al. 2003). The ECMA progressively weakens northward and eventually disappears within the northern Scotian margin, which has been identified as a non-volcanic rifted margin without evidence of excessive volcanism (Keen and Potter 1995b). However, along the central portion of the Nova Scotia margin, the magnetic anomaly is still pronounced. There is no evidence for an SDR sequence on MCS line 88-1A (Keen *et al.* 1991b), although it may be obscured by prominent diapiric salt structures. The concurrence of magnetic and seismic reflection signatures leads to an ambiguous character for the central margin segment.

1.2 Geological Setting of Eastern Canada

1.2.1 The Appalachian Orogen

Figure 1.4 is the geological map of eastern Canada, including the coastal area (after Wheeler et al. 1997). The basement rocks have recorded the history of late Precambrian rifting and the development of a Palaeozoic passive continental margin during the opening of the Iapetus Ocean, a Palaeozoic equivalent of the Atlantic Ocean (Keen et al. 1990). The Iapetus Ocean was closed in the Ordovician (Williams 1979), which produced the Appalachian Orogen after subduction and accretion of oceanic crust (Colman-Sadd 1982). The continental crust of eastern Canada, including the Nova Scotia, New Brunswick and Newfoundland, was formed during the Appalachian Orogen.

Closing of the Iapetus destroyed the Palaeozoic continental margin and several large exotic terranes were added to North America. Starting from the south, the basement of southern and central Nova Scotia consists of rocks of the Meguma Terrane, intruded by granitoid rocks (William 1979; Keppie 1989; Clarke and Chatterjee 1992). The Meguma terrane is composed of fine-grained siliciclastic turbidites and is of Gondwanan affinity based on its dispersal pattern (Schenck 1970). Keppie and Dallmeyer (1995) suggested that the basement rocks are Precambrian. Palaeozoic intrusions occurred during 380-370 Ma (Keppie and Dallmeyer 1995) and the South Mountain Batholith is the largest in the Appalachian Orogen (Benn et al. 1997). Hotspot activity may have caused the intrusion of granites and less mafic rocks (Murphy et al. 1999). The northern Nova Scotia shore, Cape Breton Island, and the eastern Grand Banks and southeastern Newfoundland belong to the Avalon Terrane (Williams and Hatcher 1982; Barr and Baeside 1989), which is separated from the Meguma Terrane to the south along the Cobequid-Chedabucto fault zone (CCFZ, Figure 1.4; Withjack et al. 1995). The fault is steep from surface to ~6 km depth (Webster et al. 1998). Off Cape Breton, the Meguma-Avalon contact dips southward (Marillier et al. 1989; Jackson et al. in preparation). Farther to the north, the Gander Terrane, the Dunnage Terrane and Humber Terrane are east to northeast trending (Figure 1.4). North of the

Appalachian Orogen is the Laurentian Shield (Figure 1.4), which was not involved in the Palaeozoic opening and closing of Iapetus Ocean.

1.2.2 Episodes of Mesozoic Rifting

Mesozoic rifting and the subsequent seafloor spreading created the North Atlantic Ocean and the contemporary Atlantic passive margin system. Figure 1.5 shows plate reconstructions for the primary Mesozoic rifting episodes between North America and Africa, Europe, and Greenland. The Nova Scotia margin was formed by separation of Africa from North America in the middle Triassic to Early Jurassic (230-175 Ma; Welsink et al. 1989). The rifted margin east of the Grand Banks, and the rifted margin northeast of Newfoundland Flemish Cap margin, the Labrador Sea margin, and their conjugates were all formed during the following episodes of Mesozoic rifting (Figure 1.5), starting in early Cretaceous (~130 Ma) and ending in late Cretaceous (~80 Ma; Hiscott et al. 1990; Watt 1969; Moullade et al. 1988; Louden and Chian 1999). The Scotian/Moroccan margin conjugates, including the US East Coast margins and their conjugates (Figure 1.1), represent the earliest episode of Mesozoic rifting along the North Atlantic (Figure 1.5; Klitgord and Schouten 1986).

1.2.3 Volcanism during Mesozoic Rifting

Two periods of magmatism were associated with early Mesozoic continental rifting of eastern Canada (Figure 1.6; Pe-Piper et al. 1990). The earlier igneous activity on the Nova Scotia margin occurred during the earliest stage of Mesozoic rifting by intrusion, which is represented by alkaline dikes in the Northumberland Strait F-25 well and in southwest Nova Scotia. The former consists of rocks of sodic high-alumina olivine tholeiites, with a whole-rock K/Ar date of 214 ± 9 Ma or older date of 239 ± 10 Ma on removal of pyroxene phenocrysts (Pe-piper and Jansa 1986). The latter contains mafic dikes of similar age (Rogers, 1985). One dike from the Wedgeport pluton (Figure 1.6) was about 225 Ma defined by $^{39}Ar/^{40}Ar$ (Reynolds et al. 1987).

The younger period of igneous activity is associated with the main phase of Mesozoic rifting (Pe-piper et al. 1990). The igneous rocks are tholeiitic basalts, represented by both dikes and extensive multiple lava flows. Large igneous dikes include the Shelburne dike (Papezik and Barr 1981) and the Caraquet dike (Burke et al. 1973; Greenough and Papezik 1986). These dikes show multiple injections of magma and are tens of meters wide and more than 100 km long. The Shelburne dike extends more than 450 km along the southern shore of Nova Scotia and into offshore region indicated by its magnetic signature (Figure 1.6). Precise dates of these dikes tend to cluster into two groups, one about 191 Ma and the other about 201 Ma (Pe-Piper et al. 1992). Short dikes are also exposed on Minister Island (near St. Andrews, New Brunswick; Figure 1.6). Basaltic lava flows from this stage of igneous activity form the landscape features in and around the Bay of Fundy. Onshore, the North Mountain of Nova Scotia extends from Cape Blomidon to Brier Island. Basaltic flows also cover much of the Grand Manan Island, New Brunswick (Pringle et al. 1974), and appear along the northern shore of the Minas Basin in Nova Scotia, at Cape d'Or near Advocate Harbour in the west, around Parrsboro-Five Islands-Bass River area

(Greenough et al. 1989), and at Economy Mountain in the east. K/Ar dates of the North Mountain Basalt range from 195 ± 4 Ma (Armstrong and Besancon 1970) to 200 ± 10 Ma (Carmichael and Palmer 1968). Offshore, the North Mountain Basalt underlies most of the Bay of Fundy (Pe-Piper et al. 1992; Figure 1.6), which has been sampled in two wells, the Chinampas N-37 (Greenough and Papezik 1987) and the Cape Spencer #1 (Pe-Piper et al. 1992). Radiometric dating suggested an age of 191 Ma for the North Mountain Basalt (Hyatsu, 1979), which is consistent with the age of the onshore North Mountain Basalt.

On the Nova Scotia shelf, basalt rocks of a total thickness of 153 m appear in the Glooscap C-63 well (Pe-Piper et al. 1992; Figure 1.6). This well is located at the center of Triassic Mohican rift graben (Given 1977), with 7 km southward dipping sediments. The volcanic rocks appear at the depths of 3893-3935 m, 3935-3998 m, and 3998-4046 m. Whole-rock K/Ar dating suggested an age of 176 ± 7 Ma. The upper layer is overlain by Toarcian and the lower unit underlain by Carnian-Norian strata with a sharp contact by red beds intercalated with thick salt layers. Basement was not reached in the well.

The two periods of magmatism are related with two phases of rifting. The earlier one occurred with the onset of Mesozoic rifting when basins formed by extension and normal dip-slip faults, and were filled by thick terrigenous clastics and evaporites. However, the associated igneous activity is of such a limited extent that rifting is lacking in volcanic rocks in most areas around eastern Canada (Pe-Piper et al. 1992) and the remaining Central Atlantic Margins (Olsen et al. 1981; Marzoli et al. 1999). The younger phase of magmatism involved flexural uplift along and landward of the hinge zone and subsidence seaward (Jansa and Wade 1975). The igneous activity in this period contains extensive extrusion, which is not only observed as outcrops onshore and in wells offshore Nova Scotia (Pe-Piper et al. 1992), but also prevailed in all the Central Atlantic Magmatic Provinces (CAMP; Figure 1.7), including once-contiguous parts of North America, South America, Africa and Europe associated with the breakup of Pangea (e.g. Sutter and Smith 1979; Olsen et al. 1981; Sutter 1985; Pe-Piper et al. 1992; Olsen 1997; Marzoli et al. 1999). However, the total volume of observed magmatic material in the circum-Atlantic region is small and most of this wide-spread magmatism event was consistently emplaced over a short time interval, within a few million years with a peak at ~200 Ma (Olsen et al. 1981; Sutter 1985; Pe-Piper et al. 1992; Olsen 1997; Marzoli et al. 1999; Hames et al. 2000). The main magmatic phase took place ~25 m.y. before the separation of continental crust and the first formation of oceanic crust (Pe-Piper et al. 1992).

1.3 Deep Seismic Observations

1.3.1 Early Seismic Refraction Profiles

Offshore Nova Scotia, a large amount of seismic refraction data was collected in the past half century. The early seismic refraction experiments were carried out by Officer and Ewing (1954), Barrett et al. (1964), Jackson et al. (1975), Keen et al. (1975) and Keen and Cordsen (1981). Location of the selected previous profiles is shown in Figure 1.8. Officer and Ewing (1954) noticed that the rifted continental crust offshore southern Nova Scotia subsides from 5,000 feet to 20,000 feet under the continental slope. Barrett et al. (1964)

measured velocities of 5.5 km/s, 6.1 km/s and 8.1 km/s for upper crust (Meguma rocks), lower crust and upper mantle, respectively. An expendable sonobuoy wide-angle reflection and refraction survey was also carried out offshore Nova Scotia, from which detailed sediment velocities were obtained (Jackson et al. 1975). Jackson et al. (1975) suggested that the continent-ocean transition off Nova Scotia may be limited to a 75-km-wide zone based on refraction data. Keen et al. (1975) reported that a 10-km-wide layer south of Sable Island with velocity of ~7.4 km/s was directly overlain by sediment.

These early seismic refraction surveys laid the framework for future research. However, the velocity models obtained are not detailed enough for understanding the rifting process of the Scotian margin. The reasons are due to a number of factors. One is that most of the previous profiles only had a few recording stations with large spacing, some of which were deployed on the coast while shooting offshore (e.g. Barrett et al. 1964). The shot spacing was also very large (e.g. 15 km for explosive shooting) such that the detailed crustal structure was not recorded by the acquisition system. This contrasts to recent studies where tens of ocean bottom seismometers (OBS) are deployed on the seabed at much narrow spacing along the survey track and with airgun shooting at about 100 m intervals coincident with the track of OBS deployment. The other limiting factor to early studies is that all of the previous profiles were short (see Figure 1.8), and none of them crossed the entire margin from un-stretched continental crust to unequivocal oceanic crust. The longest refraction profile offshore O_A is also composed of many short sections (Officer and Ewing 1954; Figure 1.8). Other refraction profiles are carried out along the strike, e.g. 78-3, 78-5 (Keen and Cordsen 1981), and they are short as well. Therefore, it is difficult to derive the full crustal structure for the rifting process across the entire margin from such limited data. In addition, it is hard to demonstrate the along strike variation of crustal structure with a number of short but scattered refraction profiles conducted along the margin.

Two long refraction profiles (99-1 and 99-2) were acquired more recently (Jackson et al. 2000; Jackson et al. in preparation). The refraction data along these lines provide detailed velocity constraint for the Meguma Supergroup and the internal structures of Mesozoic terranes, such as the geometry of the suture between the Avalon and Meguma Terranes (CCFZ, Figure 1.4). However, 99-1 is parallel and very close to the shoreline and 99-2 is partly onshore and partly on the Scotian shelf. These long profiles were not intended to investigate the crustal structure across the continent to ocean transition of this margin. To study the crustal structural variation, including the varying volcanism along the margin, a series of across-margin refraction transects are required to be carried out along the entire margin.

1.3.2 Deep Academic Seismic Reflection Profiles

Reflection seismic surveys for studies of crustal structure started as early as the refraction surveys (e.g. Jackson et al. 1975; Keen et al. 1975; Barrett and Keen 1976). Early seismic reflection profiles were acquired across the refraction lines so as to allow layers in the refraction survey to be related to particular reflectors (e.g. Jackson et al. 1975). Based on seismic reflection images offshore Nova

Scotia, Barrett and Keen (1976) identified Mesozoic magnetic anomalies M26-M28 in the Jurassic Magnetic Quiet zone (JMQZ). However, the deep structures beneath the basement surface were barely recognizable in the early seismic reflection profiles due to limited number of hydrophone groups and short streamer array (e.g. Barrett and Keen 1976). A number of seismic reflection profiles were carried out to define the internal structures of Meguma and Avalon terranes or the crustal structure of early stage of Mesozoic rifting, e.g. MCS lines 88-2, 3, 4 (Keen et al. 1991a) and 86-5A and 5B (Marillier et al. 1989). Numerous seismic reflection lines were acquired offshore Nova Scotia by industries for petroleum exploration (e.g. TGS, GSI; Figure 1.9). These lines have densely covered the Scotian slope area; but most of them are short and were intended to investigate the sedimentary structure.

In order to study the crustal extension and varying volcanism along the Nova Scotia margin, a number of across-margin MCS profiles were acquired in late 1980s (Figure 1.10), such as MCS lines 89-3, 4, 5 (Keen and Potter 1995a), 88-1,1A (Keen et al. 1991b), and 89-1 (Keen and Potter 1995b). MCS lines 89-3, 4, 5 to the southwest of Nova Scotia cross the ECMA that parallels much of the margin of eastern North America, including the southwest of Nova Scotia. Studies along the US Atlantic coast margin suggest that the ECMA may be related to the emplacement of a large thickness of late rift-stage or early drift-stage igneous wedge which is characterized by SDRs at the basement surface and by HVLC layers underneath (Austin et al. 1990; Sheridan et al. 1993; Holbrook and Kelemen, 1993). The seismic image of 89-3 (Figure 1.11) shows that the SDR are still observed southwest of Nova Scotia, indicating that the area of the southwestern Nova Scotia margin is volcanic.

MCS lines 88-1, 1A span the central Nova Scotia margin across the LaHave Platform, the Naskapi Graben Complex, and the Mohican Graben (Given 1977). In the upper crust, Mesozoic extension is reflected by normal faults (NF, Figure 1.12), which flatten and end at mid-crust. In the lower crust and upper mantle, Mesozoic rifting produced dipping reflectors, which are interpreted to be major detachment faults (DF, Figure 1.12; Keen et al. 1991b). According to Keen et al. (1991b), there are some landward dipping reflections that may be correlated with igneous rocks beneath the thinned continental crust (I, Figure 1.12). These landward dipping reflections appear roughly underneath the ECMA, which is located at the seaward edge of the slope diapiric structure (Figure 1.10), indicating that the central margin may be volcanic in character. However, the seemingly landward dipping reflections observed beneath the salt might be artifacts caused by the irregular geometry of the salt/shale diapirs. Such artifacts have been observed along recent seismic profiles offshore Nova Scotia (e.g. NovaSpan profile 1600 shown in chapter 3). In addition, it is not clear if SDR sequences exist beneath the salt/shale diapirs. The problem is that the slope diapiric salts along line 88-1A may have masked the deep structure. It is possible that large-scale volcanism has occurred beneath the diapiric salts but that the overlying salt has obscured the SDR produced by extrusive rocks. Therefore, the absence of the SDR is not sufficient to conclude that seaward dipping reflectors associated with volcanism do not exist along 88-1A. The Glooscap C-63 well on the

outer shelf did show 153 m of basalt in sediment but the well did not penetrate the basement rocks.

These facts leave uncertainties about the nature of the margin along 88-1A and the location of the volcanic/non-volcanic transition. In this case, the MCS data alone are not able to address these problems. To identify whether the central Nova Scotia margin is volcanic or non-volcanic, will rely on the following evidence: 1) whether or not a thick layer of underplated rocks exists beneath the rifted continental crust, and 2) whether or not large-scale volcanic rocks appear at the basement surface beneath the ECMA. The first problem will depend on whether a thickened layer of anomalously high velocity exists. This requires cross-margin transects of wide-angle refraction seismic experiments. To solve the second problem requires using recent migration techniques to improve the seismic reflection image such that we may be able to verify whether or not SDR sequences, indicative of volcanic lava flows, exist beneath the salt structure.

The extreme seaward end of the profile 88-1A is characterized by increasing basement relief associated with listric normal faults and linear landward-dipping intrabasement reflections. Wade and MacLean (1990) mapped the landward limit of oceanic crust at shot point (SP) 3800, as that position marked the landward extent of the diagnostic hyperbolic character of oceanic basement on unmigrated MCS sections. Keen et al. (1991b) interpreted the smooth zone (SP 3650-3800) seaward of the slope diapiric structure as basaltic rocks that extruded upon continental rocks, and used this interpretation to assign a continent-ocean boundary (COB) between the smooth and rough zones. However, this is also questionable because the deep crustal structure beneath the slope diapiric salts was masked such that the character of the basement across this region is unclear.

For the continental margins further north along the North Atlantic, the continent to ocean transition appears to be a wide transition zone with a thin upper layer of unclear character overlying partially sperpentinized mantle, such as the Newfoundland Basin continental margin (Lau et al. 2006a) and the Labrador Sea margin (Chian et al. 1995a). Such is also the case for the northern Scotian margin along 89-1 (Keen and Potter 1995b; Figure 1.13), where the OCT zone is characterized by a ~70-km-wide zone of flat basement topography (B, Figure 1.13) and a constant thickness (~2 km) of the upper basement layer. The landward limit of this zone appears to be blurred by overlying salt structures or synkinematic wedge on top of salt (shaded area, Figure 1.13; Ings and Shimeld 2006). Further seaward of this zone anomalously thin (~4 km) oceanic crust is imaged along BGR 89-12 (Wu 2007). This OCT zone was interpreted as consisting of a ~70-km-wide zone of exposed mantle which separates the rifted continental crust and the oceanic crust (Funck et al. 2004).

1.3.3 SMART Seismic Refraction Profiles

Previous refraction profiles were mostly short and none of them crossed the entire margin. A more detailed study of the crustal structure and varying volcanism can be achieved by acquiring new refraction profiles coincident with existing MCS profiles. The Scotian MARgin Transects (SMART) refraction seismic experiment was designed offshore Nova Scotia to image the along-

strike variation in crustal structure from a volcanic to a non-volcanic style of rifting. Three wide-angle seismic refraction profiles (Lines 1-3) were acquired in 2001 (Figure 1.10). Line 1 is parallel to two deep MCS lines (89-1, BGR 89-12) and extends 490 km seaward off Cape Breton Island. Line 2 runs parallel to a MCS line 88-1 and farther seaward it coincides with MCS line 88-1A (Keen *et al.* 1991b) and an unpublished BGR line 89-11, forming a 500-km-long composite profile from the continental shelf to the deep ocean basin. Line 3 crosses the southwest-most part of the Nova Scotia margin near MCS lines 89-3, 4, 5.

The purpose of the SMART refraction profiles was to reveal whether a sharp COB or a wide OCT zone exists between the continental crust and normal oceanic crust and whether the volcanic nature of the transition varies from SW to NE along the margin.

The velocity model along SMART Line 2 (Wu et al., 2006) is compared with the model for Line 1 (Funck, et al, 2004) in Figure 1.14. Both models indicate a non-volcanic character for the northeastern part of the Nova Scotia margin. Nonetheless, significant differences occur during the continental extension and the transition to seafloor spreading along the two margin segments

The velocity models for Lines 1 and 2 (Figure 1.14) show that both margin segments contain an OCT zone. The OCT zone of Line 2 consists of a partially serpentinized upper mantle (PSM), overlain by highly faulted continental crust in the northwest and oceanic crust in the southeast. Thin oceanic crust forms immediately following continental breakup with a distinct continent-ocean boundary (COB). In contrast, the OCT zone of Line 1 is characterized by a 70-km-wide upper layer that has been interpreted as exhumed and highly serpentinized mantle (HSM) overlying a layer of partially serpentinized mantle.

This suggests that at the time of breakup, limited magma supply was generated across the central margin segment while no melt was created across the northern Nova Scotia margin. The PSM layer in the OCT zone of Line 1 is ~6 km thick with velocities of 7.2-7.6 km/s; the corresponding layer for Line 2 is less than 4 km with higher velocities of 7.6-7.95 km/s. This suggests a relatively low degree of mantle serpentinization across the central margin segment, and an increasingly higher percentage of serpentinized mantle toward the northern part of the margin. The oceanic crust across the northern margin segment is only ~4 km thick compared with 7.1±0.8 km for normal oceanic crust (White et al., 1992), indicating a magma-starved margin after seafloor spreading. The oceanic crust at the seaward end of Line 2 has a more normal thickness of 6-7 km, which is 2-3 km thicker than on Line 1. The thickness variation also implies an increase of magma supply from the northern Nova Scotia margin to the central margin segment.

The preliminary results for Line 3 show an underplated lower crustal layer within the OCT zone (Dehler et al., 2003) coinciding with the SDR sequence that is observed nearby on MSC profiles 89-3 and 4 (Figure 1, Keen and Potter, 1995a). This further suggests a continuing increase of volcanism towards the southern Nova Scotia margin where the margin eventually changes its character from a non-volcanic margin to a volcanic margin.

1.4 Objectives of this Study

More recent seismic data, collected and/or re-processed for the Play Fairway Analysis of the Nova Scotian margin, will be analyzed to further constrain the rifting pattern of the margin. In particular, we will:

1) Analyze the new refraction profile collected by Geopro GmbH along the ION/GX NovaSPAN Line 2000.

2) Combine the refraction models with the ION/GX deep reflection profiles to better define the nature of the basement within the OCT.

3) Reconsider plate reconstructions of the Nova Scotia – Morocco conjugates to better constrain minimum closure (ie breakup) and maximum closure (ie pre-rift) positions of the margins.

4) Combine the revised seismic refraction models on the conjugate margins to better constrain the rifting style of the margin.

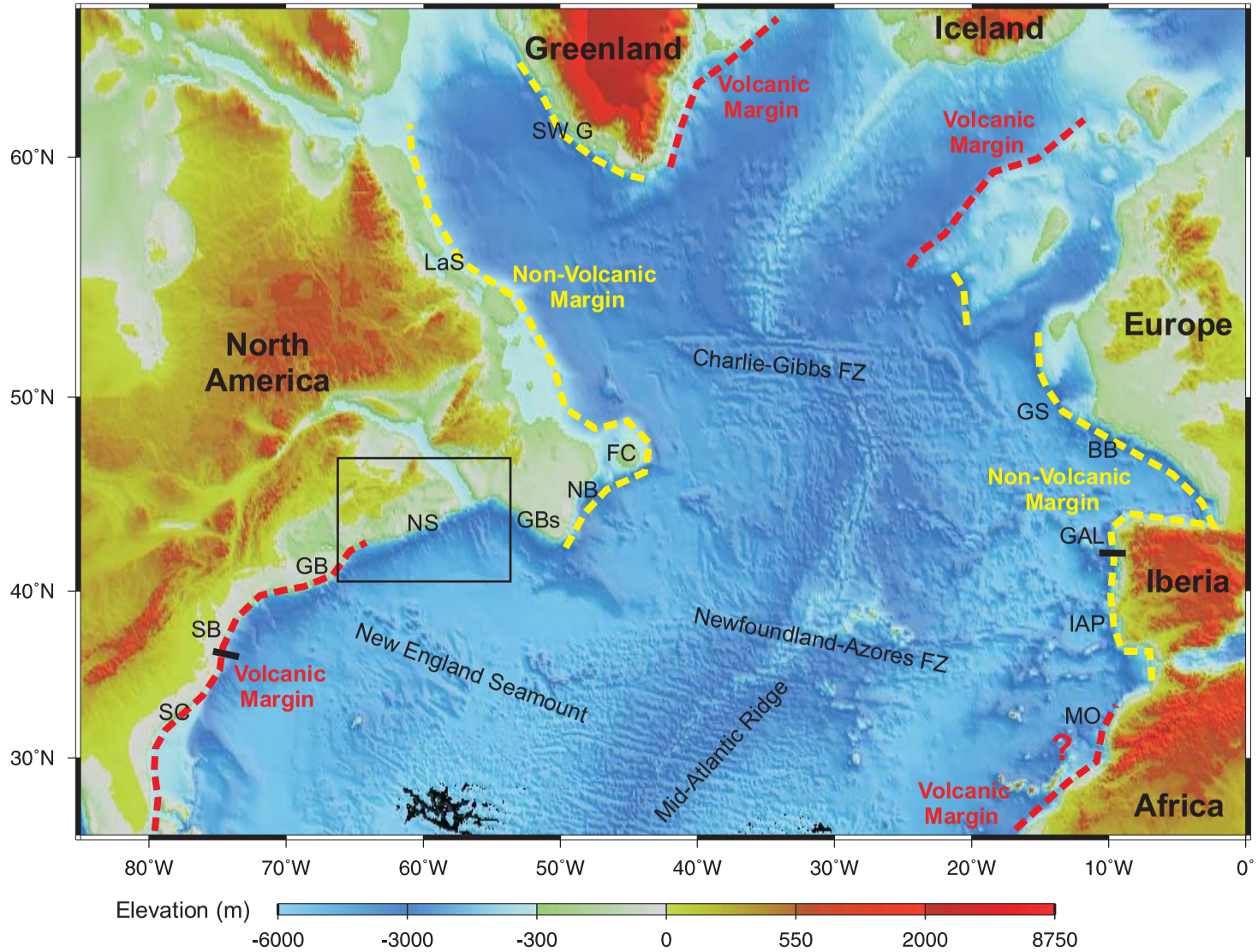
Greenland
Iceland
Volcanic Margin
Volcanic Margin
SW G
LaS
Non-Volcanic Margin
North America
Europe
Charlie-Gibbs FZ
GS
BB
Non-Volcanic Margin
FC
NB
NS
GBs
GAL
GB
Iberia
IAP
SB
Volcanic Margin
New England Seamount
Newfoundland-Azores FZ
SC
MO
?
Mid-Atlantic Ridge
Volcanic Margin
Africa
60˚N
50˚N
40˚N
30˚N
80˚W
70˚W
60˚W
50˚W
40˚W
30˚W
20˚W
10˚W
0˚
Elevation (m)
-6000
-3000
-300
0
550
2000
8750

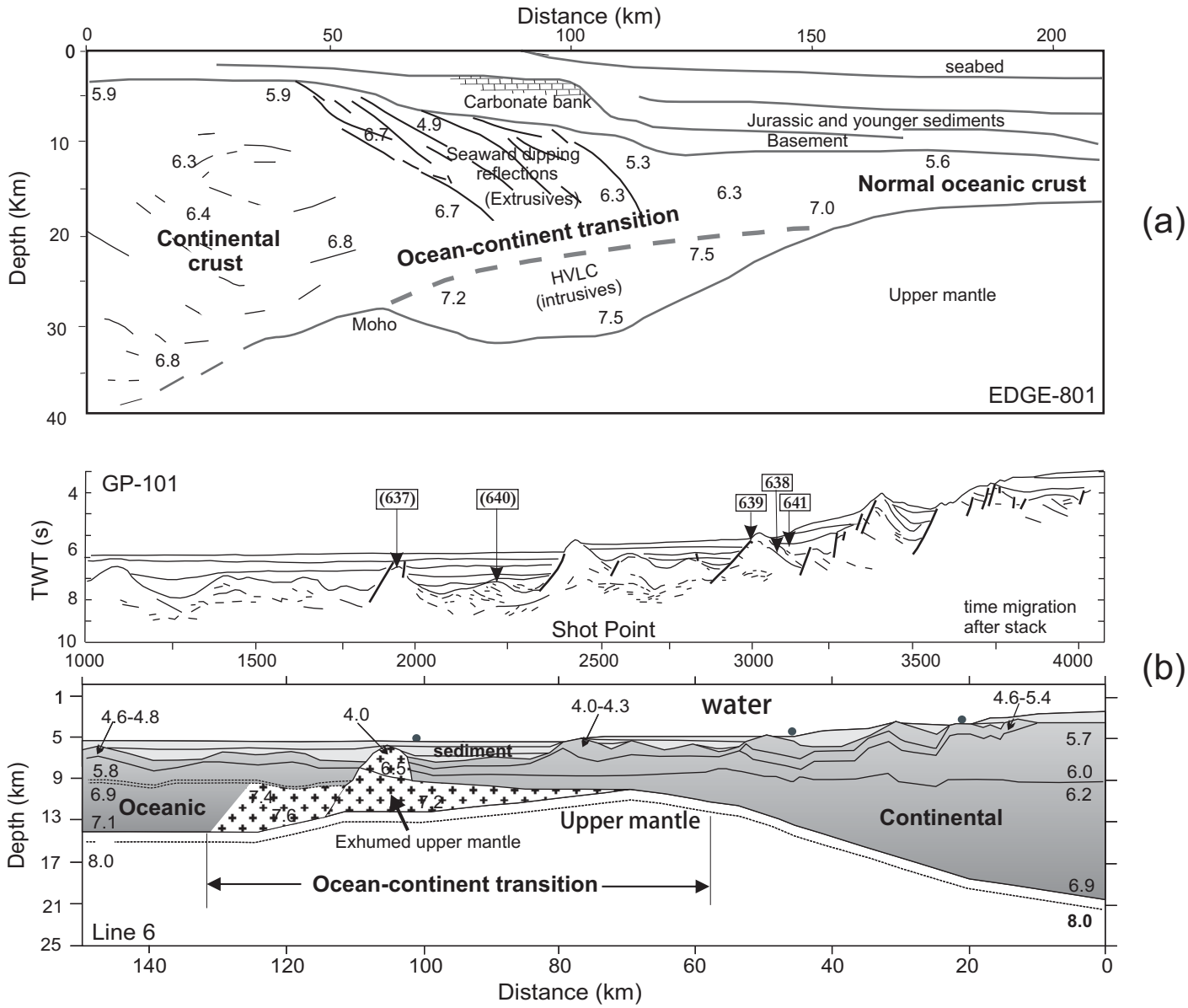

Figure 1.2. (a) A crustal section along line EDGE 801 across the southern Baltimore Canyon Trough. Major crustal layers are labeled with P-wave velocities (unit: kms-1);. SP: shot point. Area highlighted with pattern indicates a high-velocity lower crust (HVLC) layer. After Talwani and Abreu (2000). (b) A crustal section consisting of the line drawing of reflection travel time profile GP101 (Mauffret and Montadert 1987) and the velocity model for coincident refraction line 6 (Whitmarsh et al. 1996) in the west of the Galicia Bank. Boxes with arrows give locations of Ocean Drilling Program borehole sites (Shipboard Scientific Party, 1987); receiver locations (filled circles) and layer velocities (kms-1) are shown in the velocity model. The boundary between the oceanic crust and exhumed upper mantle is not well defined due to lack of seaward refraction receivers. After Louden and Chian (1999).

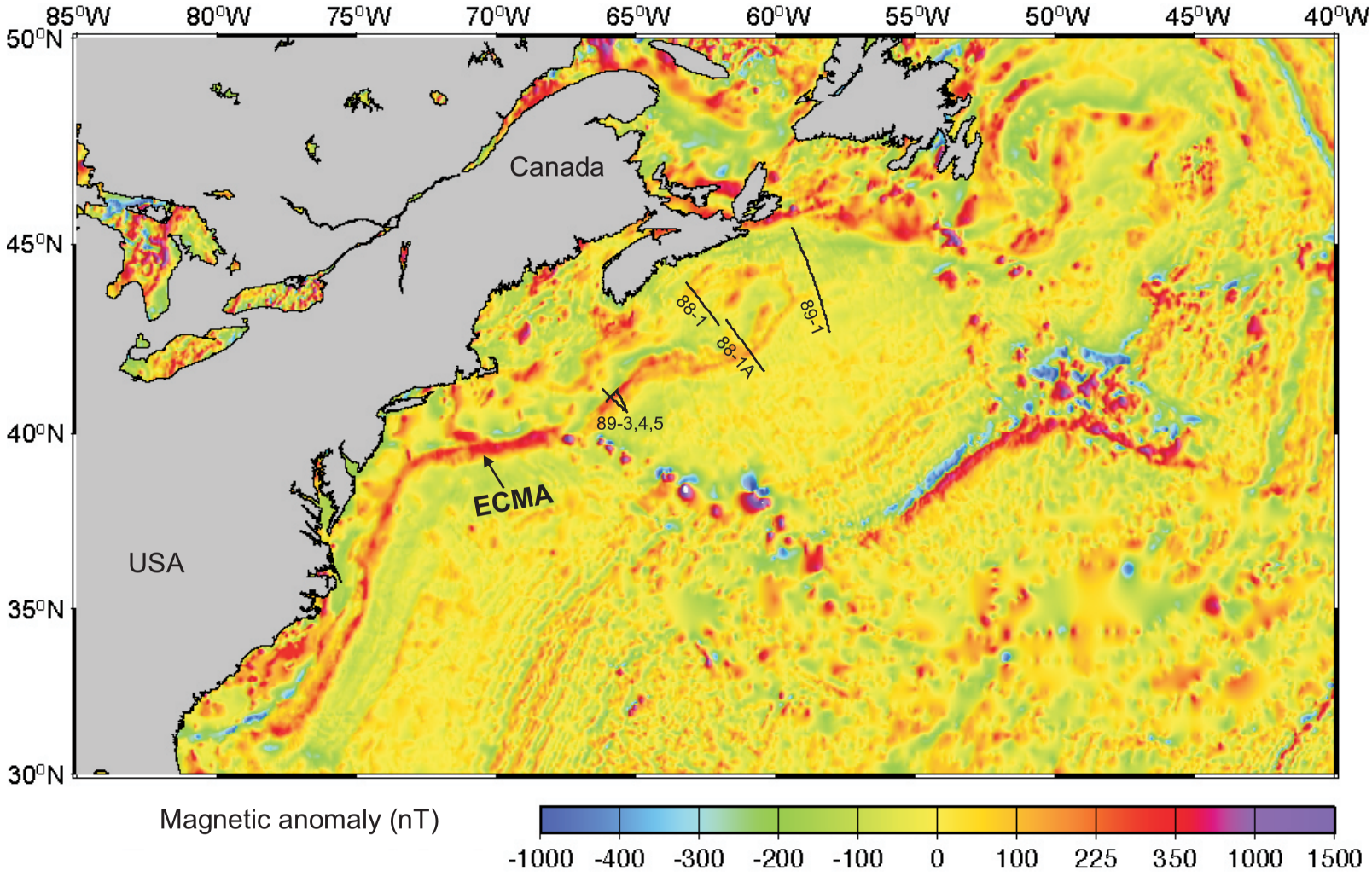

Figure 1.3. Regional magnetic anomalies offshore the east coast of the US and Canada. MCS lines are indicated for reference: 88-1, 1A (Keen et al. 1991b), 89-1 (Keen and Potter 1995b), 89-3, 4, 5 (Keen and Potter 1995a). ECMA: east coast magnetic anomaly.

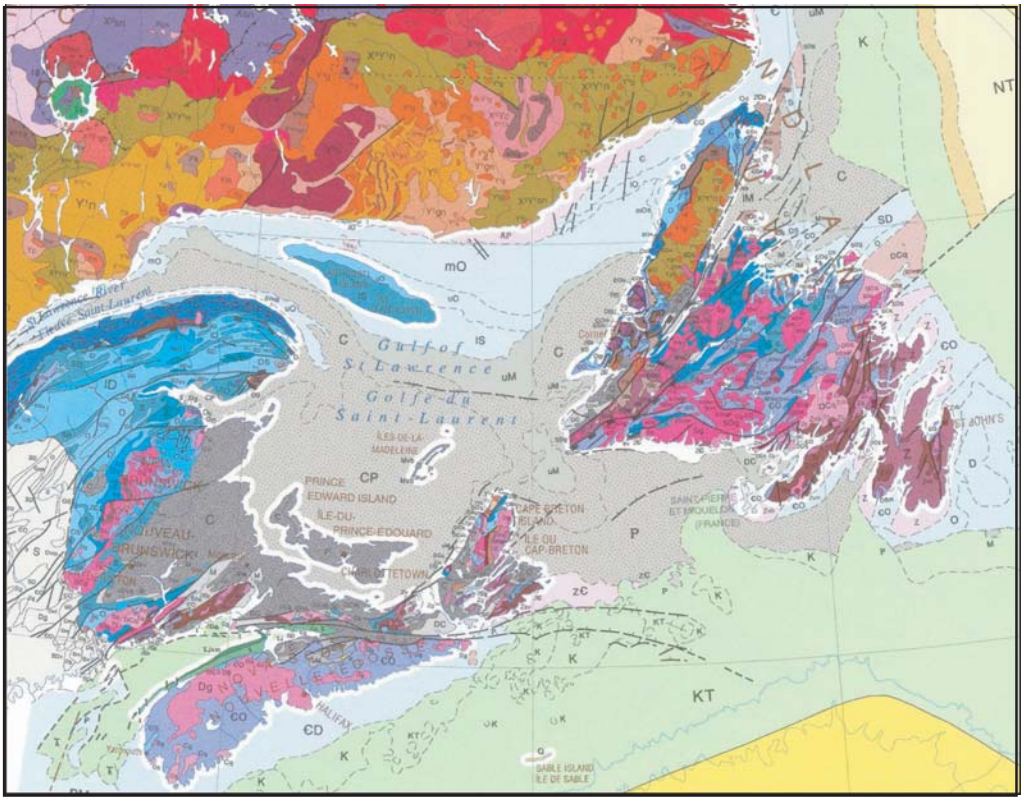
Gulf of St Lawrence
Golfe du Saint-Laurent
St Lawrence River
Fleuve Saint-Laurent
ÎLES DE LA MADELEINE
PRINCE EDWARD ISLAND
ÎLE-DU-PRINCE-ÉDOUARD
CHARLOTTETOWN
CAPE BRETON ISLAND
ÎLE DU CAP-BRETON
NOUVEAU-BRUNSWICK
NOUVELLE-ÉCOSSE
HALIFAX
SAINT-PIERRE ET MIQUELON (FRANCE)
ST JOHN'S
SABLE ISLAND
ÎLE DE SABLE
NOUVEAU-QUÉBEC
NT
KT
mO
CP
CD
zC

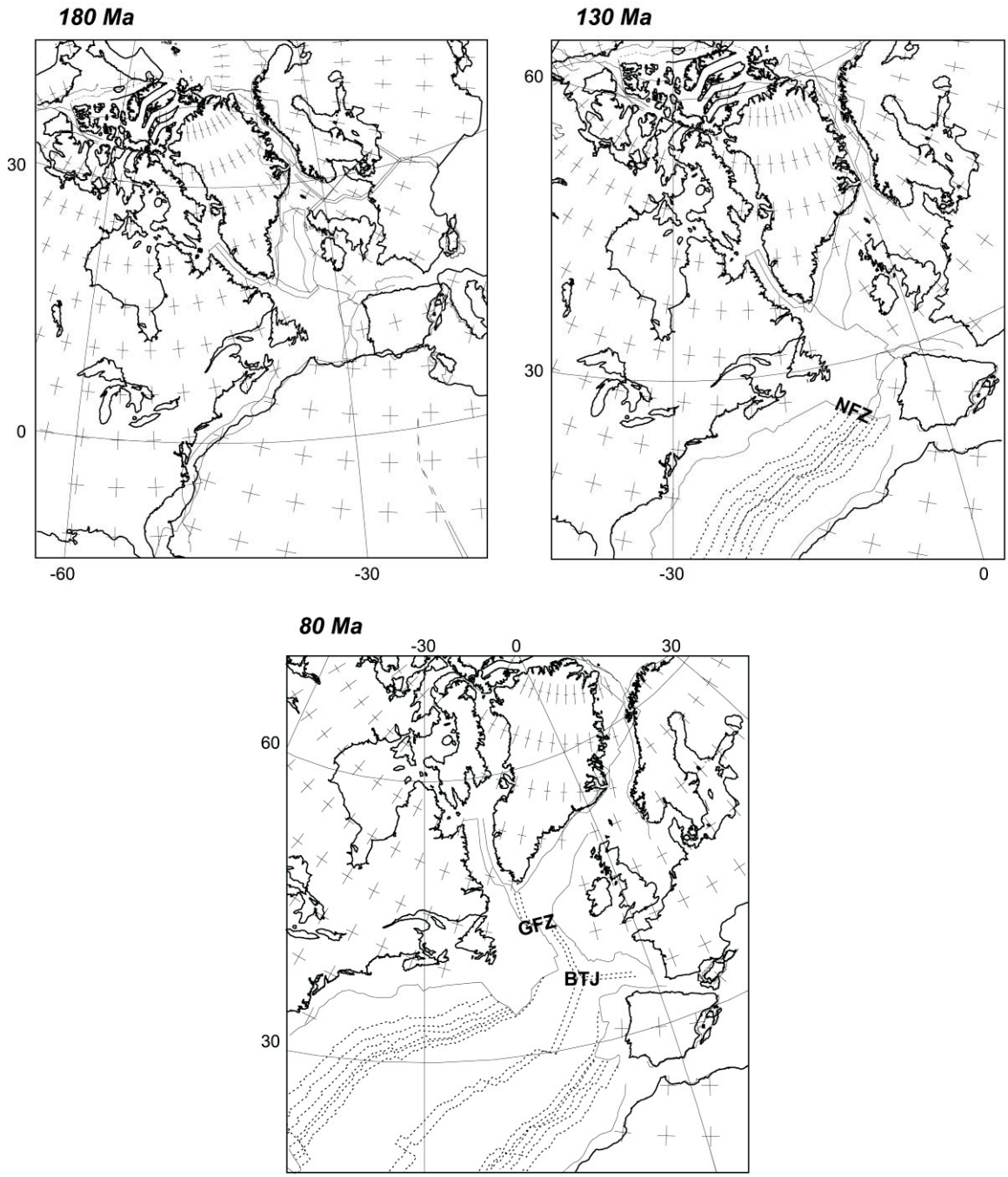

Figure 1.5. Plate reconstructions of the North Atlantic at 180 Ma, 130 Ma, and 80 Ma, respectively. Dashed lines are magnetic anomalies of oceanic crust. NFZ–Newfoundland Fracture Zone; GFZ–Charlie-Gibbs Fracture Zone; BTJ–Biscay Triple Junction. Reconstructions from Coffin et al. (1992), after Louden and Chian (1999).

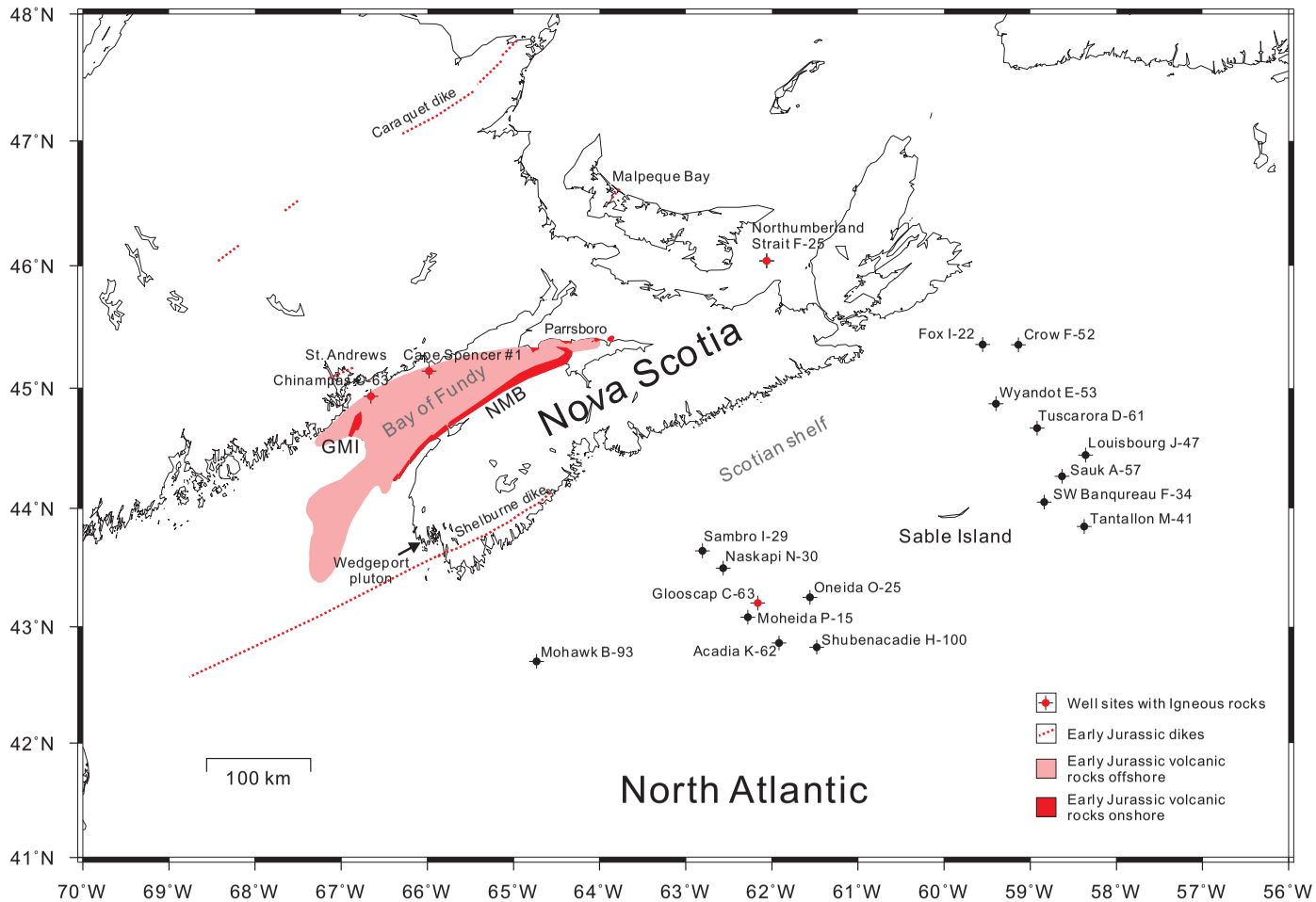

Figure 1.6. Mesezoic volcanism onshore and offshore Nova Scotia. Red areas denote the onshore igneous province of late Triassic and early Jurassic lava surface flows; dotted lines the dikes onshore and offshore. The Pink area indicates the subsurface basalt in the Bay of Fundy. Filled circles overprinted on crosses mark the location of deep exploration wells on the Scotian shelf (BASIN database, Geological Survey of Canada, Dartmouth, Nova Scotia, Canada). Igneous rocks are also presented at well sites offshore (red ones), which are described in the text. NMB: North Mountain Basalt; GMI: Grand Manan Island. The distribution of igneous rocks is based on Pe-Piper et al. (1992).

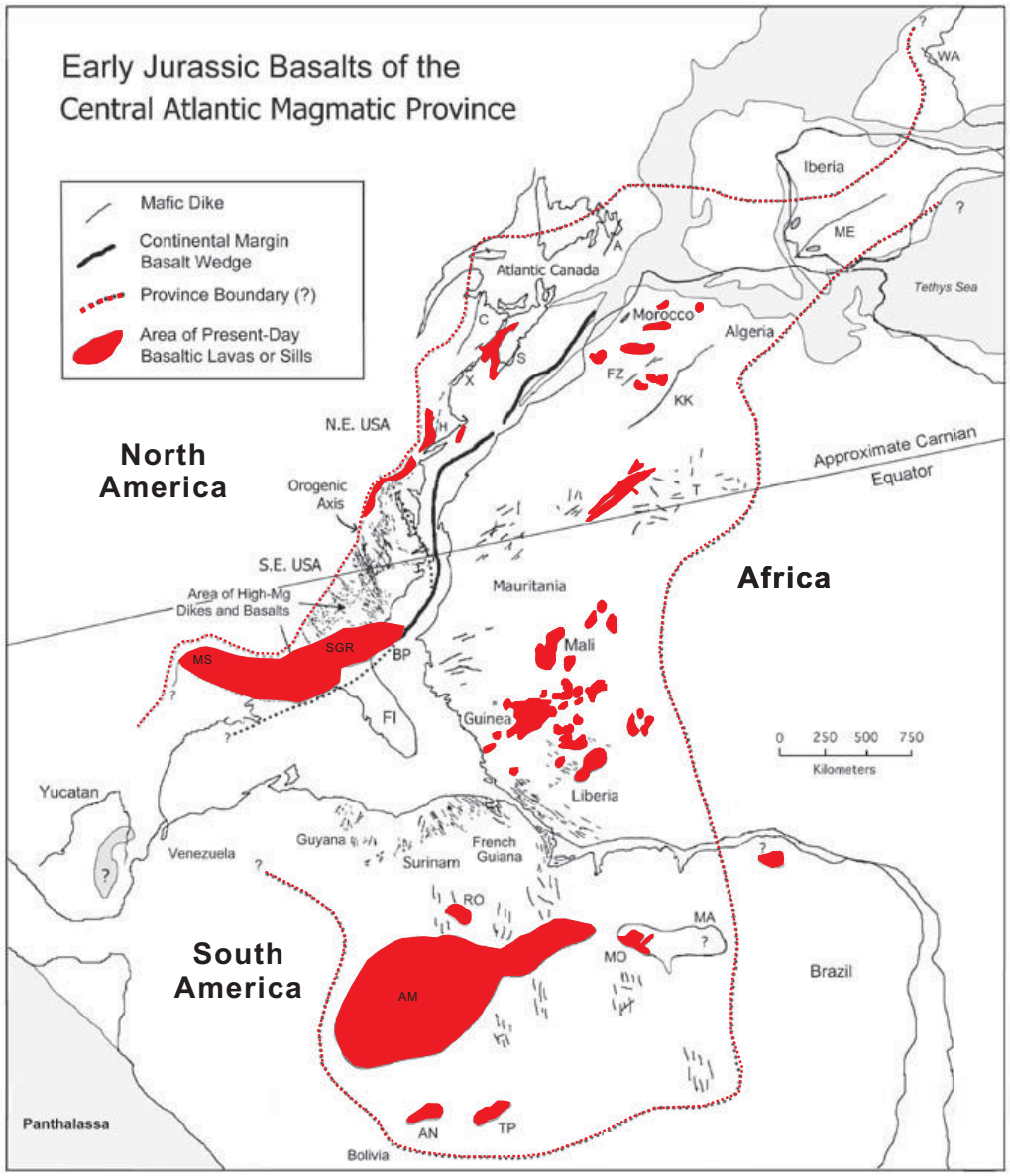

Figure 1.7. Mesozoic volcanism in the Central Atlantic Magmatic Province (CAMP). The base map is the pre-Atlantic reconstruction modified from Klitgord and Schouten (1986). The paleo-equator is from Olsen (1997). The SDR wedge basalt location is from Holbrook and Kelemen (1993). Dikes, sills and basalts in Africa are mainly as shown by Deckart et al. (1997). Basaltic rocks in Atlantic Canada were from Pe-Piper et al. (1992) and Pe-Piper et al. (1990). Volcanic features in Eastern USA were from Sutter and Smith (1979) and Sutter (1985). CAMP features in South America were collected mainly from Marzoli et al. (1999), Baksi and Archibald (1997), Montes-Lauar et al. (1994), and Oliveira et al. (1990). Labels are WA = West Armoricain dike swarm, France (Caroff et al., 1995); ME = Messejana dike, Portugal and Spain (Schermerhorn et al., 1978); A = Avalon dike, Newfoundland (Papezik and Hodych, 1980); C = Caraquet dike, New Brunswick and Maine (Greenough and Papezik, 1986); S = Shelburne dike, Nova Scotia (Papezik and Barr, 1981); X = Christmas Cove dike, Maine (McHone et al. 1995); H = Higganum-Holden-Onway dike system, Connecticut-Massachusetts-New Hampshire (Philpotts and Martello, 1986); Z = Foum Zguid dike, Morocco (Bertrand, 1991); KK = Ksi-Ksou dike, Algeria (Bertrand, 1991); CE = Ceara alkali basalt, northern Brazil (Marzoli et al., 1999); MA = Maranhao dikes and basalts, Brazil (Fodor et al., 1990); MO = Mosquito basalt, western part of the Maranhao province (Baksi and Archibald, 1997); RO = Roraima dike swarm, Brazil (Marzoli et al., 1999); AM = Amazon Basin sill province (Marzoli et al., 1999); AN = Anari basalt, western Brazil (Montes-Lauar et al., 1994); TP = Tapirapua basalt, western Brazil (Montes-Lauar et al., 1994); BP = Blake Plateau area, western Atlantic; FL = Florida, southern USA; SGR = South Georgia Rift terrane (basalts described by Sundeen, 1989; Gohn et al., 1978; Arthur, 1988; McBride, 1991); MS = Mississippi Embayment (basalt dated by Baksi, 1997). This CAMP map is adapted from Hames et al. (2002) and McHone (2000).

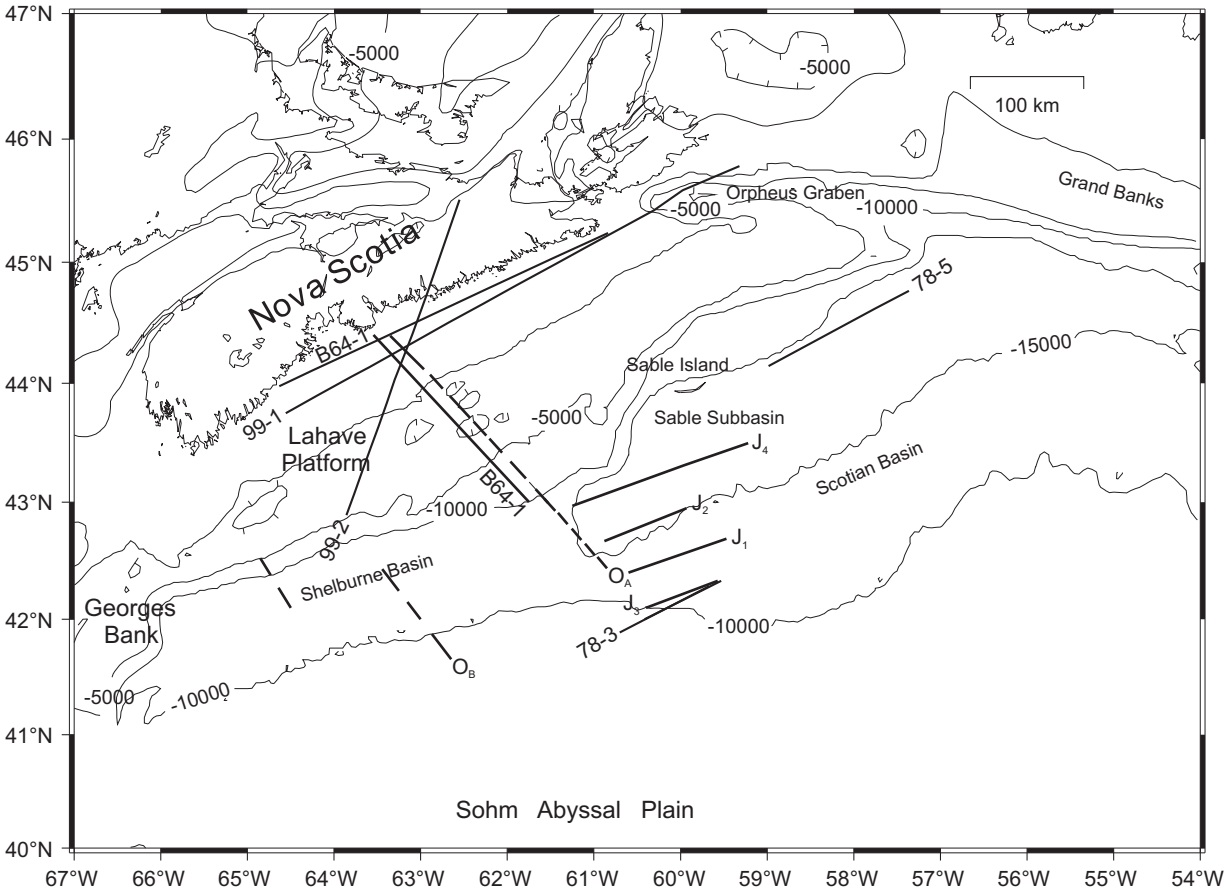

Figure 1.8. Previous refraction profiles onshore and offshore Nova Scotia: OA and OB (Officer and Ewing 1954), which were carried out in short sections indicated as broken lines, B64-1 and B64-2 (Barrett et al. 1964), J1-J4 (Jackson et al. 1975), 78-3 and 78-5 (Keen and Cordsen 1981), 99-1 (Jackson et al. submitted) and 99-2 (Jackson et al. 2000). Basement depth contours offshore are shown as thin lines (Oakey and Start 1995), with contours -5,000 m, -10,000 m, and -15,000 m labeled.

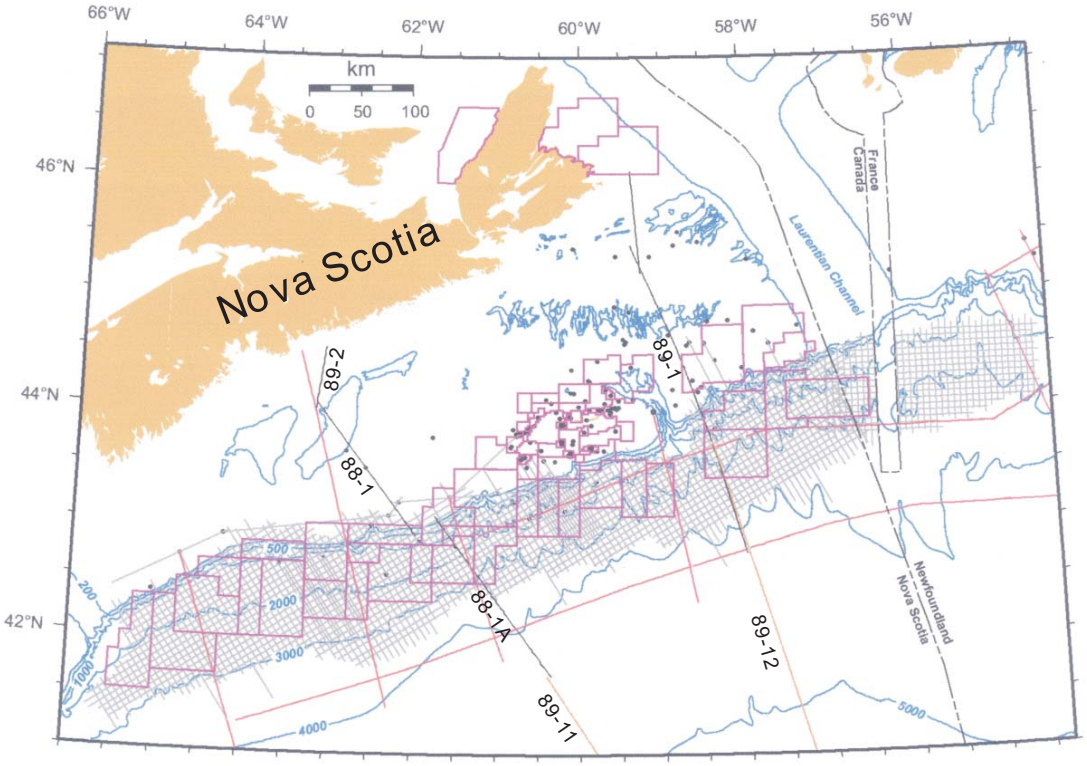
66°W
64°W
62°W
60°W
58°W
56°W
46°N
44°N
42°N
km
0 50 100
Nova Scotia
France
Canada
Laurentian Channel
Newfoundland
Nova Scotia
89-2
88-1
89-1
88-1A
89-11
89-12
200
500
1000
2000
3000
4000
5000

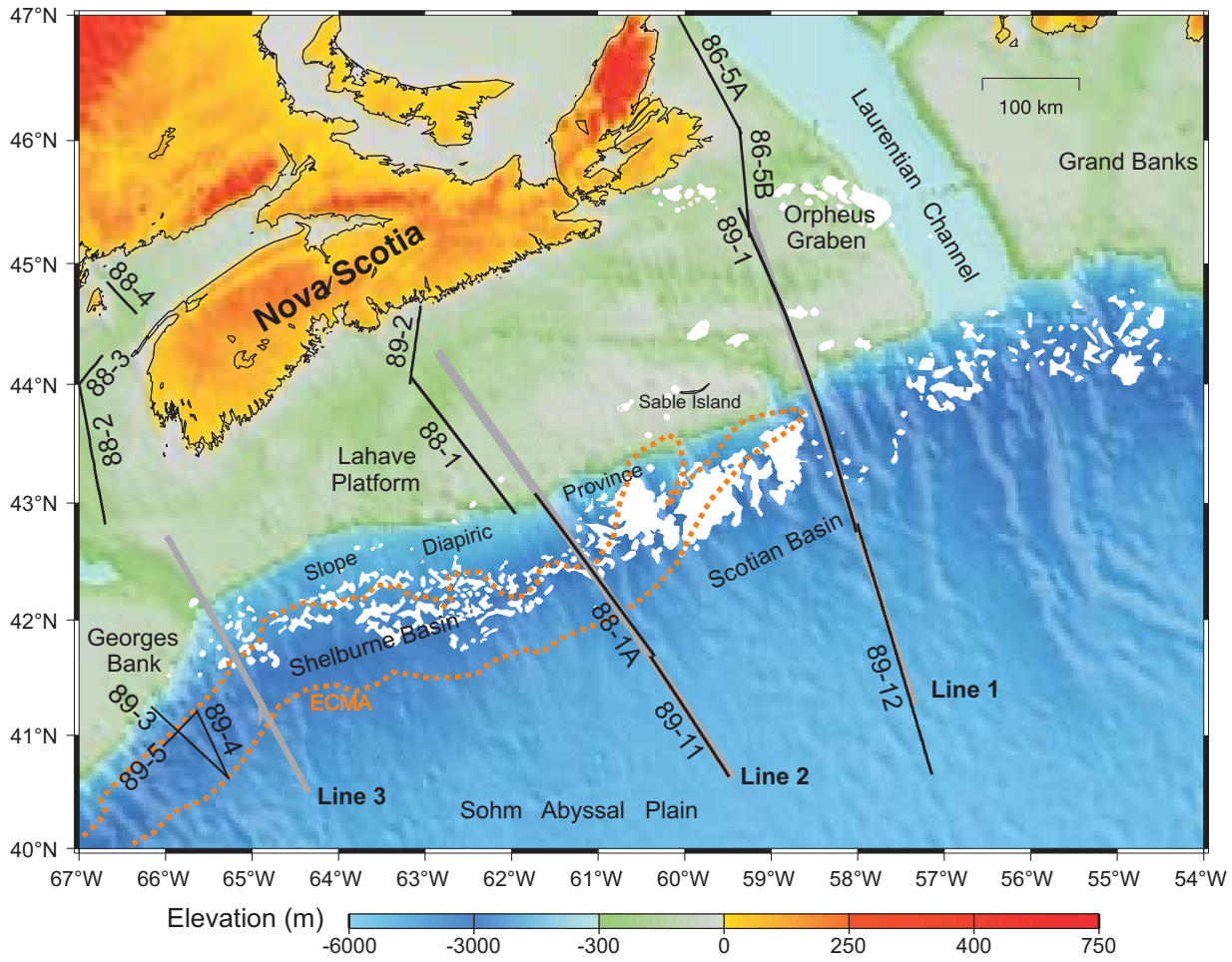
47°N
46°N
45°N
44°N
43°N
42°N
41°N
40°N
67°W
66°W
65°W
64°W
63°W
62°W
61°W
60°W
59°W
58°W
57°W
56°W
55°W
54°W
100 km
Grand Banks
Laurentian Channel
Orpheus Graben
Nova Scotia
Sable Island
Lahave Platform
Province
Diapiric
Slope
Scotian Basin
Shelburne Basin
Georges Bank
ECMA
Sohm Abyssal Plain
86-5A
86-5B
89-1
89-2
88-1
88-1A
89-11
89-12
88-4
88-3
88-2
89-3
89-4
89-5
Line 1
Line 2
Line 3
Elevation (m)
-6000
-3000
-300
0
250
400
750

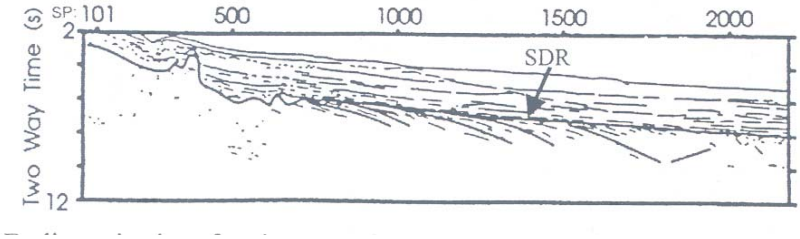

Figure 1.11. Line drawing of MCS profile 89-3. SDR: seaward dipping reflections. After Keen and Potter (1995a). See Figure 1.10 for location.

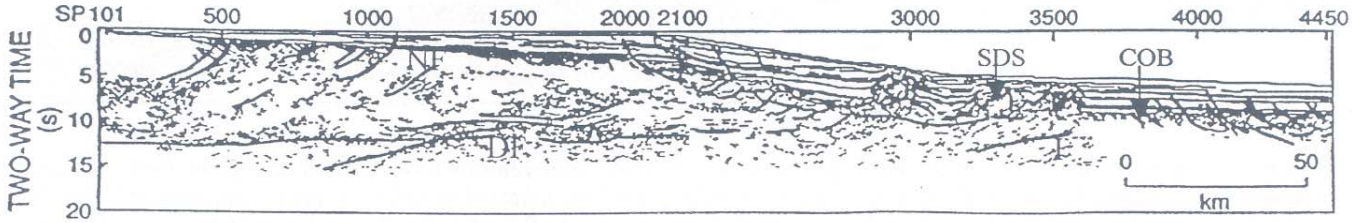

Figure 1.12. Line drawing of the composite profile of 88-1 and 88-1A. SDP: slope diapiric province; COB: continent-ocean boundary; NF: normal faults; DF: detachment faults; I: intrusives; ECMA: East Coast Magnetic Anomaly. After Keen et al. (1991b). See Figure 1.10 for location.

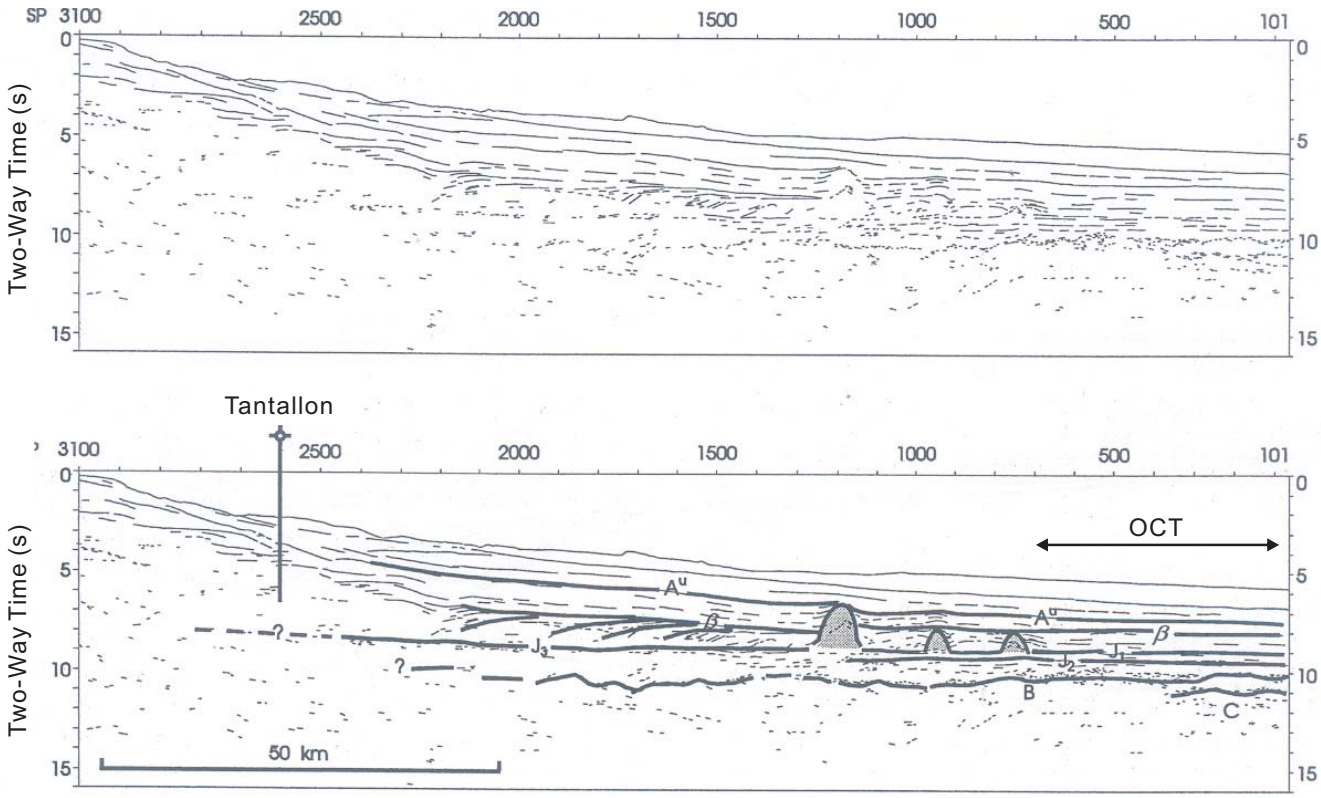

Figure 1.13. Line drawing (upper panel) and interpretation (lower panel) of MCS profile of 89-1 shot point 101-3100. Heavy lines and letters in the lower panel are the interpretation. B: top of basement; C: subbasement reflector. The ages of the sedimentary horizons are indicated by Aμ (Oligocene), β (Barremian), J1 (Top Jurassic), J2 (Callovian-early Oxfordian) and J3 (Upper/Middle Jurassic). Shaded regions are salt diapirs. After Keen and Potter (1995b). OCT: ocean-continent transition. The location of the well Tantallon is indicated in Figure 1.6.

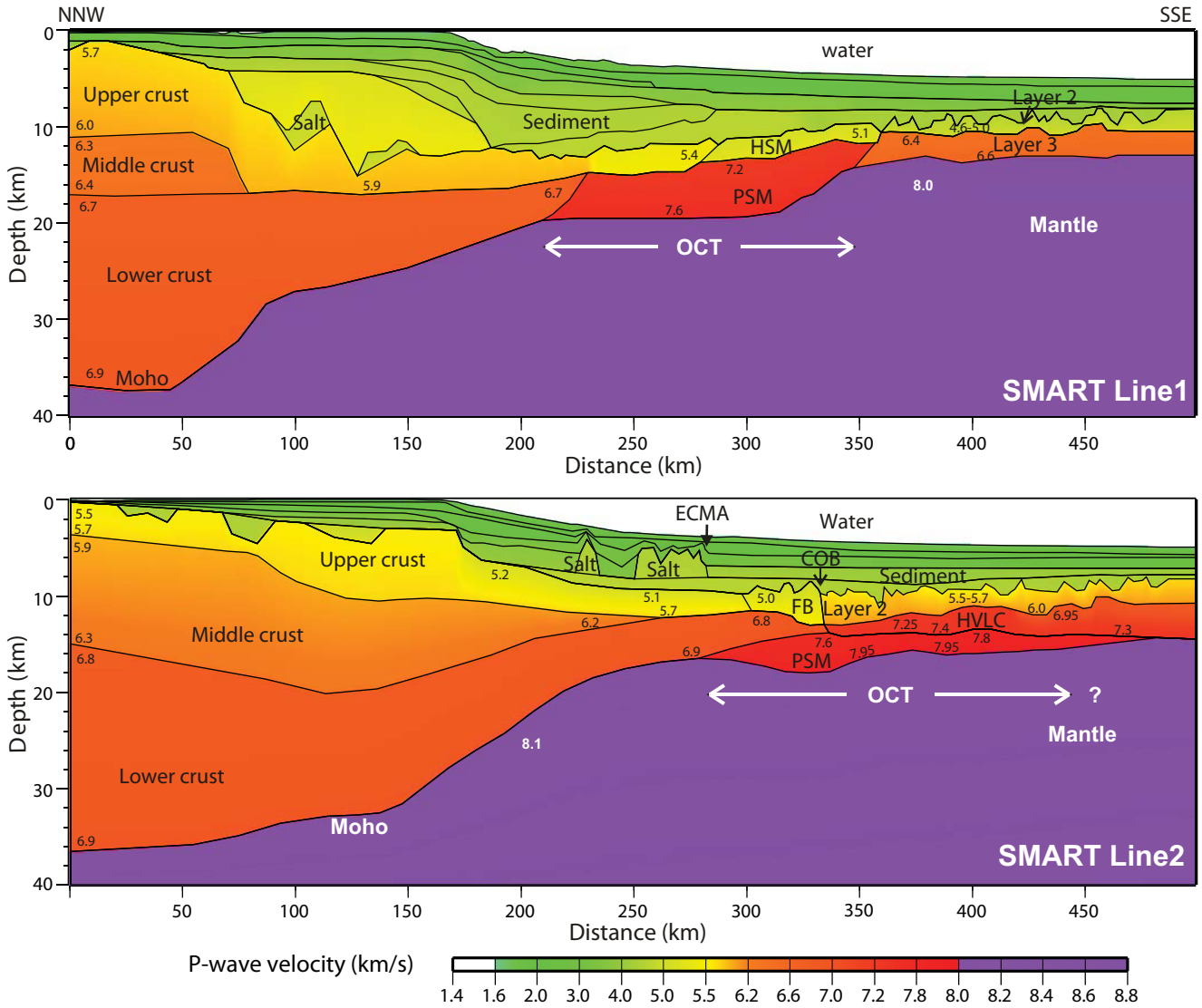

Figure 1.14. A comparison of velocity models along Line 1 (upper panel, Funck et al., 2004) and Line 2 (lower panel; Wu et al., 2006). P-wave velocities are indicated by a colour scale and numbers in the models (in km s-1). Abbreviations: COB, continent-ocean boundary; OCT, ocean-continent transition zone with a double-arrow marking its horizontal region; PSM: partially serpentinized mantle; HSM: exhumed and heavily serpentinized upper mantle; FB, faulted basement blocks; HVLC, high velocity lower crust; ECMA, East Coast magnetic anomaly.

2. OETR REFRACTION PROFILE

As part of the Play Fairway Analysis, a new refraction profile was collected by Geopro GmbH (Geopro hereafter) under contract to OETR along the pre-existing MCS reflection profile ION/GXT NovaSPAN-2000 (Figure 2.1). Geopro was also responsible for OBS data processing and velocity modeling. Our objective was to interpret their resulting velocity model based on a comparison with existing models (see Section 1). However, we first found it necessary to investigate the methodology by which the velocity model was obtained and its resolution in order to allow a more rigorous interpretation.

Therefore, in section 2.1 we will provide details of the Geopro processing sequence that are missing in their previous survey and processing reports. Then in section 2.2, we will discuss the velocity models determined from the refraction data. Finally in section 2.3, we focus on interpretations of the Geopro velocity model as provided.

2.1 Geopro Data Processing

At the beginning, we received from Geopro a set of processed OBS data. These are SEGY files of common station gathers (CSG) with one file for each of the four components of each OBS. Channels are numbered as such:

Ch1: vertical geophone

Ch2: horizontal geophone

Ch3: horizontal geophone

Ch4: hydrophone

However, contrary to the survey report, we only found in the trace headers the following information:

- Water depths at receiver (gelev)
- Receiver position on the distance axis of the velocity model (gx)
- Offset between receiver and shot positions on the model distance axis
- Delay recording time (delrt)

The problem with these values is that they are not raw values but dependent on specific aspects of the velocity model formulation. Normally, the headers should contain all of the raw acquisition geometry in geographical coordinates, so that the data can be used for differing purposes such as formulation of independent velocity models. Geopro also provided us with their first-arrival picks and the layer tomography picks. However, these were picked using the processed data mentioned above.

Based on our experience in velocity modeling of refraction data, we determined that the uncertainties present in the geometry and in the processing of the data could not be quantified sufficiently in order to justify further analysis or interpretation. Therefore, with the help of RPS Energy, we were able to retrieve the missing information from Geopro needed to fully process the data. This information will guarantee the reliability of the acquired data for other future users.

2.1.1 Geometry

In any OBS SEGY data file, each trace corresponds to a single shot. These traces should have been uniquely identified by their individual shot times and shot point numbers, which is standard practice for MCS reflection data. However, Geopro did not use shot point numbers for processing due to requirements of their modeling software. This explains why there was no shot point numbers in the headers. Unfortunately, shot times were also not recorded in the headers. Without such information, we were unable to correlate the observed trace with the shot position according to the shot time and position table (shot table, hereafter), which uses the same shot identifiers. Thus, we were unable to assign the raw shot-receiver geometry to the headers.

We contacted Geopro for this information and they sent us a new set of SEGY data files with shot point numbers in the headers. However, they did not at that time have a shot table which can correlate these shot point numbers with shot positions. In the end, a Geopro em-

ployee visited our lab to solve this problem with us. We then found that for some OBS SEGY files, both shot points and shot times were recorded in the headers. We could, therefore, obtain the shot geometry by the following steps:

- The shot time for each shot point number is obtained from the headers of those OBS SEGY files where both of these values existed. The shot times in the headers are UTC time. Fortunately, these cover all of the shots. These were used to create shot time logs.
- Ship navigation files for the dates of shooting were obtained from Geopro. The times in the ship's navigation files are UTC time, despite being identified as local times in the files. Please see Appendix A for a list of data files submitted in a hard disk together with this report. Processed navigation files are located under the *Navigation* directory with filenames "phase[#].nav" with "#" being the phase number of shooting (Figure 2.2).
- For the purpose of bookkeeping, a constant heading was assumed for each phase and was calculated using two points on the shot profile that are far away. These were added to the navigation files mentioned above but they were not used in subsequent processing.
- A shot table was created for each of the three phases of shooting using our own software. The ship's position at the time of the shot were interpolated from the ship's navigation. A gun delay of 50 ms and the difference in location between the airguns and the GPS antenna were input to determine the position and time of the shot. The ship's headings used in this calculation were also interpolated from the ship's navigation. The shot tables are located under the *Navigation* directory. Shot positions are plotted in Figure 2.2. Shots that overlap within phase 1 have been edited out both in the shot table and in the SEGY data files.

As for the receiver (OBS) geometry, we followed these steps:

- The OBS positions obtained from Geopro are the deployed positions (Figure 2.2). They are located in the *Navigation* directory. Note that the "deployed position" in the survey report is actually the planned position.
- Geopro also provided us with bathymetry along the profile and the OBS depths. These were obtained assuming a water velocity of 1.5 km/s applied to some old sea floor picks and from the ETOPO2 Grid (U.S. Department of Commerce, 2006). (N.B. The echo sounder on board did not work). However, we prefer to recalculate the OBS depths using our seafloor horizon picks from profile NovaSPAN-2000 and the GEBCO_08 Grid (30 sec) (GEBCO, 2009) to be consistent with the coincident MCS data. This also made use of the water velocity of the NovaSPAN-2000 prestack depth migration model.

The shot and OBS positions were then converted to UTM (WGS84, Zone 21 N) and offsets were calculated for each trace in the SEGY files.

2.1.2 Time corrections

Geopro has performed a time correction to the data for a gun delay, a constant receiver time delay and the OBS clock drift (see survey report for details). The file with the details of the clock drift correction is located under the *Navigation* directory. However, we also found that in addition to the above standard procedures in OBS time correction, Geopro also applied a non-standard static time shift which is specific to the individual OBS. Both the standard and the non-standard time corrections were summed into the Delay Record Time (delrt) headers. We speculate that the non-standard time correction was a quick fix to eliminate errors in OBS positions and the water depths at the OBS. Therefore, this additional time correction will prevent us from determining the correct OBS positions on the sea floor (see section 2.1.3).

As a result, we requested Geopro to separate the standard and non-standard time corrections. They then sent us the last set of SEGY files in which:

- the standard time corrections have been applied to the binary part of the data
- the non-standard time correction is pre-

For this dataset, we input the new geometry and time correction into the headers using a Linux shell script named "input_geom_head.cmd" found under the *Script* directory. The output files are located under the *OBS_data* directory. Since headers for all channels of each OBS should be identical, we only have done this for one channel (ch4). Note that all channels do not necessarily contain useful seismic data.

2.1.3 OBS repositioning

The OBS drifts as it sinks from its deployed location on the sea surface to its position on the sea floor. This drift is unknown but can be estimated by modeling the recorded seismic arrivals that travel through the water column to the OBS (direct water arrivals). This OBS repositioning is rather time consuming. However, it results in more accurate values of the receiver-to-source offsets, and hence, more accurate travel-time versus offset data for the observed reflected and refracted phases used in determining the velocity model.

Geopro used their own method for OBS repositioning, which is different from the conventional method that is used academically. Please see Appendix B for details on methodology and a comparison between the two methods. The original offset values in the SEGY data we received were calculated based on the Geopro repositioned OBS locations.

However, the Geopro method can only approximate the OBS location if it lies on the same vertical plane as the shots (i.e. the profile plane), which is not generally the case. Therefore, we decided to reposition all of the OBSs before proceeding further with velocity modeling. Unfortunately, due to time restrictions, we could reposition only three OBSs (file "*Navigation/*OBS_relocate_coord_latlon.txt"), and have updated only the header of OBS 92 (located under the *OBS_data/relocate* directory). This result is sufficient to show that we now have all the information needed to complete this task and that they give sensible results.

2.2 Velocity Modelling

2.2.1 First arrival tomography

During the period when the data processing issues were being sorted out, we continued with analysis of the initial velocity modelling results that we received from Geopro. Figure 2.3a shows the final velocity model resulting from their first arrival tomographic inversion. Geopro also provided us with their first arrival travel time picks that were used to constrain the model. However, this model does not show sufficient detail for interpretation of the crustal structure. Therefore, we found it necessary to investigate their model further by using the academic program FAST (First Arrival Seismic Tomography; Zelt and Barton, 1998).

The first step in tomographic inversion is to begin with the best possible starting model. Our initial plan was to use the final tomography model provided by Geopro, which should fit the picks reasonably well. However, a large portion of the model depends on the sediment and water velocities that are poorly constrained by first-arrivals. In contrast, the water and sediment velocities in the pre-stack depth migration model of the ION/GXT profile NovaSPAN-2000 are much better constrained.

Therefore, we replaced the Geopro velocities above the basement with the NovaSPAN-2000 migration velocities (Figure 2.3b). This profile covers only the landward part of the model (< 282 km model distance in Figure 2.3b). For greater distances, the sediment and water velocities were extrapolated following the seafloor depths. The basement horizon was picked using the pre-stack depth migrated section of profile NovaSPAN-2000 (Figure 2.4a). Beyond the seaward limit of the profile, we used the OBS data to pick the basement reflection at zero offset (Figure 2.4b). Although the geometry was not correct in these data as detailed in section 2.1, they were the best we had at the time. Finally, Moho depths were modified in our starting model to remain flat at the seaward end of the profile.

Another issue in modeling the data is that the shot line and OBS profile do not follow a great circle path, with a bend at ~ SP 2700 (Figure 2.2a). The Geopro model is, however, defined by the positions of OBS 1 and the seaward-most shot, and is not a best fit to the shot/OBS profile. To avoid this problem, we only focus on modeling the data from Phase 1, which is the seaward half of the model that covers the transitional and oceanic crust.

Figure 2.5a shows the resulting model. Although the velocities above the basement were fixed in this model, similar results were obtained by allowing the lower part of the sediment to be updated by the inversion. The velocities for distances <260 km remained essentially the same as the starting model, meaning that no improvement in fit could be made. For distances >260 km, some variations were introduced by the inversion. On average, this result is evidence in support of a thin oceanic crust and lower crustal velocities in this region compared with the initial model and compared with the crust in the landward direction (ie distances <260 km). Some instabilities also can be observed in the crust for distances >320 km, which were likely due to the lack of ray coverage in this part of the model (Figure 2.5b). These artifacts are most likely produced by the large intervals between the Geopro picks, which are often >500 m. Although this model is still not sufficient for any detailed interpretation of the crustal structures, we were primarily concerned with fixing the data processing issues and we did not proceed further with this first arrival tomography model.

2.2.2 Layer tomography

A velocity model is better constrained when second and later arrivals are considered in addition to the first arrivals. This is accomplished through a layer tomography approach. We were provided with Geopro's layer model together with the picks that were used to constrain the inversion. However, in order to justify any interpretation of the model, we first need to determine how well the model fits with the observations. The only method to do it is by ray tracing through the model.

Since we did not have access to results using Geopro's modeling software, we instead used the RayInvr program (Zelt and Smith, 1992). One advantage to this approach is that it replicates the same procedure used to determine the velocity models from the SMART profiles. We first converted the Geopro model result into the RayInvr format (v.in file format). This velocity model file (Geopro_layer.v.in) is located in *\Dalhousie\Velocity_model*. Source files for the velocity model provided by Geopro are also located in the same directory. The velocity model is plotted in Figure 2.6.

We used the OBS positions provided by Geopro since we did not have sufficient time to calculate the true OBS positions as detailed in section 2.1. The Geopro positions presumably place the apexes of the direct water waves at the vertical axis (distance=0; see Appendix B). For the same reason as in the first-arrival tomography (section 2.2.1), we redefined the model profile for Phase 1 between shotpoint 1 and shotpoint 2800 (Figure 2.2a). The OBS positions were then projected onto the velocity model profile plane and their corresponding coordinates in model distances were obtained. The OBS water depths were input using our redetermined bathymetry along the profile. This information is written in file "OBS_model_dist_depth.txt" in the *\Dalhousie\Navigation* directory.

According to Figure 2.6, the Geopro model appears quite simple in structure with very low velocity gradients in most layers. By ray tracing, we can evaluate the constraints from the data for difference parts of the model. Figures 2.7-2.10 show the ray tracing results from four different OBSs. Individual seismic phases are colour-coded and match the ray-traced paths through the various layers in the velocity model.

OBS 73 (Figure 2.7) is at the boundary between the partially serpentinized mantle layer (with velocity of 7.3 km/s) on its left and the oceanic crust on its right. It shows that the phase through the upper crust (light blue) is poorly constrained as it does not fit with any observed arrivals. The same is true for other OBSs. However, the lower and thicker layer of

the oceanic crust (green and purple) fits very well with the observed arrivals, except that the low velocity gradient of these layers causes the ray-traced arrivals to extend to greater offsets than observed. The mantle diving phase (yellow) also fits well, constraining the overall thickness of the oceanic crust.

On the other side of the OBS, the phase through the partially serpentinized mantle (pink) does not fit the observed arrivals very well. An improved fit might result if a larger velocity gradient with a lower velocity at the top is used for this layer. For OBS 76 (Figure 2.8), however, which is only slightly further seaward, the same phase fits very well, suggesting that the Geopro model is overly simple or there are errors in the data. OBS 76 also shows evidence for the seaward dipping boundary between the serpentinized mantle and the oceanic crust (purple line landward).

Farther seaward on the oceanic crust, OBS 92 (Figure 2.9) shows the presence of the oceanic crustal phase (green) on both sides of the OBS. The crustal thickness is also well constrained as the mantle phase (yellow) fits well with the data. However, the fit is not as good for OBS 95 (Figure 2.10), which is only 10 km seaward from the previous OBS, indicating that the model is overly simple or that there are errors in the data.

Although only four OBSs are shown, we have performed additional raytracing for OBSs 41-100. Fits between the modeled arrivals and the data indicate additional inconsistencies between OBS. Furthermore, our results indicate that there are insufficient constraints from the modeled data on the velocity structure of the crustal layer above the partially serpentinized mantle layer. One reason for the discrepancies between OBS could be inaccuracies in the OBS positions. Therefore, there is a need to first reposition all of the OBS to eliminate this uncertainty. We then suggest that the data be remodeled with a focus on the upper crust of the transition zone, in order to better define the crustal composition of the middle part of the model within which serpentinized mantle is interpreted.

2.3 Interpretation

The OBS repositioning and the remodeling of the data will take an extended period of time and so are not possible before the end of the present contract. We, therefore, take the original Geopro layer model to make a first-order interpretation. As major features in the model appear to be well-constrained, given the average fit between the modeled travel times and the observed arrivals, we expect that the remodeling will primarily change the detail structures (especially the velocity gradients for some layers) but not the large scale structures of the original model.

The velocity structures of the Geopro layer model (referred in following as profile OETR) show the presence of three different crustal zones (Figure 2.6 & 2.11a). In the NW, the continental crust, with the highly compact sediment above, has thinned over a relatively wide zone (> 180 km) until rupture. In the SE, oceanic crust is interpreted between 255-405 km model distance, consisting of crustal layers 2 and 3 with a total thickness of 4-5 km. Between these two zones, there is a transitional zone (COT; 180-255 km distance) that cannot be explained by either a standard continental or oceanic crustal model.

The COT is modeled as two layers above the normal mantle. The lower layer has a velocity of 7.3 km/s and thickness of ~ 6 km. We interpreted this to be partially serpentinized mantle. The upper layer has a velocity of ~ 5.3 km/s and an overall seaward decrease in thickness (4 to 2 km). Its crustal origin is the most uncertain part of the model. It is tentatively interpreted as oceanic layer 2, since it is continuous with this layer on the seaward end. This interpretation implies the formation of ultra-slow spreading oceanic crust. Such crust is usually highly tectonized (e.g. Srivastava and Keen, 1995) and therefore, is inconsistent with the low vertical velocity gradient as modeled. Results of our ray tracing in section 2.2.2 suggest, however, that such a low gradient in the model is not consistent with the observed data. An alternative interpretation of this layer as extruded basalt flows seems inconsistent with the absence of

such flows on the coincident reflection data (Figure 2.12).

Another possibility is that the layer consists in part of highly thinned continental crust. Although it is difficult to identify the basement top in the reflection profile, the Moho suggests an overall gentle thinning and so the continental crust may extend beyond the seemingly abrupt termination at ~ 170 km distance (Figure 2.6). This interpretation appears to disagree with the seaward dipping discontinuity in basement layer velocities between the upper continental crust (5.5-5.8 km/s) and the upper transitional crust (5.25-5.35 km/s) at a distance of 150-180 km. However, we note that a similar discontinuity in velocities exists in the model for SMART Line 1 (at 230 km distance in Figure 2.11b), where the continental crust was interpreted to extend over the partially serpentinized mantle until replaced by exposed highly serpentinized mantle (at 285 km). A final possibility is that this layer consists of highly serpentinized exhumed mantle, as interpreted for the seaward part of the COT on SMART Line 1 (285-360 km). However, we do not observe additional supporting evidence for this interpretation.

2.3.1 GXT 2000 reflection profile

An overlay of the NovaSPAN-2000 migrated section with the coincident Geopro layer model should facilitate direct comparison between the two (Figure 2.12). However, since the pre-stack depth migration velocity model used for NovaSPAN-2000 is not the same as the Geopro velocity model, the depths between the two cannot be correlated directly. Unfortunately, we do not have a time section of profile NovaSPAN-2000 to correct for this difference. Therefore, Figure 2.12 represents the best comparison we have at present.

This comparison shows that there are some important mismatches between the MCS profile and the velocity model. Firstly, the basement top beneath the shelf does not follow any particular reflector. If the depth of this boundary is controlled by sediment compaction rather than a change in lithology, the same should also be true beneath the continental slope where the layer instead changes depth. Another discrepancy occurs for the basement within the COT beneath the slope and the seaward basin. The basement is observed in the MCS data as an undulating surface of possible faults or small ridges, but is simplified to a relatively smooth boundary in the velocity model. It is possible that this misrepresentation of the basement in the velocity model might contribute to the misfit we observed with the OBS data. The basement reflection for distances >200 km in the model is difficult to observe in the MCS profile. It would be very helpful to have the re-processed NovaSPAN-2000 section available to us for clarifying the detailed basement geometry.

Another reason for our interest in the reprocessed GXT dataset is that we expect a strong reflection between the low velocity upper crust and the higher velocity partially serpentinized mantle layer, although such a boundary is not observed in the MCS profile. However, a strong reflection potentially equivalent to this boundary is observed on other GXT profiles such as the profile NovaSPAN-5100 (W-reflection; Figures 2.1 & 2.13). Therefore, an improved image of the upper crust in the reprocessed data will allow us to map this reflection within the COT and to discriminate between the different models for its crustal origin.

2.3.2 Comparison with SMART profiles

To compare profile OETR with profiles SMART-1 & 2, we plot them together using the same parameters and scale (Figure 2.11). A detailed discussion of the comparison can be found in Appendix C. Below is a summary of relevant points:

- Profile OETR is more similar to SMART-1 than to SMART-2.
- All three profiles display non-volcanic margin structures, showing similar characters in the three major crustal zones:
  - The continental crusts thin over a wide zone.
  - Oceanic crust is relatively thin (~ 4-6 km) for both Layers 2 and 3.
  - Within the COT, a very thin upper crust is observed above a lower layer interpreted as partially serpentinized mantle based on its

velocity and thickness.

- Despite the variable structures observed, these profiles show a general southward trend of more fully developed oceanic crust above partially serpentinized mantle.
- A mapping of the serpentinized mantle layer shows close correlation with regional structure and the presence of a strong crustal reflection (W).

2.4 Future steps

The following addition work is planned for August-October as a conclusion to the present contract:

1. Proper repositioning of all OBSs as outlined above.
2. Updating all OBS SEGY datafiles with correct geometry in the headers.

Complete remodelling of the OETR profile cannot be completed within the timeframe of the Play Fairway Project, but instead will be undertaken as a longer-term academic study.

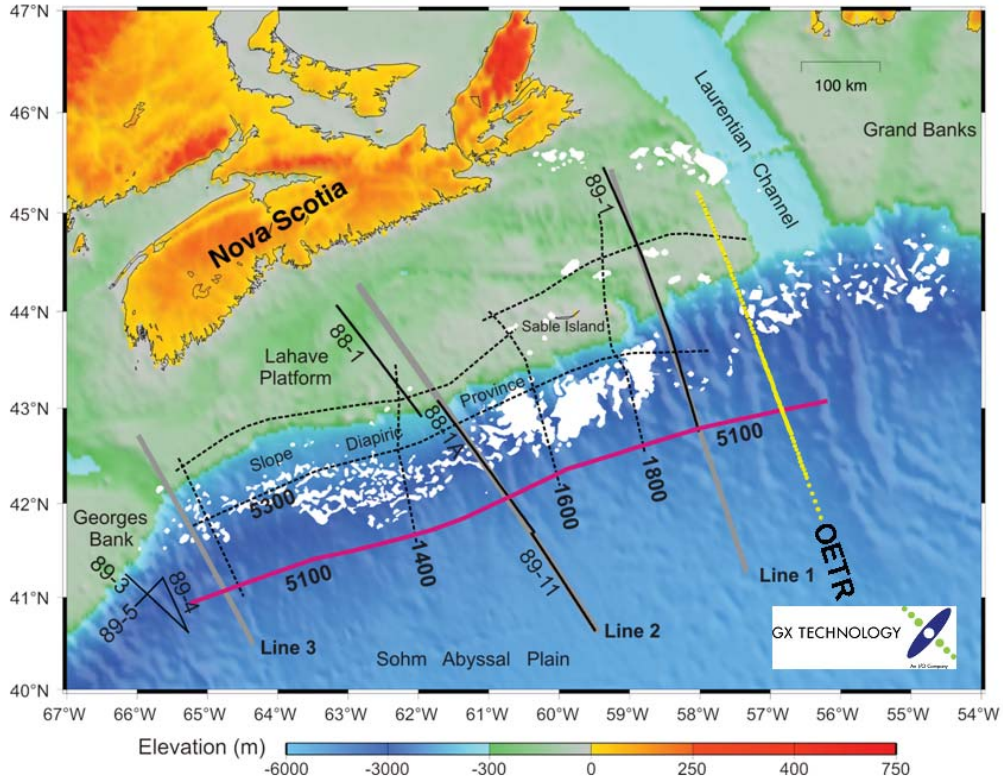

Figure 2.1. Location of profile OETR, the new refraction line (yellow dots are OBS locations). Dashed lines are ION/GXT NovaSPAN profiles. Red line is profile GXT-5100. See caption of Figure 1.10 for other features of the plot.

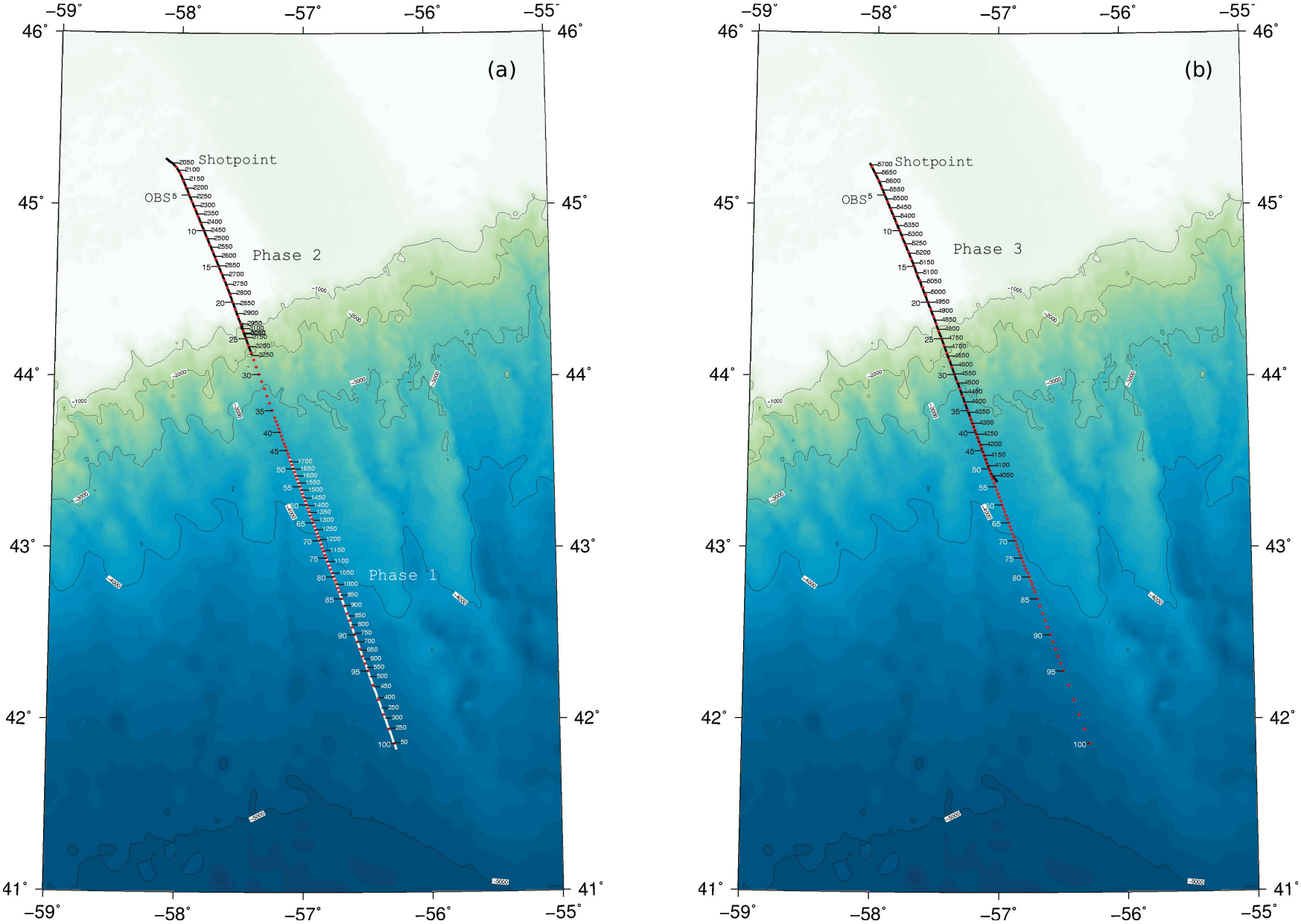

Figure 2.2. Bathymetry map showing shot profiles of (a) Phases 1 & 2 and (b) Phase 3. Red dots are deployed OBS positions. Not all OBSs were deployed during each of the phases and so most OBSs only recorded one phase of the shooting. Details of the offset coverage of each recovered OBS are in file */Dalhousie/Navigation/offset_range.txt*.

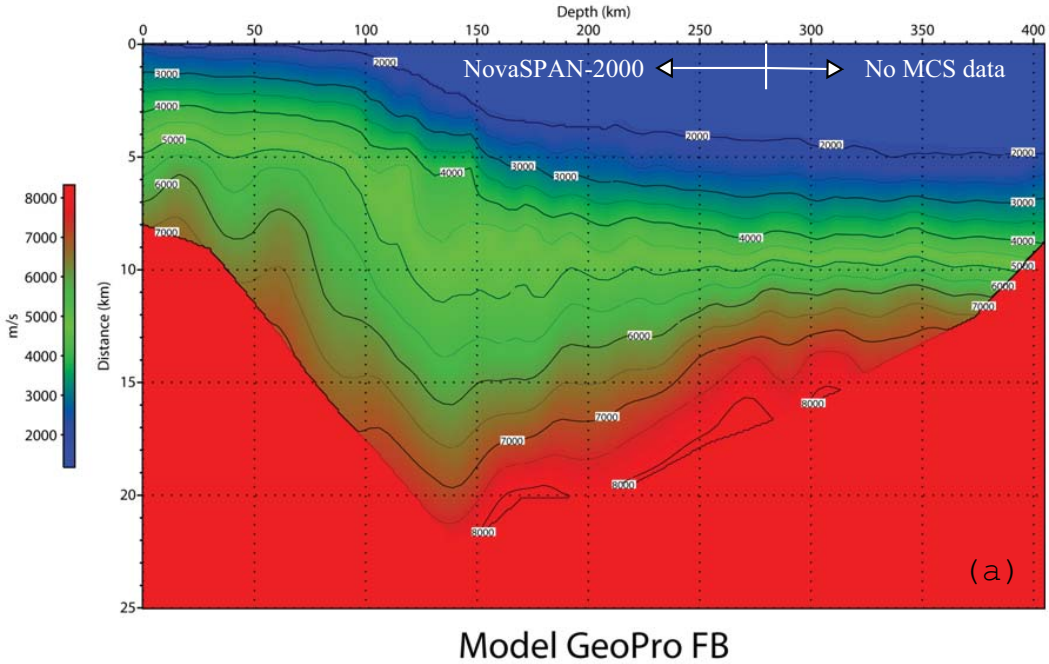

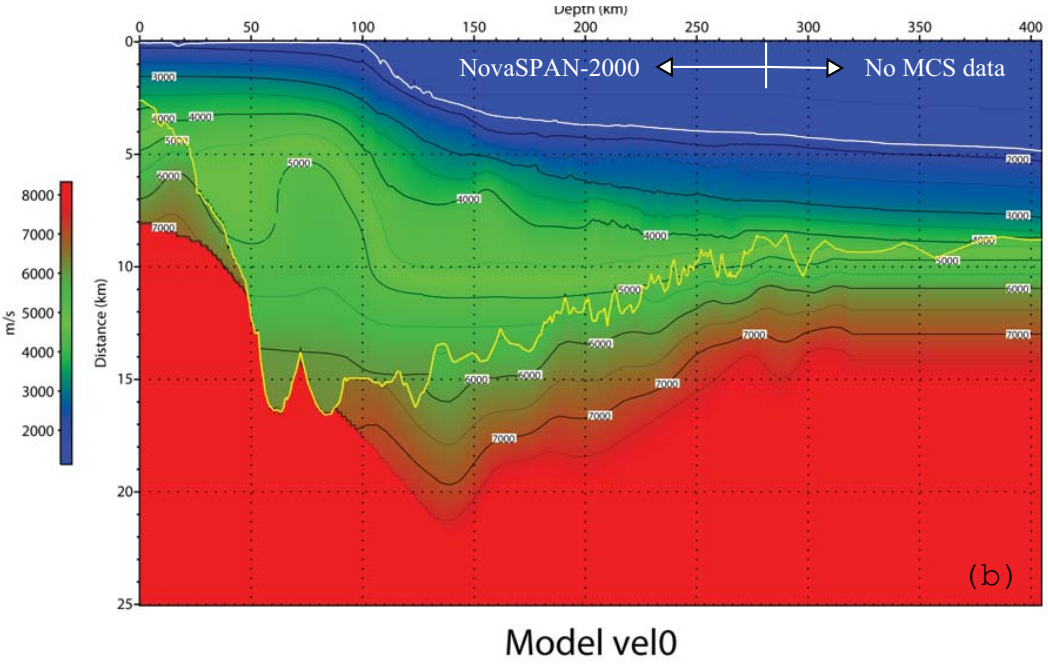

Figure 2.3. (a) Geopro first break tomography model. (b) Starting model for the FAST (First Arrival Seismic Tomography) program. Velocities above basement (yellow line) are taken from the pre-stack depth migration velocity of profile NovaSPAN-2000.

(a)

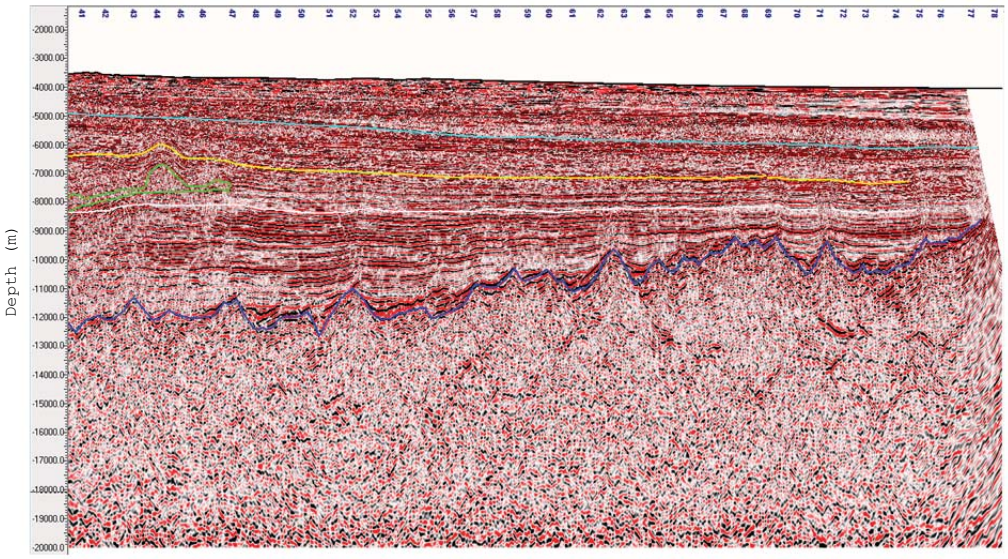

(b)

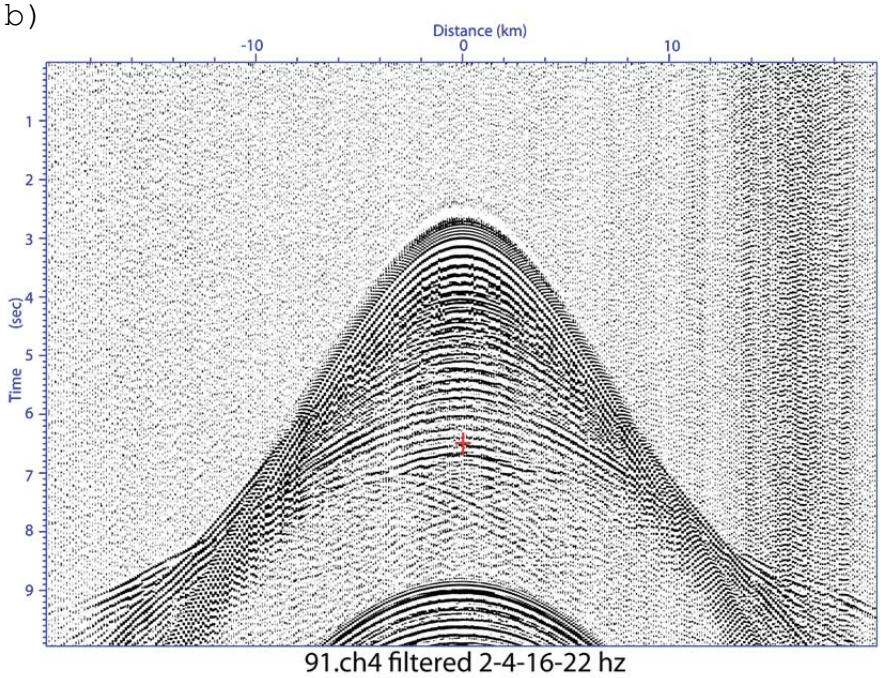

Figure 2.4. The picking of basement top on (a) profile NovaSPAN-2000 (blue line) and (b) OETR OBS data (red cross).

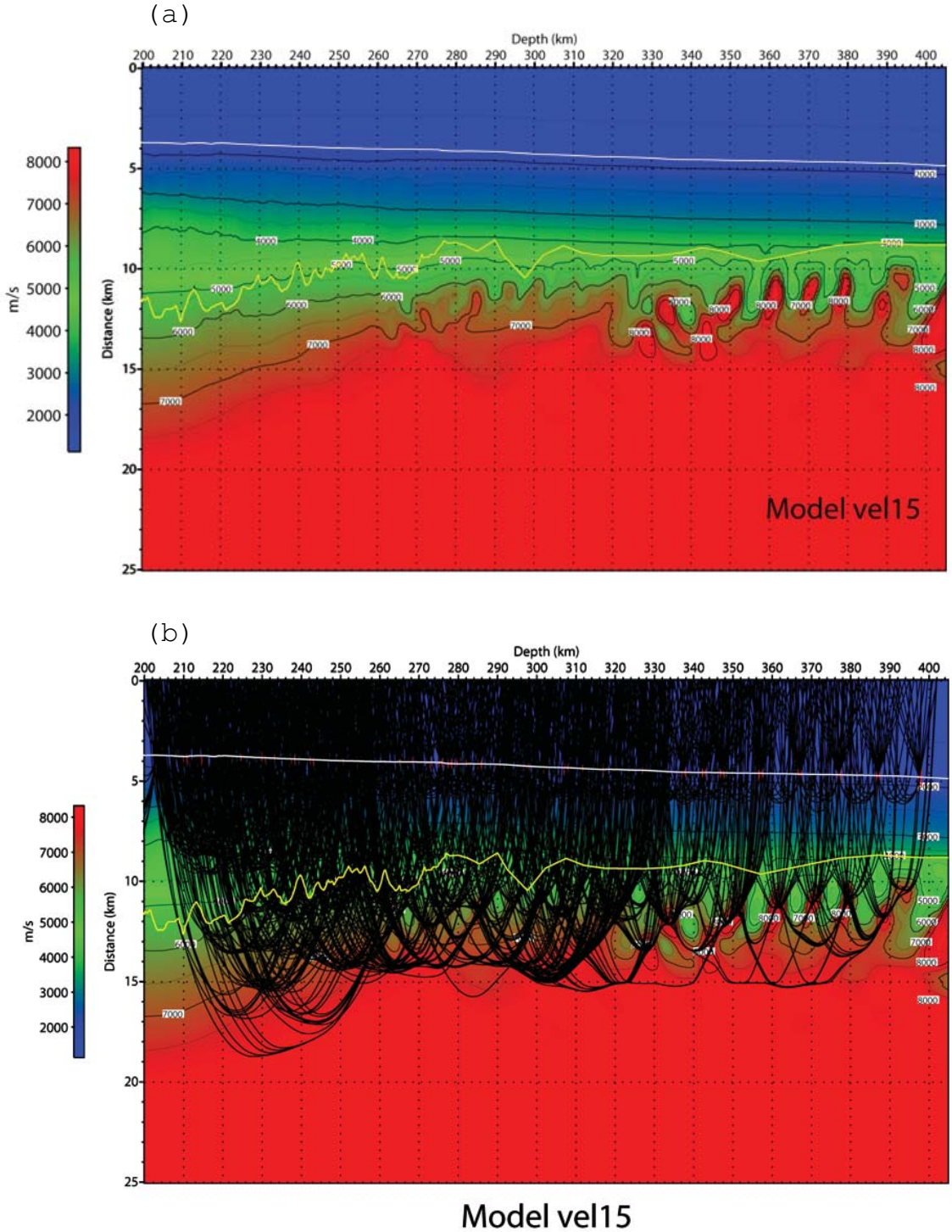

Figure 2.5. (a) Final velocity model by using FAST after 15 iterations. (b) Model overlaid with rays that constrain the inversion.

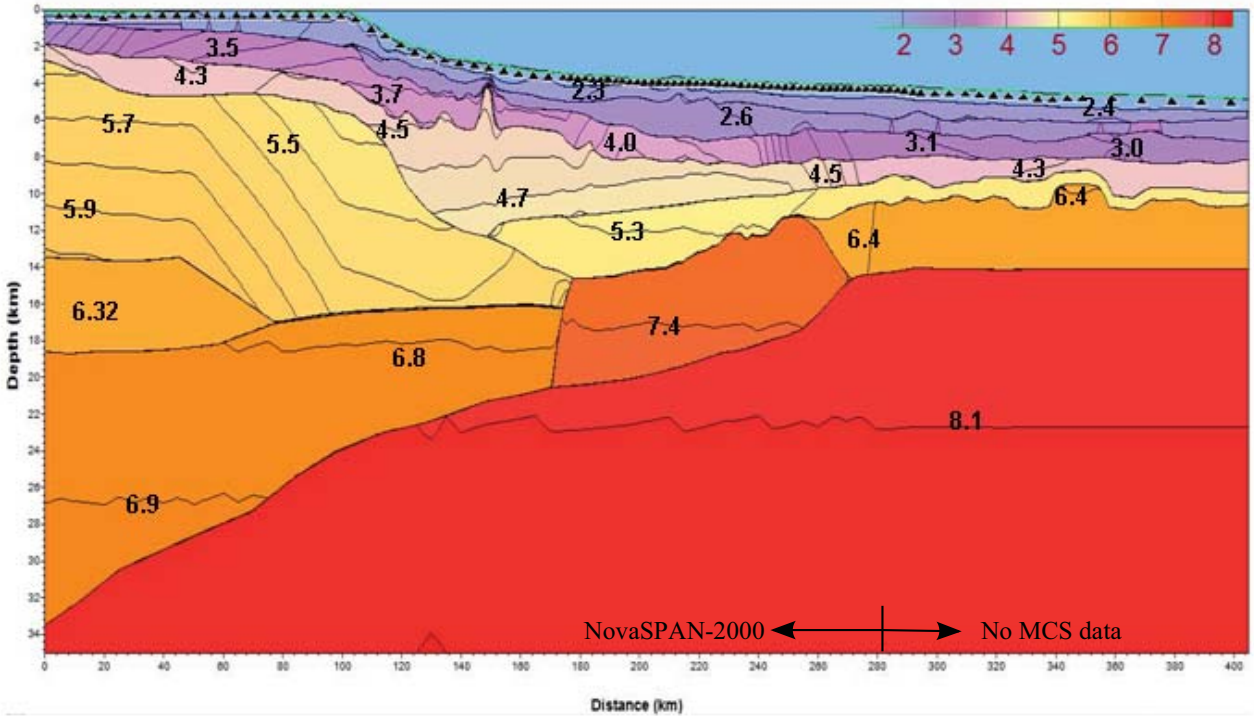

Figure 2.6. Geopro layer velocity model. Numbers in figure are p-wave velocity in km/s. The contour interval is 0.1 km/s. Triangles are OBS.

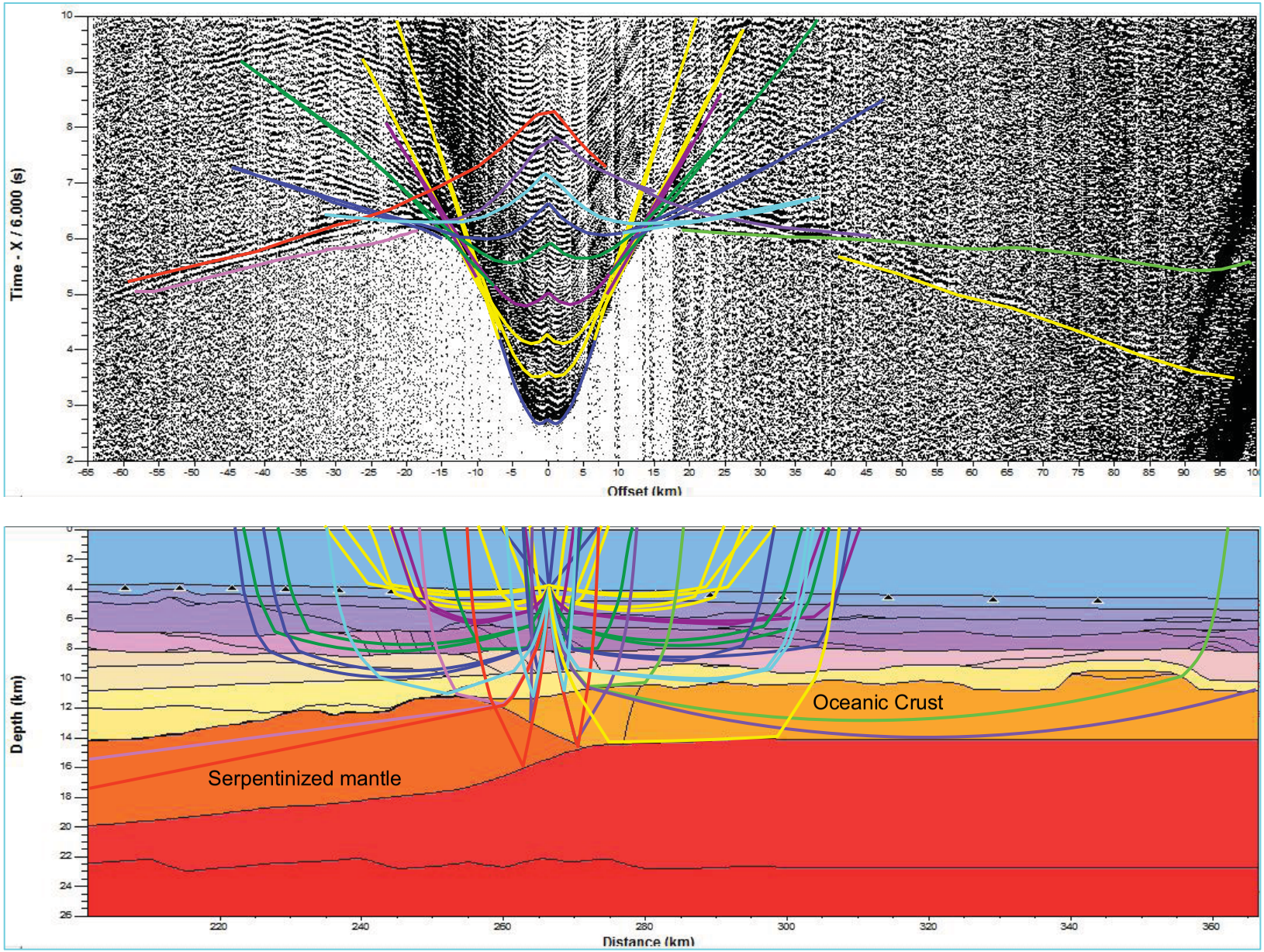

Figure 2.7. (upper panel) Common station gather (CSG) for OBS 73. Time is reduced by 6 km/s. Curves represent calculated travel times for each phases by raytracing through the Geopro layer model. (lower panel) The rays through each layer of the Geopro layer model which give rise to the travel time curves above. Phases are color coded consistently between the two plots.

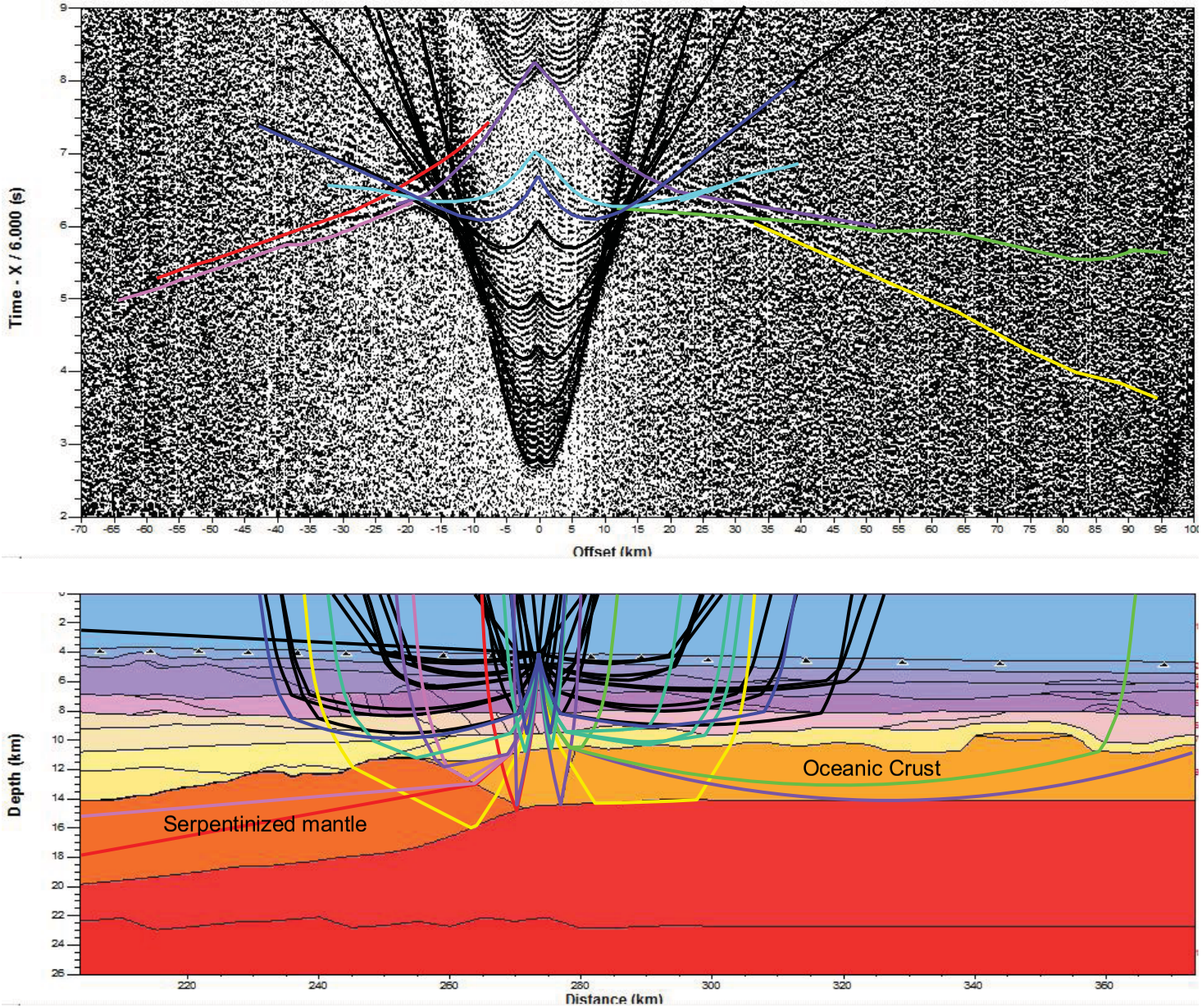

Figure 2.8. (upper panel) Common station gather (CSG) for OBS 76. Time is reduced by 6 km/s. Curves represent calculated travel times for each phases by raytracing through the Geopro layer model. (lower panel) The rays through each layer of the Geopro layer model which give rise to the travel time curves above. Phases are color coded consistently between the two plots.

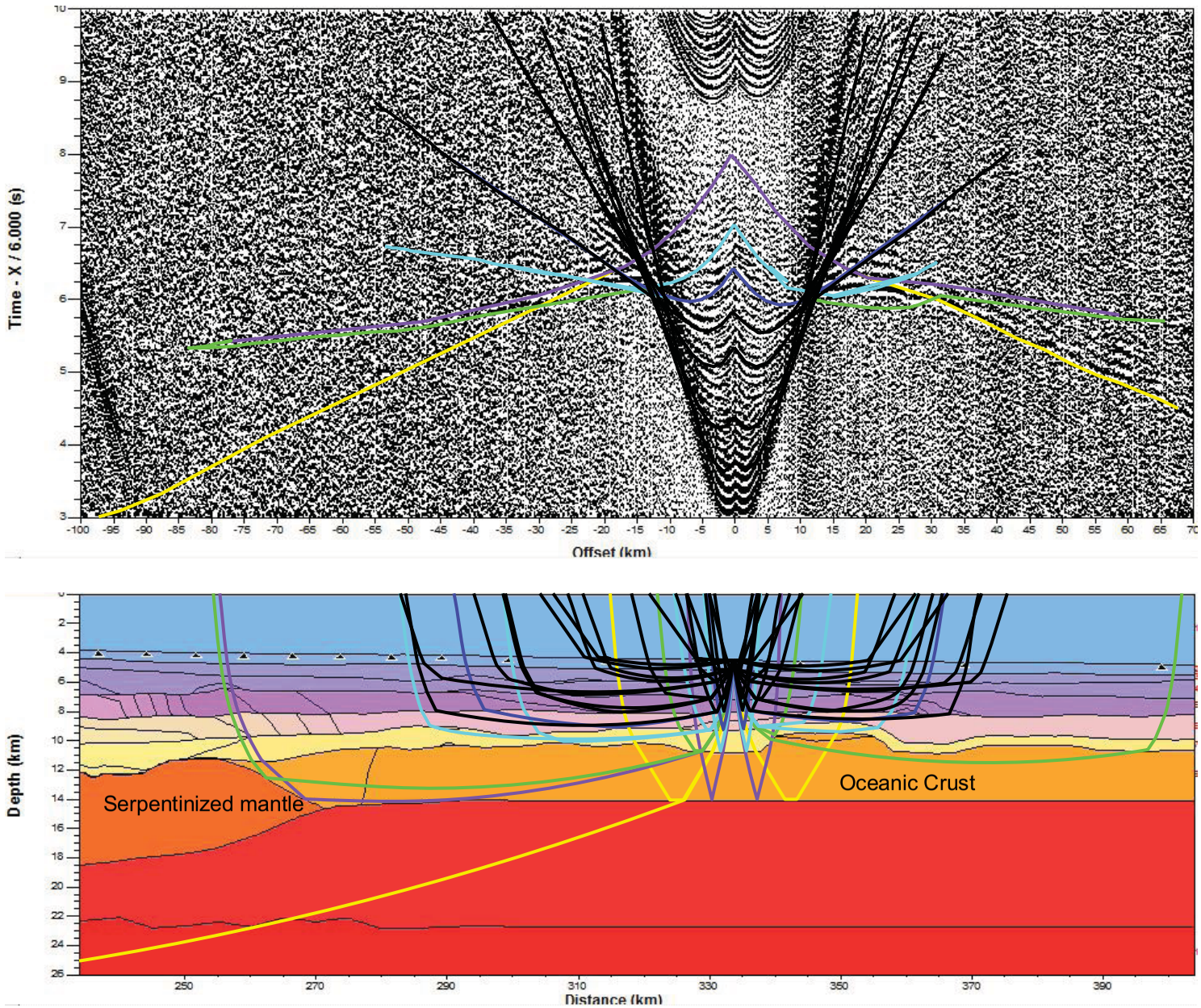

Figure 2.9. (upper panel) Common station gather (CSG) for OBS 92. Time is reduced by 6 km/s. Curves represent calculated travel times for each phases by raytracing through the Geopro layer model. (lower panel) The rays through each layer of the Geopro layer model which give rise to the travel time curves above. Phases are color coded consistently between the two plots.

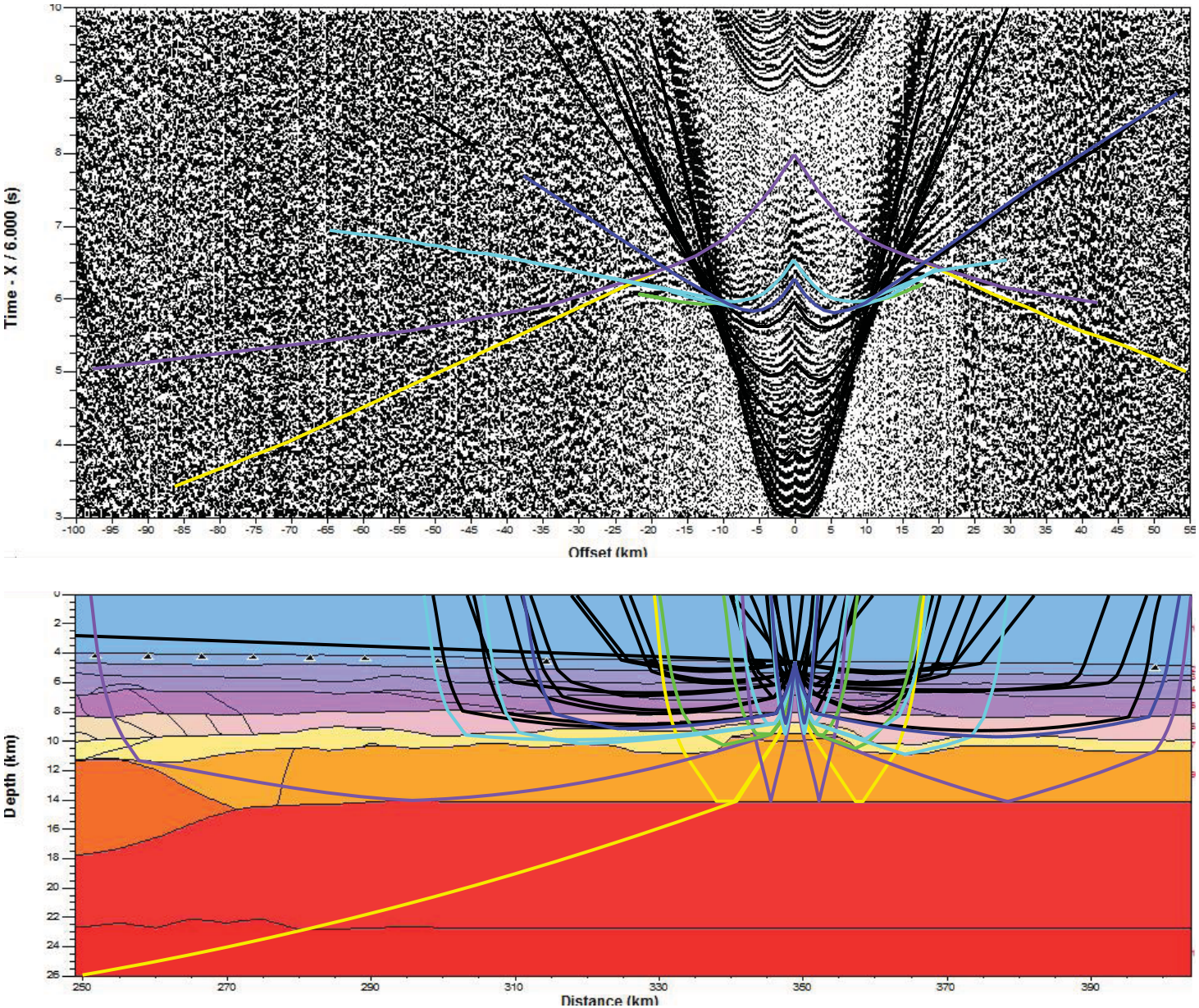

Figure 2.10. (upper panel) Common station gather (CSG) for OBS 95. Time is reduced by 6 km/s. Curves represent calculated travel times for each phases by raytracing through the Geopro layer model. (lower panel) The rays through each layer of the Geopro layer model which give rise to the travel time curves above. Phases are color coded consistently between the two plots.

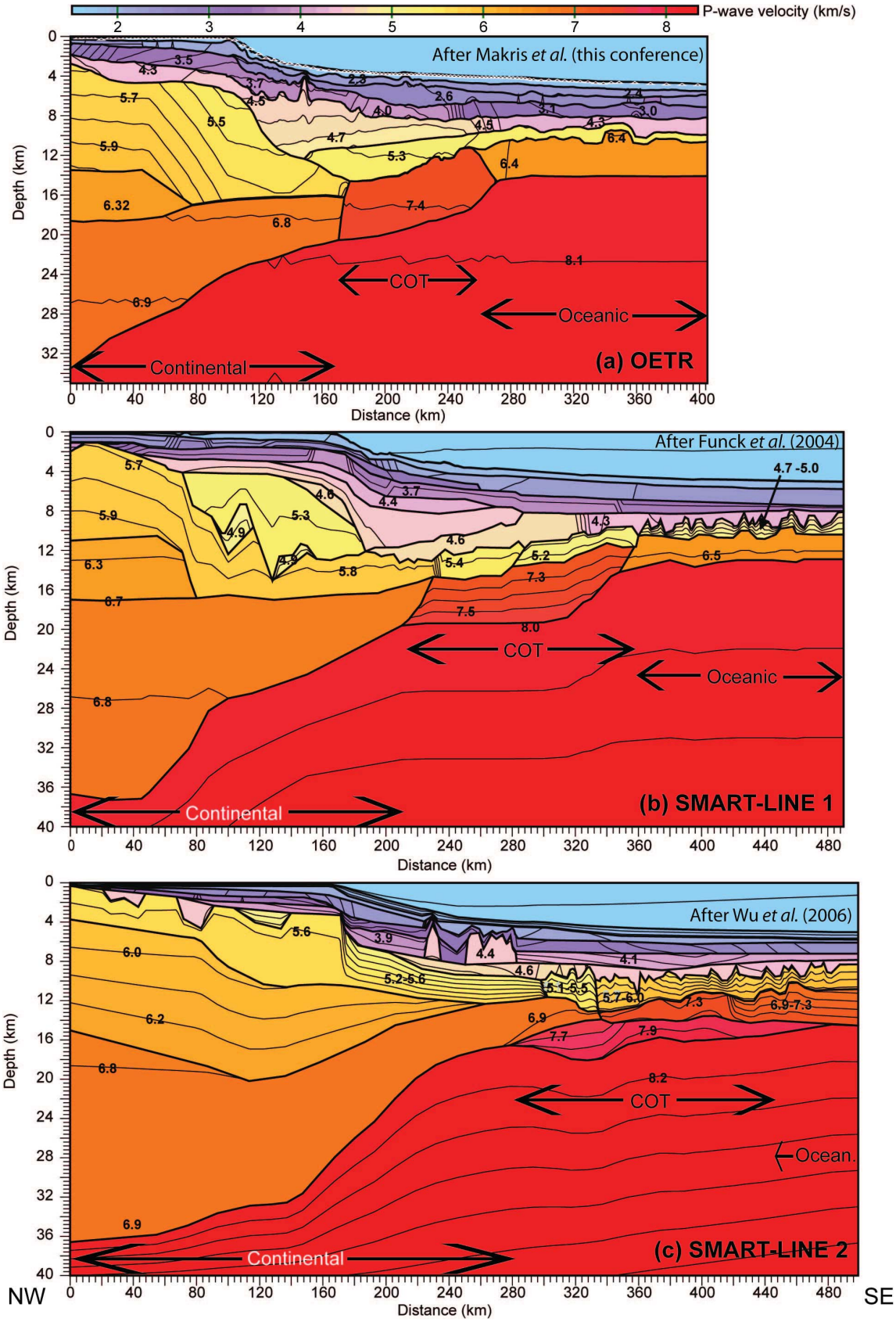

Figure 2.11. P-wave velocity models across the NE Nova Scotia margin.

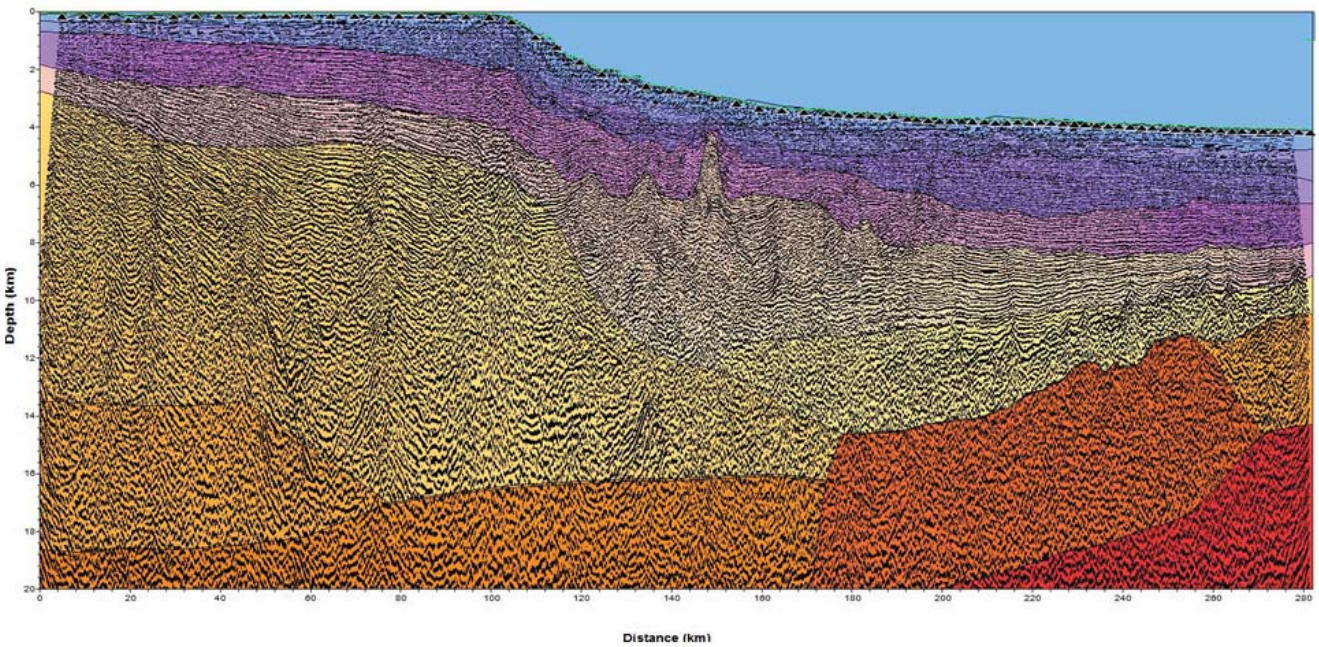

Figure 2.12. Pre-stack depth migrated section of profile NovaSPAN-2000 overlaid on Geopro layer model. Color scale is the same as in Figures 2.6 & 2.11.

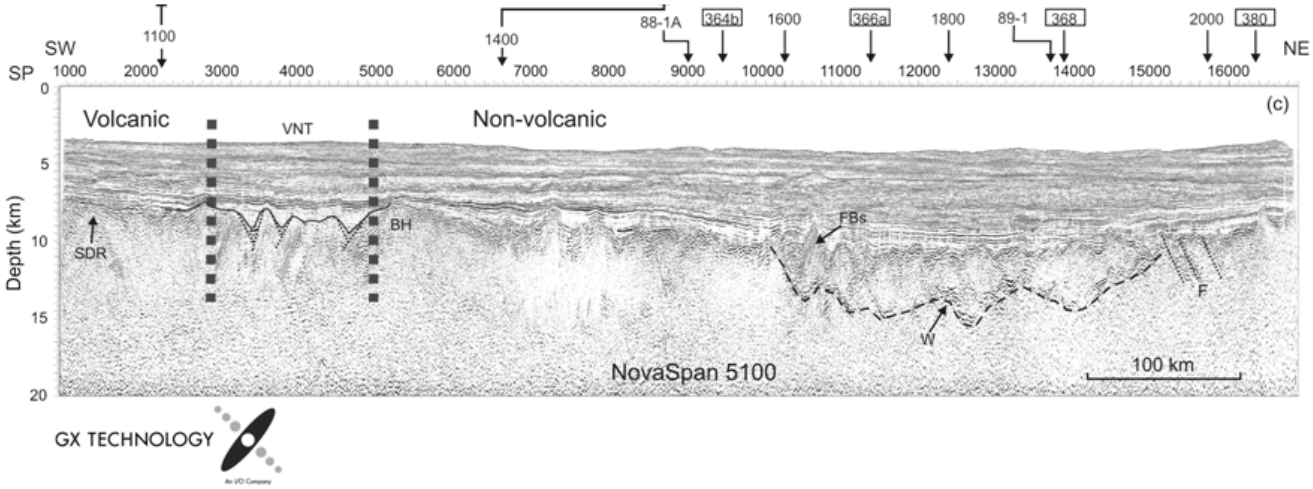

Figure 2.13. Pre-stack depth migrated section of profile NovaSPAN-5100. FB - fault block. W - a strong reflection of interest.

3. RECONSTRUCTION OF THE NOVA SCOTIA AND MOROCCO MARGINS

3.1 Introduction

Early reconstructions of the relative positions of the Nova Scotia and Morocco margin conjugates were based on geometric fits of coastlines, isobaths, seafloor spreading magnetic lineations, fracture zones, or paleomagnetic data (e.g. Bullard et al. 1965; LePichon et al. 1977; Lefort and van der Voo 1981). More recently, the slope magnetic anomalies and the relative locations of salt basins on the opposite sides were also used to match the conjugates (e.g. Klitgord and Schouten 1986; Sahabi et al. 2004). In addition, Tari and Molnar (2005) proposed a reconstruction of this margin pair by correlating the syn-rift structure based on recent seismic reflection and gravity data. Relevant plate reconstruction poles of the conjugates are listed in Table 3.1.

With the recent seismic data from the margin conjugates, the crustal structure now is better defined by detailed velocity structures. For instance across the central Nova Scotia margin, the velocity model for SMART Line 2, as well as the characteristic reflection seismic images, indicates that the continent-ocean boundary (COB) is located at the seaward edge of a series of faulted basement blocks (FB), which is ~50 km seaward of its previous interpretation (Salisbury and Keen 1993). Prestack migration of the coincident MCS data (Wu 2007) also shows that the basement changes its reflectivity pattern across the COB and therefore further supports the interpretation of the velocity model. These enhanced seismic images and more recent industry profiles (e.g. ION/GXT Nova-SPAN Project lines) across the central Nova Scotia margin demonstrate that seaward dipping reflectors (SDR) are not imaged in the basement beneath the low-amplitude East Coast Magnetic Anomaly (ECMA). The combined results of MCS data and OBS data indicate that the ECMA in this region is not caused by excessive volcanism at the COB and therefore cast doubt about the reliability of using this anomaly to reconstruct the conjugates.

The conjugate reconstructions are examined based on the new seismic processing results. This chapter begins with the reconstruction at chron M25. The conjugates are further reconstructed to pre-seafloor-spreading time based on the detailed velocity models derived from recent OBS data and the correlation with seismic reflection images, slope magnetic anomalies and salt distributions from both conjugates. The goal is to detail the formation of the Nova Scotia and Morocco conjugates from their pre-to-post-rift geometry.

3.2 Reconstruction to Chron M25

Figure 3.1 shows the reconstruction of the Nova Scotia and Morocco margin conjugates at chron M25 (Tucholke and Ludwig, 1982; Table 3.1). Magnetic anomaly M25 (155.7 Ma; Gradstein et al. 2004) is the earliest seafloor spreading magnetic anomaly that can be correlated on both sides of the conjugate margins (Klitgord and Schouten 1986; Verhoef et al. 1991). From anomaly M25 to the coasts of Nova Scotia and Morocco, until the appearance of the slope magnetic

anomalies, the seafloor is characterized by weak magnetic anomalies created during the Jurassic magnetic quiet zone (JMQZ; Vogt, 1973). Within the JMQZ, some of these weak reversal sequences were later identified as seafloor spreading magnetic anomalies prior to chron M25 along both conjugate margins (e.g. Barrett and Keen 1976; Roeser et al. 2002). However, these magnetic lineations are not continuous along the margin and can not be correlated unambiguously with each other. Therefore, ages and seafloor spreading rates older than M25 can not be determined from seafloor spreading magnetic lineations.

Figure 3.1 also shows the basement depths on both flanks of M25. The basement depth off Nova Scotia is taken from Oakey and Start (1995). The basement depth off Morocco is calculated from the bathymetry (National Geophysical Data Center, 1988) and the total sediment thickness (Divins 2007). According to this figure, the basement off Nova Scotia, particularly off Cape Breton Island, is ~5 km deeper than that around the Safi Basin off Morocco. The deep basement of the Scotian Basin may due to thick (~16 km) sediment loading, which is ~10 km thicker than the sediment fill off Morocco. The shallower basement off Morocco may have been affected by the Atlas compression in the northern region (Beauchamp et al., 1999). The wide-spread hotspot activity on the Morocco side may also have elevated the basement (Louden et al. 2004; Holik et al. 1991).

On the other hand, the basement off Nova Scotia demonstrates a gradual deepening in contrast to the basement off Morocco, which dramatically deepens offshore with dense depth-to-basement contours closely following the coastline. This indicates an asymmetry across the margin pair. The 5-km depth-to-basement contour along the Scotian margin (thick grey line) roughly follows the hinge zone based on the refraction velocity models (Dehler et al. 2003; Funck et al. 2004; Wu et al. 2006). Although this contour off Morocco is less consistent with the hinge zone (Tari and Molnar 2005), they are still close to each other from the Agadir Basin to the Safi Basin. This contour on both sides is adopted to represent the relative positions of the margin pair for further reconstructions. To restore the positions of the conjugates prior to chron M25, additional geological and geophysical information is required. This report utilizes the slope magnetic anomalies, salt distribution, and more importantly, the results of the recent seismic profiles on the opposite sides to constrain closures at continental breakup and pre-rift positions.

Figure 3.2a shows the slope magnetic anomalies (red lines) offshore Nova Scotia and Morocco. The ECMA off North America shows the distribution of positive values taken from Verhoef et al. (1996). The West African Coast Magnetic Anomaly (WACMA) consists of three components. The northeast portion, the S anomaly, is the positive anomaly taken from Roeser et al. (2002). The WACMA between 36°N and 40°N is taken from Verhoef et al. (1996). The anomaly south of 36°N (Tarfaya Basin) is digitized from the available magnetic profiles (Liger 1980), and is only shown for completeness but will not be used for further reconstruction for this margin pair. In past decades, the ECMA and WACMA were thought to mark the COB along either side of the conjugates (e.g. Roeser 1982; Klitgord and Schouten, 1986; Holik et al. 1991; Keen et al., 1991b; Keen and Potter,

1995a; Roeser et al. 2002). Based on this feature, the Nova Scotia and Morocco margins were reconstructed to continental breakup (e.g. Klitgord and Schouten, 1986; Sahabi et al., 2004), which will be presented in section 3.3.

Figure 3.2b shows the distribution of salt diapirs along the opposite sides of the conjugates (red lines). The salt limit off Nova Scotia is taken from Shimeld (2004), indicative of the distribution of autochthonous salt. The salt boundary along the Morocco margin denotes the distribution of present-day salt taken from Tari et al. (2003). Across the southern and northern portions of the margin, the seaward salt mobilization is limited based on existing MCS profiles (e.g. <10 km; Holik et al., 1991; Contrucci et al. 2004; Maillard et al. 2006). Across the central part of the Moroccan margin (near the Essaouira Basin), the salt may have mobilized ~40 km over the steepest slope area; however, the maximum salt mobilization at the seaward edge of the salt basin is estimated to be 15-20 km (Tari and Molnar 2005). Therefore, the present-day salt off Morocco is considered be autochthonous at the scale of these reconstructions. The salt basins on the opposite sides were used to indicate the relative locations of the conjugates (e.g. Sahabi et al. 2004). This study compares the distribution of autochthonous salt as a proxy for the landward and seaward limits of rifted continental crust on both sides, assuming that the salt formed in a uniform rift basin (Klitgord and Schouten 1986).

More importantly, recent wide-angle seismic refraction profiles are located across both sides of the margin conjugates (Figure 3.2). These transects extend from continental crust with full thickness into the JMQZ, almost approaching M25 where unequivocal oceanic crust exists. SMART lines S-1, S-2 and S-3 (Dehler et al. 2003; Funck et al. 2004; Wu et al. 2006) and the most recent OETR line G-1 present good coverage along the Scotian margin; while only a single refraction seismic transect, SISMAR S-4, is available across the northern Moroccan margin (Contrucci et al. 2004). Thus, no refraction data are available at the conjugate locations of SMART Lines S-2 and S-3..

Based on the velocity models derived from the modern ocean bottom seismometer (OBS) data, the seaward limit of the continental crust (SLCC) is determined by removing the oceanic basement (e.g. S-2) and exposed upper mantle (e.g. S-1, Funck et al. 2004; and G-1, see section 2). The SLCC along S-3 is interpreted half way from the landward appearance to the oceanward disappearance of the SDR sequences, assuming that the transition zone consists of half, highly-thinned continental crust and half initial oceanic crust (Dehler, personal communication, 2007). The pre-rift positions are also calculated by balancing the cross-sectional area before and after rifting. The better constrained estimations of the crustal structure across the entire margin pair provide an opportunity to re-examine and consequently, to improve the previous reconstructions.

3.3 Reconstruction to the Onset of Seafloor Spreading (Minimum Closure)

3.3.1 Minimum Closure of Klitgord and Schouten (1986)

Minimum closure is a reconstruction of a margin pair after removal of oceanic crust from both sides. Figure 3.3 shows a reconstruction of Nova Scotia and Mo-

rocco by Klitgord and Schouten (1986). It represents a minimum closure of these conjugates by rotating the NW African plate to the North American continent (Table 3.1). In this reconstruction, the SLCC along the east coast of North American plate was considered to be marked by the ECMA, which was supposed to match its counterpart, WACMA, along the NW African plate. Due to data scarcity and the weak amplitude of WACMA, this minimum closure was accomplished by placing the ECMA against the seaward edge of the NW African salt diapiric province, which was also thought to mark the oceanward limit of continental crust (Jansa and Wiedmann, 1982; Roeser et al., 2002).

To examine the fit of this minimum closure, current delineations of the WACMA and salt distribution off Morocco (Figure 3.2) were rotated to the Nova Scotia side using the pole of rotation of Klitgord and Schouten (1986). Figure 3.3a indicates that the WACMA (red) does not match very well with its counterpart ECMA (green) with an obvious longitudinal misfit of ~150 km. The overall fit of magnetic anomalies from the opposite sides can be improved by an eastward movement of the Morocco margin, as indicated by the arrow. Note that the northeast portion of the WACMA, the so-called S anomaly (Roeser et al. 2002), does not have its homologue on the Nova Scotia side and will be further discussed by correlating with results of the recent seismic data.

Figure 3.3b indicates that the distributions of salt units from the opposite sides largely overlap with each other. The autochthonous salt should indicate the original locations of the rifted basin, assuming that all autochthonous salt units from both sides formed within a uniform basin (Klitgord and Schouten, 1986). The overlap of salt distribution suggests an overlap of rifted continental crust for the closure at the SLCC. This is still true if seaward salt mobilization occurred before the continental breakup. If the salt structures on the conjugates were not deposited within a uniform basin, the exact location of the COB or SLCC can not be inferred by restoring the past positions of the salt units. However, the salt distributions from the conjugates should not overlap at the minimum closure because overlapped salt distribution suggests overlapped rifted continental crust, assuming that all autochthonous salt formed within restricted basins in the nascent Atlantic (Klitgord and Schouten, 1986; Holik et al. 1991). A better fit of the salt distributions from the conjugate margins would require less closure (indicated by an arrow).

The fit of the closure is further examined by comparing the results of recent seismic data. Figure 3.3c shows that the SLCC derived from recent OBS profiles. Across the northern part of the conjugates, SMART S-1, OETR G-1 and SISMAR S-4 are nearly conjugate to each other in this reconstruction. At this conjugate location, the continental crust derived from SMART S-1 and OETR G-1 overlaps the African continental crust. Similarly, the SLCC interpreted along S-4 (Contrucci et al. 2004) is located on the continental shelf interpreted on SMART S-1, where autochthonous salt is imaged further seaward (Shimeld 2004). Across the central and southern portions of the conjugates, the continental crust derived from S-2 and S-3 also overlaps the Moroccan continental crust, with the landward limits located at the Morocco side of the restored positions of magnetic anomalies and salt units. The overlapped continental crust also indicates less closure for the opposing sides.

The minimum closure of Tari and Molnar (2005) is based on fitting the basement embayment of the Sable sub-basin and the basement promontory off-shore Essaouira. The pole of rotation is similar to that of Klitgord and Schouten (1986). The misfit of the slope magnetic anomalies and salt distributions and overlapping of continental crust in this reconstruction will be similar to that seen above. Therefore, less closure should also be suggested as a minimum closure for this conjugate.

3.3.2 Minimum Closure of Sahabi et al. (2004)

To improve the fit of the minimum closure above, Sahabi et al. (2004) proposed a reconstruction by fitting the magnetic anomalies and salt basins from the conjugate sides (Figure 3.4). In this case, both the ECMA and WACMA are still thought to mark the COBs (i.e. SLCC in this case) along both margins. One difference for this closure is that the conjugate margins are less closed compared to the closure of Klitgord and Schouten (1986). The other difference is that the WACMA is divided at a position near the Agadir Basin into a southern portion and a northern portion, which are rotated to fit the ECMA using separate poles of rotation (Table 3.1). The main purpose of a separate rotation for the northern part is to account for the younger Atlas compression (Beauchamp et al. 1999) and to improve the overall fit with ECMA.

Figure 3.4a demonstrates an improved fit of the WACMA and ECMA. The WACMA presents an almost identical shape to the ECMA, with a slight overlap across the SW Nova Scotia margin. A problem for this fit is that the S anomaly does not have a clear homologue on the Nova Scotia side, which casts doubt about the reliability of using this anomaly to constrain the minimum closure of the margin pairs. If the S anomaly is generated by the SLCC, similar magnetic anomalies should be observed on the Scotian side. Lack of a magnetic homologue for the S anomaly indicates that this anomaly may not mark the SLCC. The recent refraction velocity models also show that the high-amplitude ECMA across the SW Scotian margin along S-3 roughly coincides with the SLCC. However, the low-amplitude ECMA from SMART S-2 (Wu et al. 2006) to S-1 (Funck et al. 2004) does not represent the location of the SLCC. Therefore, the magnetic anomalies from the central part of the conjugates to the north should not be used to match the seaward termination of the continental crust.

Figure 3.4b shows the restored salt distributions from the conjugate sides. Across the southwest conjugate locations, the salt limits fit very well. Across the northeastern-most conjugate locations, the salt limits still overlap with each other (e.g. along SISMAR S-4), suggesting less closure at the time of continental breakup. Hence, a separate rotation, which is intended to improve the fit of magnetic anomalies, is not required for this part of the conjugates. Across the central margin conjugates (from S-2 to S-1), a gap exists between the seaward limits of the salt. Since the autochthonous salt across the southwest and northeast conjugate locations is well defined by MCS profiles (Holik et al., 1991; Contrucci et al. 2004; Maillard et al. 2006), the misfit for the central conjugates suggests that the salt structures from the opposing sides may not form within a uniform basin. Alternatively, salt may form in one rifted basin but it

may be truncated over basement highs during syn-rift times, such as some area of the Tafelney Plateau off Morocco that is conjugate to the central Nova Scotia margin (Molnar et al. 2002).

The SLCCs derived from recent OBS profiles are projected onto this closure (Figure 3.4c). Although the fit of continental crust for the central and southern conjugate locations are not constrained by OBS data on the Morocco side, the SLCCs interpreted along S-2 (Wu et al., 2006) and S-3 (Dehler, personal communication, 2007) are close to the matched magnetic anomalies (grey lines). Across the northern part of the conjugates, the seismically derived continental crust overlaps with each other for more than 100 km, unless this part of the margin separated along a transform zone. However, this seems to be unlikely because the SLCC (short dashed line) derived from S-4 is situated on the Nova Scotia shelf, where extensive autochthonous salt is observed (Figure 3.4b; Shimeld, 2004). The overlapped continental crust from the opposite sides also suggests less closure, which is consistent with the implications derived from the overlap of oceanward salt limits. Therefore, a separate rotation for the northern part of the conjugates is not required.

3.3.3 A Modified Minimum Closure

A modified minimum closure is suggested below based on the combined correlation of magnetic anomalies, salt limits, and seismic results. For this modified closure, the southern and northern conjugate locations are fit by different types of constraints. Across the southern conjugate locations, no OBS data are available on the Morocco side. However, this part of the conjugates is volcanic and the slope magnetic anomaly is directly related with rifting volcanism (Keen and Potter 1995a). The ECMA on the Nova Scotia side has been modeled as a result of extrusives evidenced by SDR sequences that occupy the seaward end of the rifted continental crust (Alsop and Talwani 1984; Dehler, et al. 2003). Therefore, the slope magnetic anomalies from the opposite sides are still utilized to fit the southern part of the conjugates.

For the northern conjugate locations, the minimum closure is constrained by seismic results derived from the recent OBS profiles S-1, G-1 and S-4. However, the COB or SLCC along S-4 is previously based on the location of the S anomaly. This relationship of the SLCC and the S anomaly is re-examined in the velocity model and adjacent MCS data. Figure 3.5a shows the original and revised velocity models along S-4. No major velocity boundary or significant velocity variation is observed across the S anomaly (Contrucci et al., 2004; Sibuet, personal communication, 2010). Rather, the main change in basement velocity occurs further landward where the velocities decrease. We also observed that along both SMART S-1 and S-2 off Nova Scotia, the thinned continental crust extends ~50 km seaward of the ECMA (Funck et al. 2004; Wu et al. 2006). This suggests that the S anomaly, or even most of the WACMA in this region, does not mark the COB or SLCC on the Morocco margin.

Figure 3.5b shows the seismic image for a perpendicular MCS profile SISMAR 10 (see Figure 3.2 for location). According to this profile, the continental crust pinches out against a northeast dipping reflector L (Maillard et al. 2006), and its seaward limit, based on this profile, has been delimited by the last occurrence of salt. This seismic image shows

that the S anomaly is about 30-40 km further seaward of the SLCC and obviously related with a basement high underneath and therefore, it does not mark the COB or SLCC. Similar seismic images with salt diapiric structure are observed along S-4 (Contrucci et al., 2004; Maillard et al. 2006), suggesting that the SLCC should also be delimited by the last salt diapir (SLCC' between OBS 8 and 9, Figure 3.5b). This re-interpretation is supported by the velocity model where strong lateral gradients are present landward of the salt unit but vanish seaward of the salt structure, consistent with a transition from continental crust to oceanic crust.

With the above constraints, the modified reconstruction is represented in Figure 3.6. The pole of rotation of this reconstruction is same as that of Sahabi et al. (2004) for the southern part of the conjugates (Table 3.1), but only one rotation is required to reconstruct the entire Morocco margin with its conjugate Nova Scotia margin. This produces a reduced closure for the northern conjugate locations, but the same fit as that of Sahabi et al (2004) for the central and southwestern conjugate segments.

In this reconstruction, the ECMA and WACMA fit very well across the southern conjugates, but they start to separate from the central part of the conjugate to the north (Figure 3.6a), indicating a change in character across the central margin segment. The salt limits from the opposite sides fit very well across the southern and northern parts of the conjugates respectively (Figure 3.6b). A gap still exists between the restored salt distributions across the middle part of the conjugates. This gap may be due to the basement highs that lack salt deposition during syn-rift time, such as the faulted basement blocks off Nova Scotia and the Tafelney plateau off Morocco. With the re-interpretation of SLCC (SLCC', Figure 3.6c) along S-4, the continental crust across the northern margin conjugates are matched with each other.

3.4 Reconstruction to Pre-Rift Position (Maximum Closure)

3.4.1 Maximum Closure of Klitgord and Schouten (1986)

Maximum closure is a reconstruction of a margin pair to the pre-rift position after removal of extended continental crust from both sides. Reconstruction to the pre-rift position requires the estimation of the landward limit of crustal extension. Klitgord and Schouten (1986) used the landward edge of the rifted basins to represent the pre-rift positions, from which the pole of rotation was calculated (Table 3.1). Their maximum closure of the Nova Scotia and Morocco margin conjugates is presented in Figure 3.7.

With the recent wide-angle seismic refraction data carried out on both sides of the conjugates, the landward limits of crustal extension can be better estimated from the well-defined velocity models by balancing the cross sectional area before and after rifting, assuming that the continental material is volumetrically conserved. The pre-rift position is obtained from the total cross sectional area of continental crust, including the rifted portion, divided by the thickness of unstretched continental crust. The calculated pre-rift positions are projected onto the maximum closure. Across the northern part of the conjugates, the SMART S-1 and S-4 were exactly conjugate to each other at the pre-rift position. According to this projection, the interpreted continental crust with full thickness from

the opposite sides still overlaps more than 50 km, indicating the maximum closure should be placed further apart about 50 km. Unfortunately, there are no refraction seismic lines available so far at the conjugate locations of S-2 and S-3.

3.4.2 A Modified Maximum Closure

An alternate reconstruction to the pre-rift positions is determined so as to eliminate the overlapping of continental crust. Section 3.3 demonstrated that the modified minimum closure of Sahabi et al. (2004) improved the correlation of the seismically derived results as well as the slope magnetic anomalies and salt distributions from both sides of the conjugates. Using this modified minimum closure as starting point (Figure 3.8a), the conjugates are further reconstructed to match the full thickness continental crust on both sides (Figure 3.8b), assuming a constant pole of rotation from the initial rift to final continental breakup. In the modified maximum closure, the transect S-4 is more closely conjugate to G-1 than S-1, although both S-1 and G-1 contain similar structures. The overlapped continental crust in the closure of Klitgord and Schouten (1986; Figure 3.7) is eliminated by a reduced closure. The reconstruction pole for this maximum closure is shown in Table 3.1. This maximum closure may be further constrained if additional OBS transects become available across the central and southern Morocco margin.

3.5 Conclusions

A number of reconstructions of the Scotian/Moroccan margin conjugates have been re-examined based on the latest results derived from the recent seismic refraction and reflection data, as well as magnetic and salt distribution from both sides of the conjugates. The seismic data show that the pre-rift full thickness continental crust overlaps in the maximum closure determined by Klitgord and Schouten (1986). A new maximum closure of this margin pair is suggested by eliminating the overlapped pre-rift full thickness continental crust between the northern margin conjugates.

The minimum closure of Sahabi et al. (2004) improved the fit of the two sides of the margin pair compared to that of Klitgord and Schouten (1986); however, the S magnetic anomaly off NW Morocco does not have a clear homologue offshore Nova Scotia. In addition, velocity models of refraction data show that the rifted continental crust still overlaps in the minimum closure after two separate rotations of the southern and northern Morocco margin. A modified minimum closure is suggested so as to eliminate the overlapped rift crust across the northern margin conjugates. This proposed minimum reconstruction is similar to the rotation of Sahabi et al. (2004) for the southern portion of the conjugates, but no additional rotation is required for the northern part of conjugates. This minimum reconstruction also improved the correlation of magnetic anomalies and salt distribution from the opposing sides of the conjugates.

The final reconstructions shown in Fig. 3.8 demonstrate two first-order patterns to the geometry of the continental rifting.

(a) There is a major asymmetry between the Nova Scotian and Moroccan conjugate structures in the northeastern section. The Nova Scotia margin shows a very wide region of extended crust, while the Moroccan side shows a narrow region.

(b) No major discontinutities exist in large-scale structures along the margin conjugates from the beginning to the end of rifting. However, further comparison of conjugate reflection profiles need to be made using these reconstructions in order to define possible second-order variations. Such variations are suggested by the termination of the volcanic sequences north of S-3 that may be coincident with changes in the salt basins, and by the presence of the large tilted fault blocks observed on several profiles near S-2 that may be linked to similar structures on the Tafalney Plateau (Wu 2007).

Table 3-1 Plate reconstruction poles of the NW African plate (Morocco) relative to the North American plate.

Closure	Age (Ma)**	Latitude	Longitude	Angle of rotation	Reference*
M25	156	66.7°	-15.85°	-64.9°	[1]
Minimum	175	66.97°	-12.34°	-74.57°	[2]
	195	64.31°	-15.19°	-77.09° (south)	[3]
		66.31°	-11.78°	-72.59° (north)	
	N/A	66.92°	-12.45°	-74.42°	[4]
	N/A	66.92°	-12.45°	-74.42°	[5]
	167	64.31°	-15.19°	-77.09°	[8]
Maximum	175	66.95°	-12.02°	-75.55°	[2]
	N/A	67.6°	-14.0°	-74.8°	[6]
	N/A	66.95°	-13.35°	-76.74°	[7]
	176	64.31°	-15.19°	-80.58°	[8]

* [1] Tucholke and Ludwig (1982), [2] Klitgord and Schouten (1986), [3] Sahabi et al. (2004), [4] Tari and Molnar (2005), [5] LePichon et al. (1977), [6] Bullard et al. (1965), [7] Lefort and van der Voo (1981); [8] Wu (2007).

** Ages for the modified minimum and maximum closure [8] are determined from chron M25 (155.7 Ma; Gradstein et al. 2004) using a spreading rate of 1.9 cm/y (Klitgord and Scouten 1986). The ages for the remaining minimum or maximum closures come from the original references [2] and [3].

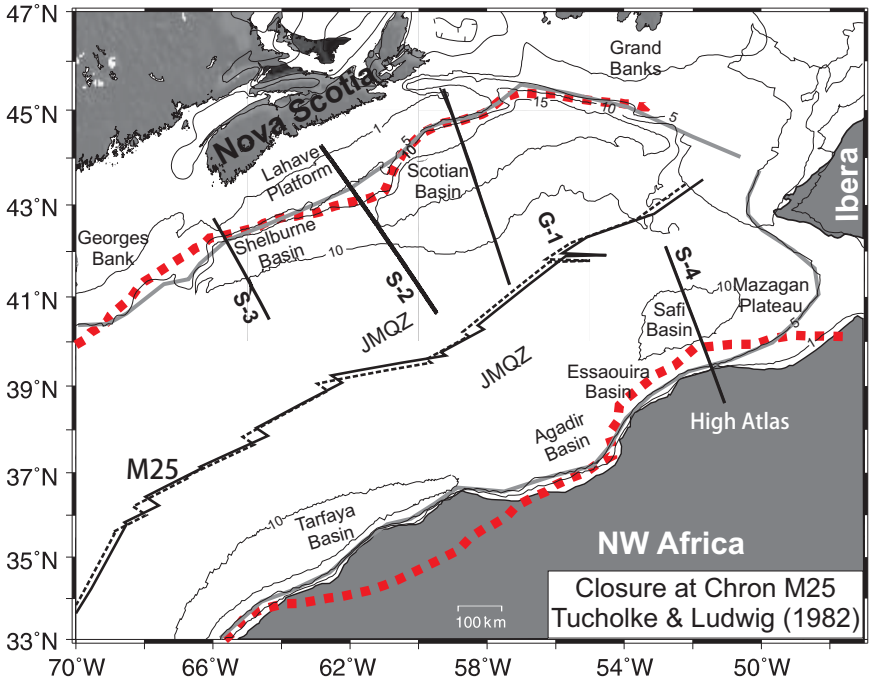
47˚N
45˚N
43˚N
41˚N
39˚N
37˚N
35˚N
33˚N
70˚W
66˚W
62˚W
58˚W
54˚W
50˚W
Grand Banks
Nova Scotia
Lahave Platform
Scotian Basin
Georges Bank
Shelburne Basin
S-3
S-2
G-1
S-4
Mazagan Plateau
Safi Basin
JMQZ
JMQZ
Essaouira Basin
Agadir Basin
High Atlas
Ibera
M25
Tarfaya Basin
NW Africa
100 km
Closure at Chron M25
Tucholke & Ludwig (1982)

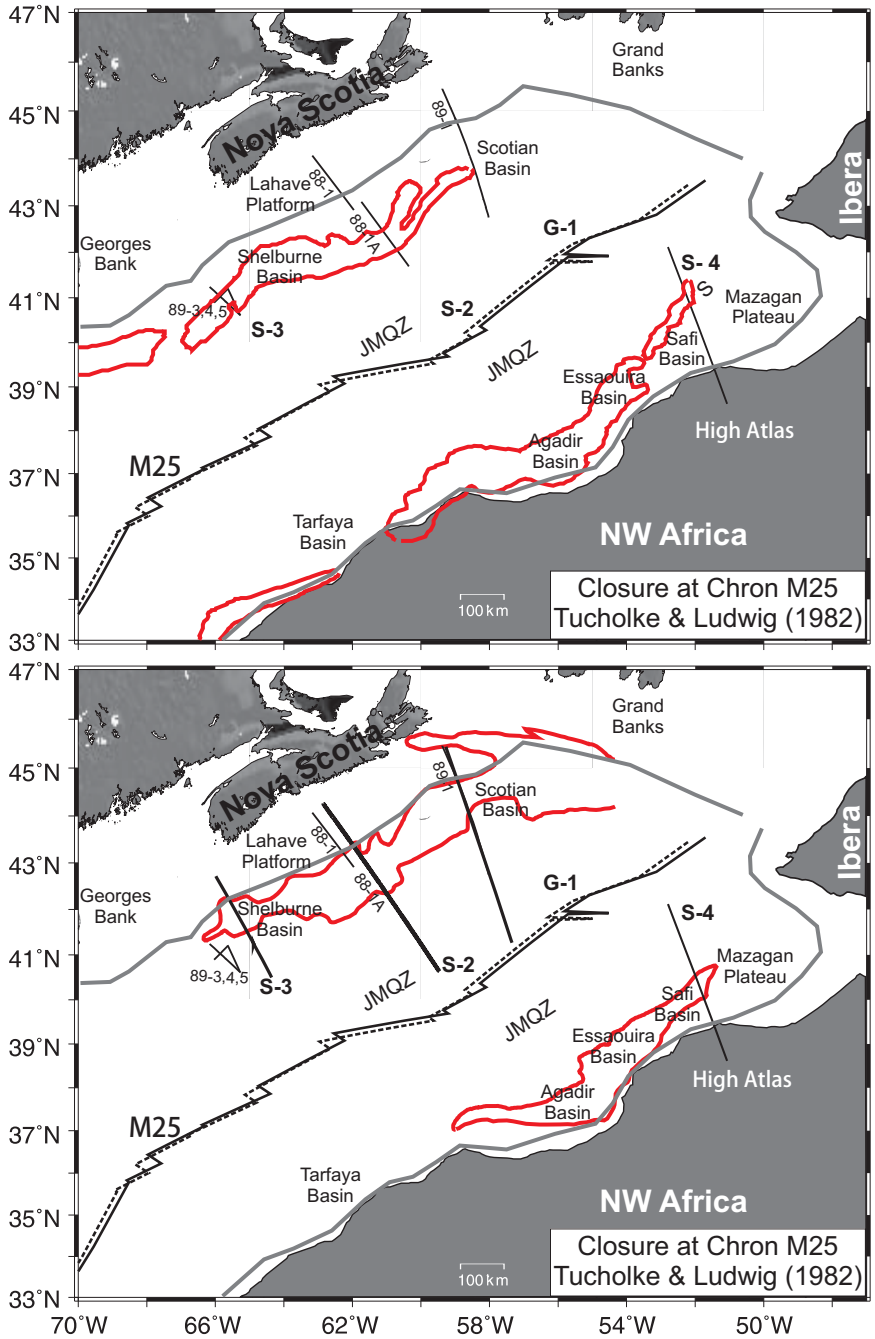
47˚N
45˚N
43˚N
41˚N
39˚N
37˚N
35˚N
33˚N
70˚W
66˚W
62˚W
58˚W
54˚W
50˚W
Nova Scotia
Grand Banks
Scotian Basin
Lahave Platform
Georges Bank
Shelburne Basin
89-3,4,5
S-3
S-2
G-1
S- 4
Mazagan Plateau
Safi Basin
Essaouira Basin
Agadir Basin
High Atlas
Ibera
JMQZ
M25
Tarfaya Basin
NW Africa
100 km
Closure at Chron M25
Tucholke & Ludwig (1982)

(a)

47˚N
45˚N
43˚N
41˚N
39˚N
37˚N
35˚N
33˚N
70˚W
66˚W
62˚W
58˚W
54˚W
50˚W
Nova Scotia
Grand Banks
Scotian Basin
Lahave Platform
Georges Bank
Shelburne Basin
89-3,4,5
S-3
S-2
G-1
S-4
Mazagan Plateau
Safi Basin
Essaouira Basin
Agadir Basin
High Atlas
Ibera
JMQZ
M25
Tarfaya Basin
NW Africa
100 km
Closure at Chron M25
Tucholke & Ludwig (1982)

(b)

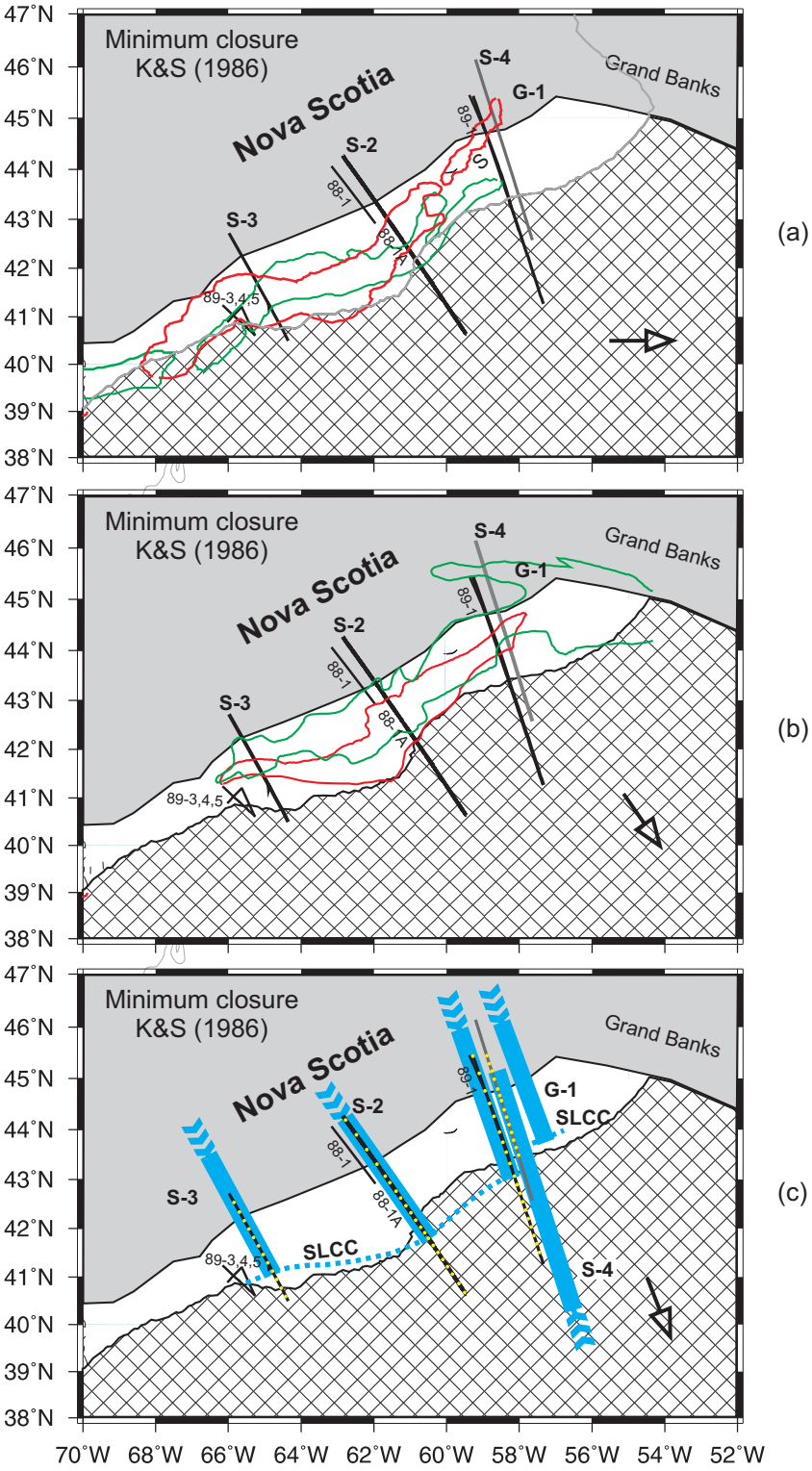
Minimum closure
K&S (1986)
Nova Scotia
Grand Banks
S-4
G-1
S-2
S-3
89-1
88-1
88-1A
89-3,4,5
SLCC
(a)
(b)
(c)
47˚N
46˚N
45˚N
44˚N
43˚N
42˚N
41˚N
40˚N
39˚N
38˚N
70˚W
68˚W
66˚W
64˚W
62˚W
60˚W
58˚W
56˚W
54˚W
52˚W

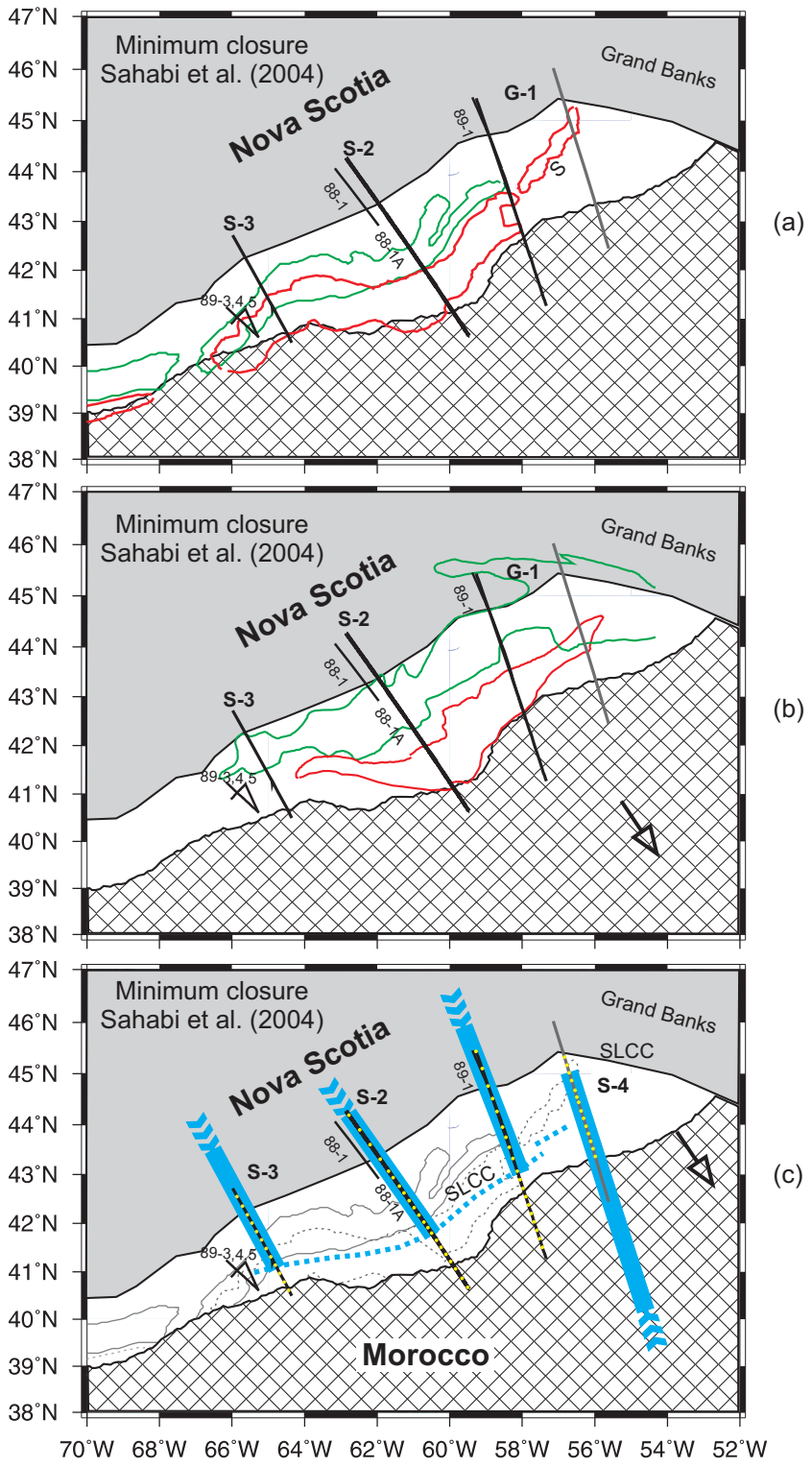
Minimum closure
Sahabi et al. (2004)
Nova Scotia
Grand Banks
G-1
S-2
S-3
S-4
89-1
88-1
88-1A
89-3,4,5
S
SLCC
Morocco
(a)
(b)
(c)
47˚N
46˚N
45˚N
44˚N
43˚N
42˚N
41˚N
40˚N
39˚N
38˚N
70˚W
68˚W
66˚W
64˚W
62˚W
60˚W
58˚W
56˚W
54˚W
52˚W

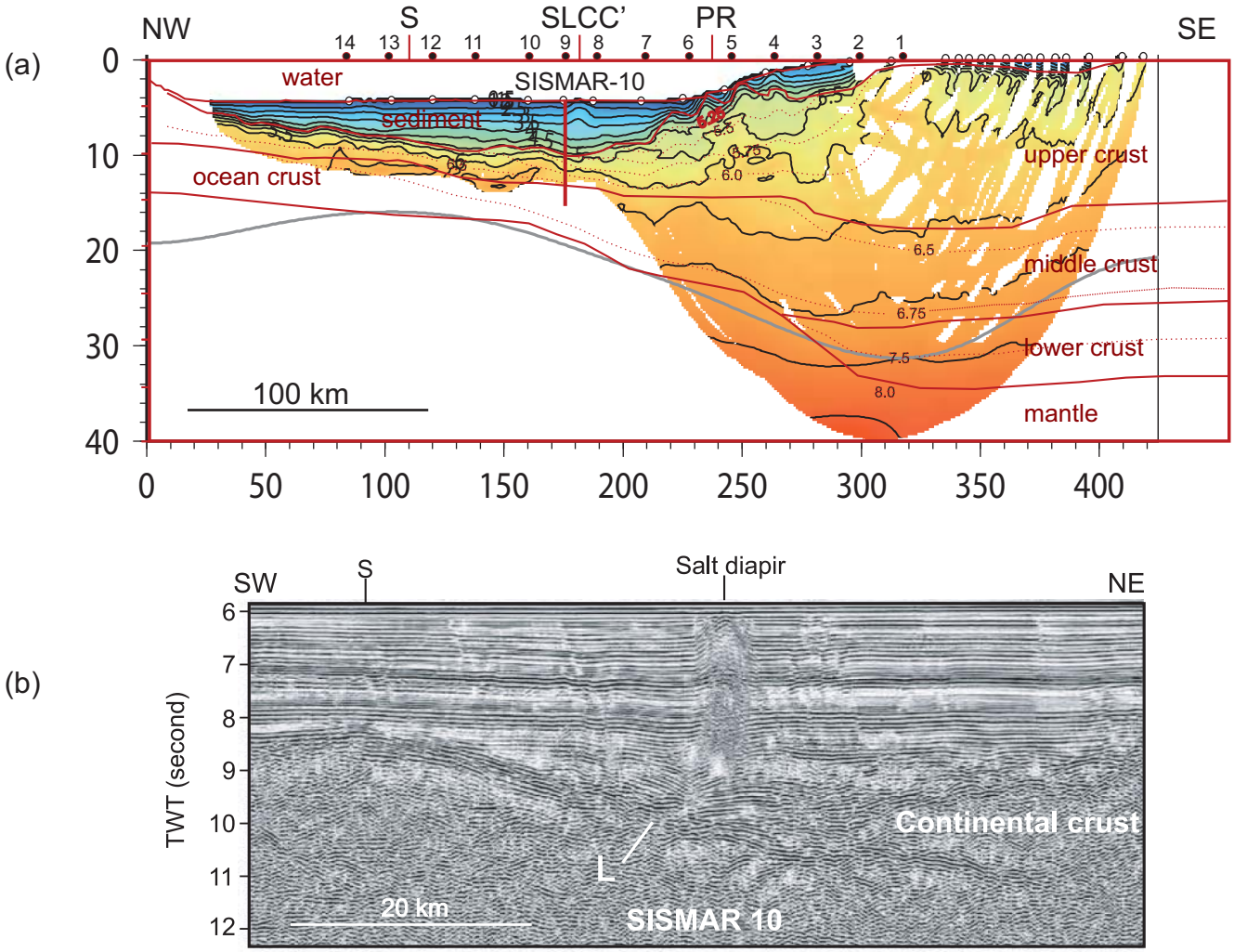

Figure 3.5. (a) Original and revised velocity models along SISMAR 4. The red lines indicate the original velocity contours (dotted lines in km/s) and crustal bouondaries (solid lines) of Contrucci et al. (2004). The colours and solid black lines indicate the revised model of J.-C. Sibuet (personal communication, 2010). The filled circles above the velocity model mark the locations of OBS instruments, labelled by numbers. S denotes the location of S anomaly, which was thought to represent the COB. SLCC' is the seaward limit of continental crust re-interpreted from the combined results of velocity structure and seismic image. PR: pre-rift position. (b) The seismic image of MCS profile SISMAR 10 (Maillard et al. 2006). Its location is shown in Figure 3.2, and also indicated by a vertical bar below OBS 9 in (a). L: landward dipping reflector.

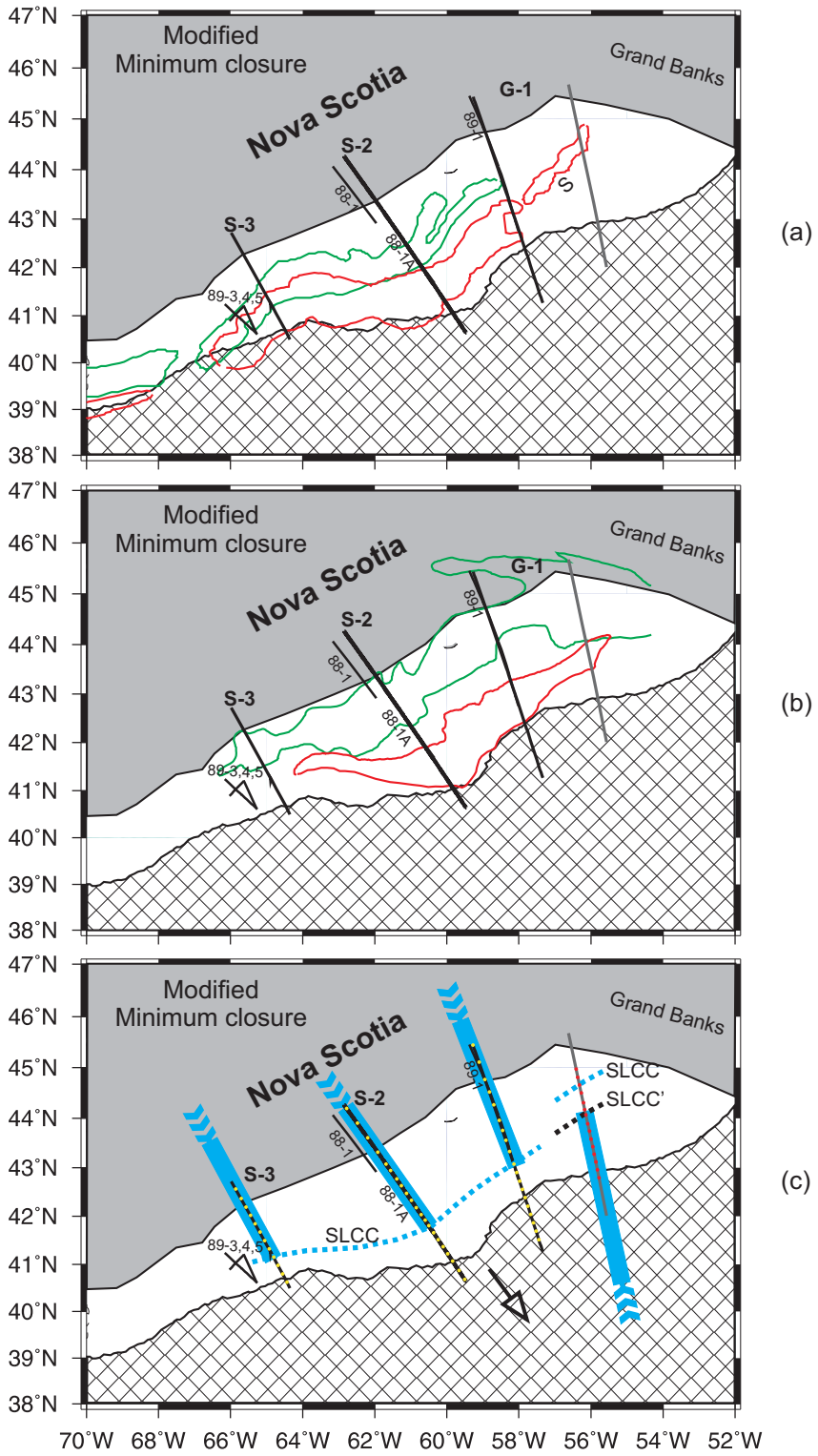
Modified
Minimum closure
Nova Scotia
Grand Banks
G-1
S-2
S-3
89-1
88-1
88-1A
89-3,4,5
S
(a)
(b)
(c)
SLCC
SLCC'
47°N
46°N
45°N
44°N
43°N
42°N
41°N
40°N
39°N
38°N
70°W
68°W
66°W
64°W
62°W
60°W
58°W
56°W
54°W
52°W

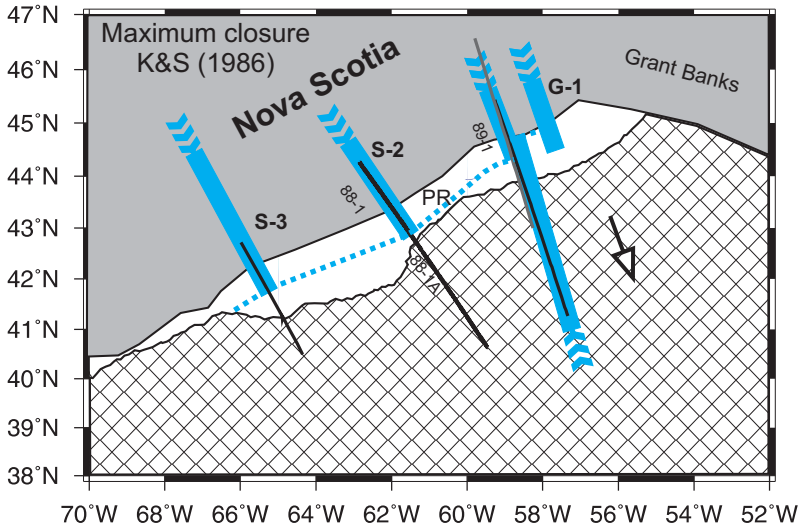
Maximum closure
K&S (1986)
Nova Scotia
Grant Banks
S-3
S-2
G-1
88-1
88-1
88-1A
PR
47˚N
46˚N
45˚N
44˚N
43˚N
42˚N
41˚N
40˚N
39˚N
38˚N
70˚W
68˚W
66˚W
64˚W
62˚W
60˚W
58˚W
56˚W
54˚W
52˚W

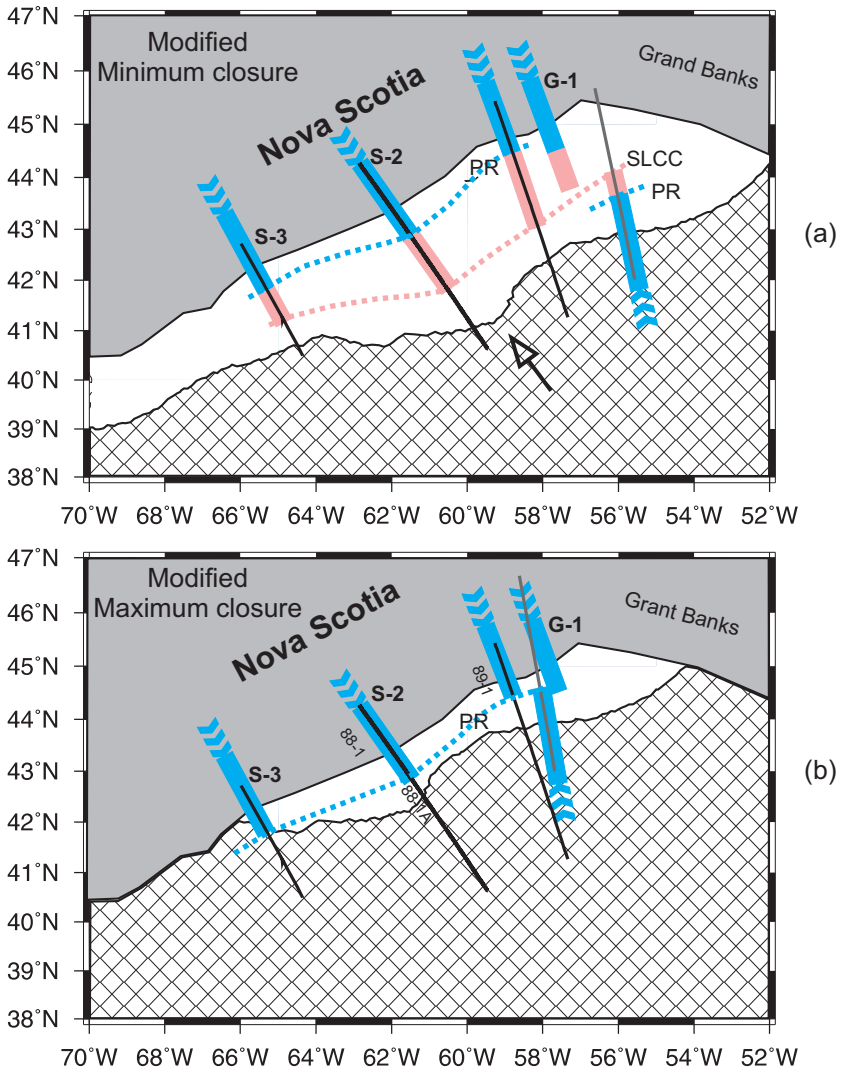
Modified
Minimum closure
Nova Scotia
Grand Banks
G-1
S-2
S-3
PR
SLCC
PR
(a)
Modified
Maximum closure
Nova Scotia
Grant Banks
G-1
S-2
S-3
89-1
86-1
88-1A
PR
(b)
47˚N
46˚N
45˚N
44˚N
43˚N
42˚N
41˚N
40˚N
39˚N
38˚N
70˚W
68˚W
66˚W
64˚W
62˚W
60˚W
58˚W
56˚W
54˚W
52˚W

4. REFERENCES

Alsop L. E., and Talwani, M., 1984. The East Coast Magnetic Anomaly, Science, New Series, 226, No. 4679, 1189-1191.

Anderson, D. L., Y.-S. Zhang, and T. Tanimoto, 1992. Plume heads, continental lithosphere, flood basalts and tomography, in Magmatism and the Causes of Continental Break-up, vol. 68, edited by B. C. Storey, T. Alabaster, and R. J. Pankhurst, 99-124, Geol. Soc. Lond., London.

Armstrong, R. L., and Besancon, J., 1970. A Triassic time scale dilemma: K-Ar dating of Upper Triassic mafic igneous rocks, Eastern U.S.A. and Canada and post-Upper Triassic plutons, Western Idaho, U.S.A. Eclogae Geol. Helv. 63, 15–28.

Arthur, J. D., 1988. Petrogenesis of early Mesozoic tholeiite in the Florida basement, and an overview of Florida basement geology: Florida Geological Survey, Tallahassee, Report of Investigation no. 97, 39 p.

Austin, J. A., Jr., Stoffa, P. L., Phollips, J., D., Oh, J., Sawer, D. S., Purdy, G. M., Reiter, E.,Makris, J., 1990. Crustal structures of the southeast Georgia embayment-Carolina trough: Preliminary results of a composite seismic image of a continental suture (?) and a volcanic passive margin, Geology, 18, 1023-1027.

Baksi, A.K., 1997. The timing of Late Cretaceous alkalic igneous activity in the northern Gulf of Mexico basin, southeastern USA: Journal of Geology, 105, 629-643.

Baksi, A. K., and Archibald, D. A., 1997. Mesozoic igneous activity in the Maranhao province, northern Brazil: $^{40}Ar/^{39}Ar$ evidence for separate episodes of basaltic magmatism: Earth and Planetary Science Letters, 151, 139-153.

Barr, S. M. and Raeside R. P., 1989. Tectono-stratigraphic terranes in Cape Breton Island, Nova Scotia: Implications for the configuration of the northern Appalachian orogen, Geology, 17, 822-825.

Barrett, D. L., M. J. Berry, J. E. Blanchard, M. J. Keen, and R. E., McAllister, 1964. Seismic studies on the eastern seaboard of Canada: the Atlantic coast of Nova Scotia, Can. J. Earth Sci., 1, 10-22.

Barrett, D. L. and Keen, C. E., 1976. Mesozoic magnetic lineations, the magnetic quiet zone, and sea floor spreading in the northwest Atlantic, J. Geophys. Res., 81, 4875-4884.

Beauchamp, W., R. W. Allmendinger, M. Barazangi, A. Demnati, M. El Alji, and M. Dahmani, 1999. Inversion tectonics and the evolution of the High Atlas Mountains, Morocco, based on a geological-geophysical transect, Tectonics, 18(2), 163–184.

Benn, K., Horne, R. J., Kontak, D. J., Pignotta, G. S. and Evans, N. G., 1997. Syn-Acadian emplacement model for the South Mountain batholith, Meguma Terrane, Nova Scotia: Magnetic fabric and structural analyses, Geological Society of America Bulletin, 109, 1279-1293.

Bertrand, H. 1991. The Mesozoic tholeiitic province of northwest Africa: A volcano-tectonic record of the early opening of the central Atlantic.In Kampunzo, A. B. and R. T. Lubala, eds., The Phanerozoic African plate, pp. 147-191. New York: Springer-Verlag.

Bown, J. W. and White, R. S., 1995. Effect of finite extension rate on melt generation at rifted continental margins, J. Geophys. Res., 100, 18011-18029.

Broughton, Paul, and André Trepaniér, 1993. Hydrocarbon Generation in the Essaouira Basin of Western Morocco. A.A.P.G. Bull., 77, Nº 6, 999 -1015.

Bullard, E. C., Everett, J. E. and Smith, A. G., 1965. The fit of the continents around the Atlantic, Royal Society of London Philosophical Transactions Series A, 258, 41–51.

Burke, K.B.S., Hamilton, J.B., and Gupta, V.K., 1973. The Caraquet dike: Its tectonic significance, Can. J. Earth Sci., 10, 1760-1768.

Carmichael, C.M., and Palmer, H.C. 1968. Paleomagnetism of the Late Triassic North Mountain Basalt of Nova Scotia, J. Geophys. Res., 73, 2811– 2822.

Caroff, M., Bellon, H., Chauris, L., Carron, J.-P., Chevrier, S., Gardinier, A., Cotten, J., Le Moan, Y., Neidhart, Y., 1995. Magmatisme fissural Triasico-Liasique dans l'ouest du Massif Armoricain (France): Petrologie, age, et modalities des la mise en place. Can. J. Earth Sci. 32, 1921-1936.

Chian, D., Louden, K. E. and Reid, I., 1995a. Crustal structure of the Labrador Sea conjugate margin and implications for the formation of non-volcanic continental margins, J. Geophys. Res., 100, 24239-24253.

Clarke, D.B., and Chatterjee, A.K. 1992. Origin of peraluminous granites in the Meguma Zone of southern Nova Scotia: a synthesis. Joint Annual Meeting of GAC/AGC, Wolfville, abstract, 17, A18.

Coffin, M. F., Gahagan, L.M., Lawver, L.A., Lee, T.-Y., and Rosencrantz, E., 1992. Atlas of Mesozoic/Cenozoic reconstructions (200 Ma to Present Day), Plates Progress Report No. 1-0192, University of Texas Institute for Geophysics Technical Report 122, 49 pp.

Cole, P. B., Minshull, T. A. and Whitmarsh, R. B., 2002. Azimuthal seismic anisotropy in a zone of exhumed continental mantle, West Iberia margin, Geophys. J. Int., 151, 517-533

Colman-Sadd, S.P., 1982. Two stage continental collision and plate driving forces, Tectonophysics, 90, 263-282.

Contrucci I., F. Klingelhofer, J. Perrot, R. Bartolome, M. A. Gutscher, M. Sahabi, J. Malod and J. P. Rehault, 2004 - The crustal structure of the NW Moroccan continental margin from wide-angle and reflection seismic data, Geophys. J. Int., 159, 1, 117-128.

Dean, S. M., Minshull, T.A., Whitmarsh, R. B. and Louden, K. E., 2000. Deep structure of the ocean-continent transition in the southern Iberia Abyssal Plain from seismic refraction profiles: The IAM-9 transect at 40˚20'N, J. Geophys. Res., 105, 5859-5885.

de Boer, J.Z., McHone, J.G., Puffer, J.H., Ragland, P.C. and Whittington, D. 1988. Mesozoic and Cenozoic magmatism, In The Geology of North America, Volume I-2: The Atlantic Continental Margin, U.S. Sheridan R.E. and Grow J.A. (eds.), Geological Society of America, Boulder, Colorado, 217-241.

Deckart, K., G. Féraud, and H. Bertrand. 1997. Age of Jurassic continental tholeiites of French Guy-

ana/Surinam and Guinea: Implications to the initial opening of the central Atlantic Ocean. Earth Plan. Sci. Let., 150, 205-220

Dehler, S.A., Keen, C.E., Funck, T., Jackson, H.R., and Louden, K., 2003. Structure of a volcanic to non-volcanic transitional margin segment off Nova Scotia, Atlantic Canada, EGS/AGU/EUG Joint Annual Meeting, April 2003, Nice, France.

Dehler, S. A., Keen, C. E., Funck, T., Jackson, H. R. and Louden, K. E., 2004. The limit of volcanic rifting: A structural model across the volcanic to non-volcanic transition off Nova Scotia. Eos Trans. AGU, 85(17), Jt. Assem. Suppl., Abstract T31D-04.

Divins, D.L., 2007. NGDC, Total Sediment Thickness of the World's Oceans and Marginal Seas, Retrieved date from http://www.ngdc.noaa.gov/mgg/sedthick/ sedthick.html.

Eldholm, O. and Thiede, J. and ODP Leg 104 Shipboard Scientific Party 1986. Ocean drilling at the Vøring Plateau in the Norwegian Sea. Nature, 319, 360–361.

Ernst, R.E. and Buchan, K.L., 2001. Large mafic magmatic events through time and links to mantle plume heads, in Ernst, R.E. and Buchan, K.L. (eds.), Mantle Plumes: Their Identification Through Time: Geological Society of America, Special Paper 352, 483-575.

Fitton J.G., Saunders A.D., Larsen L.M., Fram M.S., Demant A., Sinton C., 1995. Leg 152 Shipboard Scientific Party Magma sources and plumbing systems during break-up of the SE Greenland margin: preliminary results from ODP Leg 152. Journal of the Geological Society, London, 152, p.985-990.

Fodor, R.V., Sial, A.N., Mukasa, S.B., McKee, E.H., 1990. Petrology, isotope characteristics, and K-Ar ages of the Maranhao, northern Brazil, Mesozoic basalt province. Contr. Min. Pet. 104, 555-567.

Funck, T., Hopper, J. R., Larsen, H. C., Louden, K. E., Tucholke, B. E. and Holbrook, W. S., 2003. Crustal structure of the ocean-continent transition at Flemish Cap: Seismic refraction results, J. Geophys. Res., 108(B11), 2531, doi: 10.1029/2003JB002434.

Funck, T., Jackson, H. R., Louden, K. E., Dehler, S. A. and Wu, Y., 2004. Crustal structure of the northern Nova Scotia rifted continental margin (Eastern Canada), J. Geophys. Res., 109, B09102, doi: 10.1029/2004JB003008.

GEBCO, 2009. The GEBCO_08 Grid, http://www.gebco.net/data_and_products/gridded_bathymetry_data/documents/gebco_08.pdf.

Given, M. M., 1977. Mesozoic and early Cenozoic geology of offshore Nova Scotia, Bulletin of Canadian Petroleum Geology, 25 (1), 63-91.

Gohn, G. S., Gottfried, D., Lanphere, M. A., and Higgins, B. B., 1978. Regional implications of Triassic or Jurassic age for basalt and sedimentary red beds in the South Carolina Coastal Plain: Science, 202, 887-890.

González, A., Córdoba, D. and Vales, D., 1999. Seismic crustal structure of Galicia continental margin, NW Iberian Peninsula, Geophys. Res. Lett., 26, 1061-1064.

Gradstein, F.M., Ogg, J.G. and Smith, A.G., 2004. A Geologic Time Scale 2004. Cambridge University Press.

Greenough, J. D., Jones, L. M., and Mossman, D. J., 1989. Petrochemical and stratigraphic aspects of North Mountain basalt from the north shore of the Bay of Fundy, Nova Scotia, Canada, Can. J. Earth Sci., 26, 2710-2717.

Greenough, J.D., and Papezik, V.S., 1986. Petrology and geochemistry of the early Mesozoic Caraquet dyke, New Brunswick, Canada, Can. J. Earth Sci., 23, 193–201.

Greenough, J.D., and Papezik, V.S. 1987. The petrology of North Mountain Basalt from the wildcat oil well Mobil Gulf Chinampas N-37, Bay of Fundy, Can. J. Earth Sci., 24: 1255–1260.

Hames, W.E., McHone, J.G., Ruppel, C., and Renne, P. (editors), 2002. *The Central Atlantic Magmatic Province: Insights from Fragments of Pangea:* Am. Geophys. Union Monograph, 136, 267 p.

Hames, W.E., Renne, P.R., and Ruppel, C., 2000. New evidence for geologically instantaneous emplacement of earliest Jurassic Central Atlantic magmatic province basalts on the North American margin, Geology, 28, 9, 859-862.

Hayatsu, A., 1979. K-r isochron age of the North Mountain basalt, Nova Scotia, Can. J. Earth Sci. 16, 973–975.

Hiscott, R.N., Wilson, R.C.L., Gradstein, F.M., Pujalte, V., García-Mondéjar, J., Boudreau, R.R. and Wishart, H.A., 1990. Comparative stratigraphy and subsidence history of Mesozoic rift basins of North American, Am. Ass. Petrol. Geol. Bull., 74, 60-76.

Holbrook, W. S. and Kelemen, P. B., 1993. Large igneous province on the US Atlantic margin and implications for magmatism during continental breakup, Nature, 364, 433-436.

Holik, J.S., Rabinowitz, P. D. and Austin, J. A., 1991. Effects of Canary hotspot volcanism on structure of oceanic crust off Morocco, J. Geophys. Res., 96, 12039-12067.

Ings, S.J. and Shimeld, J.W., 2006. A new conceptual model for the structural evolution of a regional salt detachment on the northeast Scotian margin, offshore eastern Canada. American Association of Petroleum Geologists Bulletin, 90: 1407-1423.

Jackson, H.R., Chian, D., Louden, K. and M. Salisbury, M., submitted. Crustal Structure of the Meguma Terrane Offshore of Nova Scotia and its Tectonic Implications, Can. J. Earth Sci..

Jackson, H.R., Chian, D., Salisbury, M. and Shimeld, J., 2000. Preliminary crustal structure from the Scotian margin to the Maritimes Basin from wide-angle reflection/refraction profiles, Geocanada 2000, The Millennium Geoscience Conference Cdrom, May 29-June 2, Calgary, Alberta.

Jackson, H. R., Keen, C. E. and Keen, M. J., 1975. Seismic structure of the continental margins and ocean basins of southeastern Canada, Geol. Surv. Can. Pap. 74–51, p. 13.

Jansa, L.F., and Pe-Piper, G., 1985, Early Cretaceous volcanism on the northeastern American margin and implications for plate tectonics: Geological Society of America Bulletin, 96, 83–91.

Jansa, L.F. and Wade, J.A., 1975, Geology of the continental margin off Nova Scotia and Newfoundland: in Offshore Geology of Eastern Canada, Vol. 2, Regional Geology, Van

der Linden, W.J.M. and Wade, J.A. (Eds.), Geol. Sur. Can., Paper 74-30, 51-106.

Jansa, L.F., and Wiedmann, J., 1982. Mesozoic-Cenozoic development of the eastern North American and northwest African continental margins: a comparison, 215–269. In: Geology of the northwest African Margin. Ed.U. von Rad, K. Hinz, M. Sarnthein and E. Seibold. Springer-Verlag, Berlin/Heidelberg/New York.

Keen, C. E. and Cordsen, A., 1981. Crustal structure, seismic stratigraphy, and rift processes of the continental margin off eastern Canada: ocean bottom seismic refraction results off Nova Scotia, Can. J. Earth Sci., 18, 1523-1538.

Keen, C. E., Kay, W. A., Keppie, D., Marillier, R., Pe-Piper, G. and Waldron, J. W. F., 1991a. Deep seismic reflection data from the Bay of Fundy and marine: tectonic implication for the northern Appalachian, Can. J. Earth Sci., 28, 1096-1111.

Keen, C. E., Keen, M. J., Barrett, D. L., and Heffler, D. E., 1975. Some aspects of the ocean-continent transition at the continental margin off eastern North America. In Off-shore Geology of Eastern Canada, Vol. 2, Regional geology, edited by W. J. M. van der Linden and J. A. Wade, Geological Survey of Canada, 189-197.

Keen, C. E., and B. D., Loncarevic, I. Reid, J. Woodside, R. T. Howorth, and H. Williams, 1990. Tectonic and geophysical overview, In Geology of Canada, No. 2, Geology of the continental margins of eastern Canada, Edited by M. J., Keen, G. L. Williams. Geological Survey of Canada, Ottawa, Ont., 31-85.

Keen, C. E., MacLean, B. C. and Kay, W. A., 1991b. A deep seismic reflection profile across the Nova Scotia continental margin, offshore eastern Canada, Can. J. Earth Sci., 28, 1112-1120.

Keen, C. E. and Potter, P., 1995a. The transition from a volcanic to non-volcanic rifted margin off eastern Canada, Tectonics, 14, 359-371.

Keen, C. E. and Potter, P., 1995b. Formation and evolution of the Nova Scotian rifted margin: Evidence from deep seismic reflection data, Tectonics, 14, 918-932.

Kelemen, P. B. and Holbrook, W. S., 1995. Origin of thick, high-velocity igneous crust along the U.S. East Coast Margin, J. Geophys. Res., 100, B7, 10,077-10,094.

Keppie, J. D., 1989. Northern Appalachian terranes and their accretionary history, in Terranes in the circum-Atlantic Paleozoic Orogens, edited by Dallmeyer, R. D., Geological Society of America, Special Paper, 230,159-192.

Keppie, J.D., and Dallmeyer, R.D. 1995. Late Paleozoic collision, delamination , short-lived magmatism, and rapid denudation in the Meguma Terrane, (Nova Scotia, Canada): constraints from 40Ar/39Ar isotopic data, Can. J. Earth Sci., 32: 644-659.

Klitgord, K. D. and Schouten, H., 1986. Plate kinematics of the central Atlantic, in The Geology of North America, Volume M, The Western North Atlantic Region, edited by Vogt P. R. and Tucholke, B. E., 351-378, Geological Society of America, Boulder, Colo.

Lau, K. W. H., Louden, K. E., Funck, T., Tucholke, B.E., Holbrook, W.S., Hopper, J.R., and Larsen, H.C., 2006a. Crustal structure across the

Grand Banks - Newfoundland Basin continental margin (Part I) - Results from a seismic refraction profile, Geophys. J. Int. 167, 127-156.

Lau, K. W. H., Louden, K.E., Deemer, S., Hall, J., Hopper, J.R., Tucholke, B.E., Holbrook, W.S., and Larsen, H.C., 2006b. Crustal structure across the Grand Banks - Newfoundland Basin continental margin (Part II) - Results from a seismic reflection profile, Geophys. J. Int. 167, 157-170.

Lefort, J. -P. and Van der Voo, R., 1981. A kinematic model for the collision and complete suturing between Gondwanaland and Laurasia in the Carboniferous, J. Geol., 89, 537-550.

LePichon, X., Sibuet, J. C. and Francheteau, J., 1977. The fit of the continents around the North Atlantic Ocean. Tectonophysics, 38, 169–209.

Liger, J.-L.,1980. Structure profonde du bassin sénégalo-mauritanien– Interprétation des données gravimétriques et magnétiques, Trav. Lab. Sci. Terre, Saint-Jérôme, Marseille, 16.

Louden, K. E. and Chian, D., 1999. The deep structure of non-volcanic rifted continental margins, Phil Trans. Roy. Soc. Lond., Ser. A., 357, 767-804.

Louden, K. E., Tucholke, B. E. and Oakey, G. N. 2004: Regional anomalies of sediment thickness, basement depth and isostatic crustal thickness in the North Atlantic Ocean. Earth and Planetary Science Letters, 193-211.

Maillard A., J. Malod, E. Thiébot, F. Klingelhoefer and J.-P. Réhault, 2006 - Imaging a lithospheric detachment at the continent–ocean crustal transition off Morocco, Earth Planet. Sci. Lett., 241, 686-698.

Marillier, F., Keen, C. E., Stockmal, G. S., Quinlan, G., Williams, H., Colman-Sadd, S. P. and O'Brien, S. J., 1989. Crustal structure and surface zonation of the Canadian Appalachians: implications of deep seismic reflection data, Can. J. Earth Sci., 26, 305-321.

Marzoli, A., Renne, P. R., Piccirillo, E. M., Ernesto, M., Bellieni, G. and Min, A. De, 1999. Extensive 200-million-year-old continental flood basalts of the Central Atlantic Magmatic Province, Science 284: 616-618.

Mauffret A. and Montadert L., 1987. Rift tectonics on the passive continental margin off Galicia (Spain). Mar. Petrol. Geol., 4, 49-70.

McBride, J.H., 1991. Constraints on the structure and tectonic development of the Early Mesozoic South Georgia rift, southeastern United States; seismic reflection data processing and interpretation. Tectonics 10, 1065-1083.

McHone, J. G., D. P. West, Jr., A. M. Hussey II., and N. W. McHone.1995. The Christmas Cove dike, coastal Maine: Petrology and regional significance. Geol. Soc. Am. Abs. with Prog., 27, 67-68.

McHone, J.G., 2000. Volatile emissions of Central Atlantic Magmatic Province basalts: Mass assumptions and environmental consequences, in Hames, W.E., McHone, J.G., Renne, P.R., and Ruppel, C., editors, *The Central Atlantic Magmatic Province*: American Geophysical Union, Geophysical Monograph, 136, 241-254.

Minshull, T.A., Dean, S.M., White, R.S., and Whitmarsh, R.B., 2001. Anomalous melt production after continental break-up in the southern Iberia Abyssal Plain. In Wilson,

R.C.L., Whitmarsh, R.B., Taylor, B., and Froitzheim, N. (Eds.), Non-volcanic Rifting of Continental Margins: Evidence From Land and Sea. Geol. Soc. Spec. Publ. London.

Molnar, J, Tari, G., Ashton P. and Thompson P., 2002. Correlation of syn-rift structural elements across the central Atlantic between Morocco and Nova Scotia, AAPG distinguished lecture 2002.

Montes-Lauar, C. R., Pacca, I. G., Melfi, A. J., Piccirillo, E. M., Bellieni, G., Petrini, R., and Rizzieri, R., 1994, The Anari and Tapirapua Jurassic formations, western Brazil: paleomagnetism, geochemistry, and geochronology: Earth and Planetary Science Letters, v. 128, p. 357-371.

Moullade, M., Brunet, M.-F. and Boillot, G., 1988. Subsidence and deepening of the 160 Galicia margins: the paleoenvironmental control. In Proceedings of the Ocean Drilling Program, Scientific Results, Vol. 103, pp. 733-740, ed. Mazullo, E.K., Ocean Drilling Program, College Station, TX.

Murphy, J.B., van Staal, C.R. and Keppie, J.D.1999. Middle to Late Paleozoic Acadian orogeny in the northern Appalachians: a Larmide-style plume-modified orogeny? Geology, 27: 653- 656.

Mutter, J.C., W.R. Buck and C.M. Zehnder, 1988. Convective Partial Melting 1. A model for the formation of thick basaltic sequences during the initiation of spreading, J. Geophys. Res., 93, 1031-1048.

National Geophysical Data Center, 1988. ETOPO-5 Bathymetry/Topography data, Data announcement 88-MG-02, National Oceanic and Atmospheric Administration, U.S. Dept. of Commerce, Boulder, Colo.

Oakey, G.N. and Start, A., 1995. ADigital Compilation of Depth to Basement and Sediment Thickness for the North Atlantic and Adjacent Coastal Land Areas: Geological Survey of Canada Open File Report No. 3039.

Officer, C. B. and Ewing, M., 1954. Geophysical investigations in the emerged and submerged Atlantic coastal plain. Part VII. Continental shelf, continental slope, and continental rise south of Nova Scotia, Geol. SOC. Am. Bull., 65, 653-670.

Oliveira, E.P., Tarney, J., Joao, X.J., 1990. Geochemistry of the Mesozoic Amapa and Jari dyke swarms, northern Brazil: Plume-related magmatism during the opening of the central Atlantic. In: Parker, A.J., Rickwood, P.C., Tucker, D.H. (Editors), Mafic dikes and emplacement mechanisms. Balkemia, Rotterdam, Netherlands, 173-183.

Olsen, P.E., 1997. Stratigraphic record of the early Mesozoic breakup of Pangea in the Laurasia-Gondwana rift system: Annual Reviews of Earth and Planetary Science, 25, 337-401.

Olsen, P. E., Hubert, J. F. and Mertz, K. A., 1981. Eolian dune field of Late Triassic age, Fundy Basin, Nova Scotia, Geology, 9: 557-559

Papezik, V.S., and Barr, S.M. 1981. The Shelburne dike, an early Mesozoic diabase dike in Nova Scotia: mineralogy, petrology, and regional significance, Can. J. Earth Sci., 18: 1346–1355.

Papezik, V. S. and Hodych, J. P., 1980. Early Mesozoic diabase dikes of the Avalon Peninsula, Newfoundland: Petrochemistry, mineralogy, and origin: Canadian Journal of Earth Sciences, 17, 1417-1430.

Pe-Piper, G. and Jansa, L.F., 1986: Triassic olivine- normative diabase from Northumberland Strait, Eastern Canada: implications for continental rifting. Can. J. Earth Sci., 23, 1013-1021.

Pe-Piper, G., Jansa, L.F., and Lambert, R., St.J., 1992, Early Mesozoic magmatism on the eastern Canadian margin: Petrogenetic and tectonic signifi cance, in Puffer, J.H., and Ragland, P.C., eds., Eastern North American Mesozoic Magmatism: Geological Society of America Special Paper 268, 13–36.

Pe-Piper G., Piper, D.J.W., Keen, M.J., and McMillan, N.J., 1990. Igneous rocks of the Eastern Canadian continental margin. Chapter 2 in: Geology of the continental margin off Eastern Canada, M.J.Keen and G.L. Williams (ed.); Geological Survey of Canada, Geology of Canada, no.2, 75-85.

Pérez-Gussinyé, M. and Reston, T. J., 2001. Rheological evolution during extension at nonvolcanic rifted margins: onset of serpentinization and development of detachments leading to continental breakup, J. Geophys. Res., 106, 3961-3975.

Philpotts, A. R. and A. Martello. 1986. Diabase feeder dikes for the Mesozoic basalts in southern New England. Am. Jour. Sci. 286,105-126.

Pringle, G.J., Trembath, L.T., Pajari, G.J., Jr., 1974. Crystallization history of a zoned plagioclase. Mineral. Mag. 39, 867–877.

Reid, I. D., 1994. Crustal structure of a nonvolcanic rifted margin east of Newfoundland, J. Geophys. Res., 99, 15161-15180.

Reston, T. J.; Perez-Gussinye, M.; Phipps Morgan, J., 2003. Numerical Modelling of the Transition from Continental Rifting to Mantle Exhumation at the West Iberia Margin, American Geophysical Union, Fall Meeting 2003, abstract #T12A-0433.

Reynolds, P. H., Elias, P., Muecke, G. K. and Grist, A. M., 1987. Thermal history of the southwestern Meguma Group, Nova Scotia, from 40Ar/39Ar and fission track dating study of intrusive rocks;, Can. J. Earth Sci., 24, 1952-1965.

Roeser, H. A., 1982, Magnetic Anomalies in the Magnetic Quiet Zone off Morocco, in von, Rad, U., Hinz, K., Sarnthein, M., and Seibold, E. (eds.), Geology of the Northwest African Continental Margin, Springer Verlag, Berlin, pp. 60–68.

Roeser, H.A., Steiner, C., Schreckenberger, B., Block, M., 2002. Structural development of the Jurassic Magnetic Quiet Zone off Morocco and identification of Middle Jurassic Magnetic Lineations, J. Geophys. Res., (B10), 107.

Roest, W., R., Danobeitia, J., Verhoef, J., and Collette, B. J., 1992. Magnetic anomalies in the Canary Basin and the Mesozoic evolution of the Central North Atlantic. Marine Geophysical Research, 14, 1-24.

Rogers, H. D. 1985. Geology of the Igneous-Metamorphic Complex of Shelburne and eastern Yarmouth counties, Nova Scotia; in Current Research, Part A, Geological Survey of Canada, Paper 85-1A, 773-777.

Sahabi, M., Aslanian, D. and Olivet, J.-L., 2004. Un nouveau point de départ pour l'histoire de l'Atlantique central, Comptes Rendus Geosciences, 336, 12,1041-1052.

Salisbury, M.H. and Keen, C.E., 1993. Listric faults imaged in oceanic crust, Geology, 21, 117-120.

Sawyer, D.S., Whitmarsh, R.B., Klaus, A., et al. (including Milliken, K. L.), 1994. Proceedings of the Ocean Drilling Program, Initial Reports, 149, College Station, TX, 719.

Schermerhorn, L. J. G., Priem, H. N. A., Boelrijk, N. A., Hebeda, E.H., Verdumen, E. A. Th., and Verschure, R. H., 1978. Age and origin of the Messejana dolerite fault-dike system (Portugal and Spain) in the light of the opening of the North Atlantic Ocean: Journal of Geology, 86, 299-309.

Schenk, P. E., 1970. Regional variation of the flysch-like Meguma Group (Lower Paleozoic) of Nova Scotia compared to recent sedimentation off the Scotia Shelf; Geological Association of Canada, Special Paper 7, 127-153.

Sheridan, R. E., D. L., Musser, L., Glover III, J, I., Ewing, W. S., Holbook, G. M., Purdy, R., Hawman, and S. Smithson, 1993. Deep seismic reflection data of EDGE U.S. mid-Atlantic continental-margin experiment: Implications for Appalachian sutures and Mesozoic rifting and magmatic underplating, Geology, 21, 563-567.

Shimeld, J., 2004. A comparison of salt tectonic subprovinces beneath the Scotian Slope and Laurentian Fan, in Salt Sediment Interactions and Hydrocarbon Prospectivity: Concepts, Applications, and Case Studies for the 21st Century, 24th Annual Conference, Post, P., Olson, D., Lyons, K., Palmes, S., Harrison, P. and Rosen N., editors. Gulf Coast Section Society of Economic Paleontologists and Mineralogists Foundation (GCSSEPM), Houston, TX (CD format).

Shipboard Scientific Party, 1987. Site 637. *In* Boillot, G., Winterer, E.L., Meyer, A.W., et al., *Proc. ODP, Init. Repts.,* 103: College Station, TX (Ocean Drilling Program), 123–219.

Sleep, N. H., 1996. Lateral flow of hot plume material ponded at sublithospheric depths, J. Geophys. Res., 101(B12), 28,065–28,084.

Sleep, N.H. and Barth, G.A., 1997. The nature of oceanic lower crust and shallow mantle emplaced at low spreading rates, Tectonophysics, 279, 181–191.

Srivastava, S.P. and Keen, C.E., 1995. A deep seismic reflection profile across the extinct Mid-Labrador Sea spreading center: Tectonics, v. 14, p. 372–389.

Sundeen, D.A., 1989. Note concerning the petrography and K-Ar age of Cr-spinel-bearing olivine tholeiite in the subsurface of Choctaw County, north-central Mississippi: Southeastern Geology, 30, 137-146.

Sutter, J. F. and Smith, T. E., 1979. $^{40}Ar/^{39}Ar$ ages of diabase intrusions from Newark Trend Basins in Connecticut and Maryland: Initiation of Central Atlantic Rifting, *Am. J. Sci.* 279, 808–831.

Sutter, J. F., 1985. Progress on geochronology of Mesozoic diabase and basalts, US Geological Survey Circular 946, chapter 21, Page 110-114.

Talwani, M. and Abreu, V., 2000. Inferences regarding initiation of oceanic crust formation from the U.S. east coast margin and conjugate south Atlantic margins, in Atlantic rifts and continental margins, edited by Mohriak W. and Talwani, M., 211-233, American geophysical Union, Geophysical Monograph 155, Washington, DC.

Tari, G., Molnar, J. and Ashton, P., 2003. Examples of salt tectonics from West Africa: a comparative approach. In: T.J. Arthur, D.S. Macgregor and N.R. Cameron (Editors), Petroleum geology of Africa: New themes and developing technologies. The Geological Society, London, pp. 85-104.

Tari, G., and Molnar, J., 2005. Correlation of syn-rift structural between Morocco and Nova Scotia, Canada, 25th Annual GCSSEPM Foundation Bob F. Perkins Research Conference, Petroleum Systems of Divergent Continental Margin Basins, Houston, Texas.

Tucholke, B. E. and Ludwig, W. J., 1982, Structure and Origin of the J Anomaly Ridge, Western North Atlantic, J. Geophys. Res. 87, 9389–9407.

U.S. Department of Commerce, National Oceanic and Atmospheric Administration, National Geophysical Data Center, 2006. 2-minute Gridded Global Relief Data, ETOPO2v2.

Vauchez, A., Tommasi, A., Barruol, G. and Maumus, J. 2000. Upper mantle deformation and seismic anisotropy in continental rifts. Phys. Chem. Earth (A), 25 (2): 111-117.

Verhoef, J., Collette, B. J., Danobeitia, J. J., Roeser, H. A., and Roest, W. R., 1991, Magnetic Anomalies off West-Africa (20°–38° N), Marine Geophys. Res. 13, 81–103.

Verhoef, J., W.R. Roest, R. Macnab, J. Arkani-Hamed, and Project Team, 1996. Magnetic anomalies of the Arctic and North Atlantic Oceans and adjacent land areas, Geol. Surv. Can. Open File Rep., 3125a.

Vogt, P.R., 1973. Early events in the opening of the North Atlantic. In implications of continental drift to the Earth Sciences (D.H. Tarling and S.K. Runcorn, ed.), Vol. 2, pp. 693–712.

Vogt, P.R., 1991. Bermuda and Appalachian-Labrador rises: Common non-hotspot processes? Geology, 19, 41-44.

Wade, J. A. and MacLean, B. C., 1990. The geology of the southeastern margin: aspects of the geology of the Scotian Basin from recent seismic and well data, in Geology of the Continental Margin Eastern Canada, edited by Keen, M. J. and Williams, G. L., Geological Survey of Canada, Geology of Canada, No. 2, 167-238.

Watt, W.S., 1969. The coast-parallel dike swarm of southern Greenland in relation to the opening of the Ladrador Sea, Can. J. Earth Sci., 6, 1320-1321.

Webster, T.L., Murphy, J.B. and Barr, S.M. 1998. Anatomy of a terrane boundary, an integrated structural, geographic information system and remote sensing study of the Late Paleozoic Avalon-Meguma terrane boundary drift. Can. J. Earth Sci., 35: 787-801.

Welsink, H. J., Dwyer, J. D. and Knight, R. J., 1989. Tectono-stratigraphy of the passive margin off Nova Scotia, in Extensional tectonics and stratigraphy of the North Atlantic margin, edited by Tankard, A. J. and Balkwill, H.R., American Association of Petroleum Geologists, Memoir 46, 215-231.

Wheeler, J.O., Hoffman, P.F., Card, K.D., et al., 1997. Geological Map of Canada, Geological Survey of Canada, Map D1860A, Ottawa Geological Survey of Canada.

White, R. S. and McKenzie, D. P., 1989. Magmatism at rift zones: the generation of volcanic continental mar-

gins and flood basalts, J. Geophys. Res., 94, 7685-7729.

White, R. S., McKenzie, D. and O'Nions, K., 1992. Oceanic crustal thickness from seismic measurements and rare earth element inversions, J. Geophys. Res., 97, 19683-19715.

Whitmarsh, R.B. and Miles, P.R. 1995. Models of the development of the West Iberia rifted continental margin at 40°30'N deducted from surface and deep-tow magnetic anomalies, J. Geophys. Res., 100, 3789-3806.

Whitmarsh R. B., White R. S., Horsefield S. J., et al, 1996. The ocean-continent boundary off the western continental margin of Iberia: Crustal structure west of Galicia Bank, J. Geophys. Res. Sol 101 (B12): 28291-28314.

Williams, H., 1979. Appalachian Orogen in Canada, Can. J. Earth Sci., 16, 792-807.

Williams, H., and Hatcher, R. D. 1982. Suspect terranes and accretionary history of the Appalachian Orogen. Geology, 10: 530-536.

Withjack, M.O., Schlische, R.W., and Olsen, P.E., 1998, Diachronous rifting, drifting, and inversion on the passive margin of central eastern North America: An analog for other passive margins: AAPG Bulletin, 82, 817-835.

Wu, Y., 2007. Crustal Structure of the Central Nova Scotia Margin and the Transition from Volcanic to Non-Volcanic Rifting off Eastern Canada, Ph.D. Thesis, Dalhousie University, 341 pp.

Wu, Y., Louden, K.E., Funck, T., Jackson, H.R., and Dehler, S.A., 2006. Crustal structure of the central Nova Scotia margin off Eastern Canada, Geophys. J. Int. 166 (2), 878-906.

Zelt, C. A. & Barton, P. J. 1998. Three–dimensional seismic refraction tomography: A comparison of two methods applied from the Faeroe Basin. *Journal of Geophysical Research*, 103, 7187–7210.

Zelt, C. A. & Smith, R. B. 1992. Seismic traveltime inversion for 2-D crustal velocity structure. *Geophysical Journal International*, 108, 16–34.

Appendix A – List of Files

```
Folder PATH listing for volume Expansion Drive
Volume serial number is 00090178 D0A5:C0F1

Dalhousie:.
|   list_of_files.txt
|
+---Navigation
|       all_shot_utm.txt
|       deep_water_vel.txt
|       drift
|       OBS_deploy_coord_latlon.txt
|       OBS_deploy_coord_UTM.txt
|       OBS_model_dist_depth.txt
|       OBS_relocate_coord_latlon.txt
|       offset_range.txt
|       phase1.nav
|       phase2.nav
|       phase3.nav
|       seafloor_depth_new.txt
|       shot_table_1.txt
|       shot_table_2.txt
|       shot_table_3.txt
|
+---OBS_data
|   |   obs10.ch4.sgy
|   |   obs100.ch4.sgy
|   |   obs11.ch4.sgy
|   |   obs12.ch4.sgy
|   |   obs13.ch4.sgy
|   |   obs14.ch4.sgy
|   |   obs15.ch4.sgy
|   |   obs16.ch4.sgy
|   |   obs17.ch4.sgy
|   |   obs18.ch4.sgy
|   |   obs19.ch4.sgy
|   |   obs2.ch4.sgy
|   |   obs20.ch4.sgy
|   |   obs21.ch4.sgy
|   |   obs22.ch4.sgy
|   |   obs23.ch4.sgy
|   |   obs24.ch4.sgy
|   |   obs25.ch4.sgy
|   |   obs27.ch4.sgy
|   |   obs28.ch4.sgy
|   |   obs29.ch4.sgy
|   |   obs3.ch4.sgy
|   |   obs30.ch4.sgy
|   |   obs32.ch4.sgy
|   |   obs33.ch4.sgy
|   |   obs34.ch4.sgy
|   |   obs35.ch4.sgy
|   |   obs36.ch4.sgy
|   |   obs37.ch4.sgy
```

```
|   |   obs38.ch4.sgy
|   |   obs39.ch4.sgy
|   |   obs4.ch4.sgy
|   |   obs40.ch4.sgy
|   |   obs41.ch4.sgy
|   |   obs42.ch4.sgy
|   |   obs43.ch4.sgy
|   |   obs44.ch4.sgy
|   |   obs45.ch4.sgy
|   |   obs46.ch4.sgy
|   |   obs47.ch4.sgy
|   |   obs48.ch4.sgy
|   |   obs49.ch4.sgy
|   |   obs5.ch4.sgy
|   |   obs50.ch4.sgy
|   |   obs51.ch4.sgy
|   |   obs52.ch4.sgy
|   |   obs53.ch4.sgy
|   |   obs55.ch4.sgy
|   |   obs56.ch4.sgy
|   |   obs57.ch4.sgy
|   |   obs58.ch4.sgy
|   |   obs59.ch4.sgy
|   |   obs6.ch4.sgy
|   |   obs60.ch4.sgy
|   |   obs62.ch4.sgy
|   |   obs63.ch4.sgy
|   |   obs64.ch4.sgy
|   |   obs65.ch4.sgy
|   |   obs66.ch4.sgy
|   |   obs67.ch4.sgy
|   |   obs69.ch4.sgy
|   |   obs7.ch4.sgy
|   |   obs70.ch4.sgy
|   |   obs73.ch4.sgy
|   |   obs74.ch1.sgy
|   |   obs74.ch4.sgy
|   |   obs75.ch4.sgy
|   |   obs76.ch4.sgy
|   |   obs77.ch4.sgy
|   |   obs78.ch4.sgy
|   |   obs79.ch4.sgy
|   |   obs8.ch4.sgy
|   |   obs80.ch4.sgy
|   |   obs81.ch4.sgy
|   |   obs83.ch4.sgy
|   |   obs84.ch4.sgy
|   |   obs85.ch4.sgy
|   |   obs86.ch4.sgy
|   |   obs87.ch4.sgy
|   |   obs88.ch4.sgy
|   |   obs89.ch4.sgy
|   |   obs9.ch4.sgy
|   |   obs91.ch4.sgy
|   |   obs92.ch4.sgy
|   |   obs93.ch4.sgy
|   |   obs94.ch4.sgy
|   |   obs95.ch4.sgy
|   |   obs96.ch4.sgy
```

```
|   |   obs97.ch4.sgy
|   |   obs98.ch1.sgy
|   |   obs98.ch2.sgy
|   |   obs98.ch3.sgy
|   |   obs98.ch4.sgy
|   |   obs99.ch4.sgy
|   |
|   \---relocate
|           obs92.ch4.relo.sgy
|
+---Script
|       input_geom_head.cmd
|
\---Velocity_model
        10.layer
        11.layer
        12.layer
        13.layer
        14.layer
        2.layer
        3.layer
        4.layer
        5.layer
        6.layer
        7.layer
        8.layer
        9.layer
        Geopro_layer.v.in
        NovaScotia_vmodel.xyz
```

Appendix B - OBS Relocation

A brief note on Geopro approach and Dalhousie approach

June 24, 2010

By Helen Lau

Dalhousie University

Geopro data as is

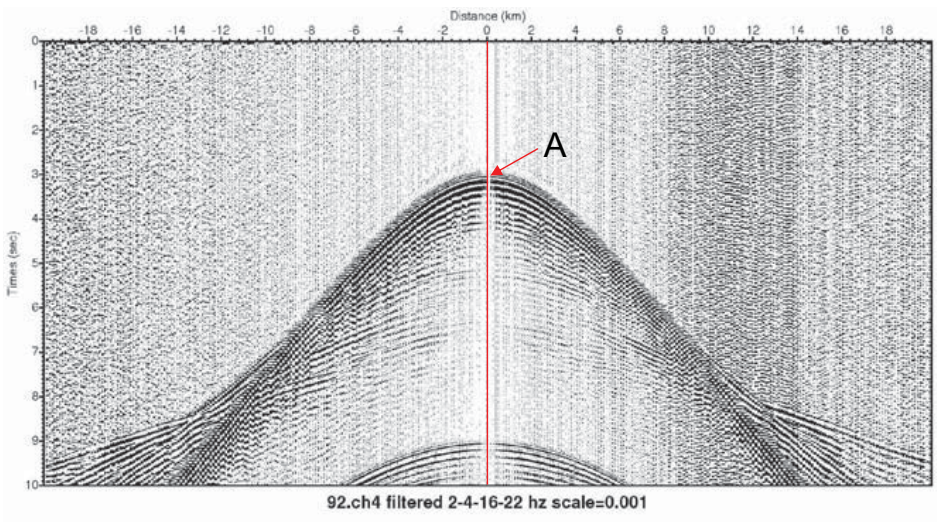

- An example plot of bandpass filtered OBS data as is provided by Geopro
- Odd: data are observable very near to zero (offset) distance (red line), implying that OBS did not drift much from its deployment position (unusual for deep water)
- At the beginning, we found no geographical positions of both shots and OBSs in the trace headers → unable to trace the cause
- We later understood that the offsets as provided are between shots and planned OBS position plus an along profile shift such that the minimum water arrival time (A) is at zero offset. A new OBS position is obtained accordingly.
- There is also a static shift applied to the data to fit the modeled water arrival times

True geometry considered

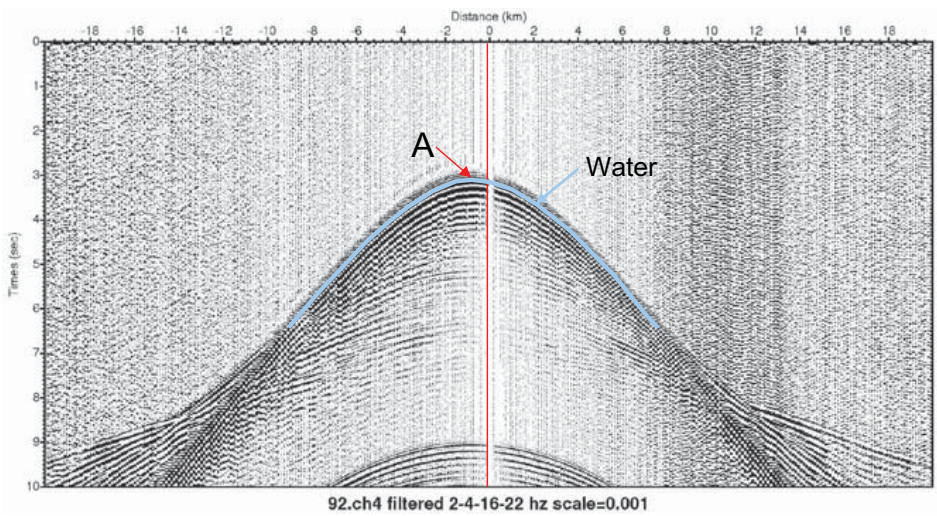

Requirements

- shot locations on all traces
- water depth of OBS
- velocity profile above the OBS
- the deployed OBS position
- Undo static time shifts

- To determine if the Geopro approach is in agreement with conventional methods, we tested on a few OBSs using our usual approach honouring the listed requirements.
- Geopro later provided us with the required shotpoint and static shift information we needed for our processing
- A new OBS record section is plotted using true geometry information to calculate offsets.
- The minimum point (A) is observed to be in the negative quadrant, implying a drift in the negative distance direction
- The direct water arrivals were then picked using given shotpoint locations and without filtering.

Relocation using water arrival picks

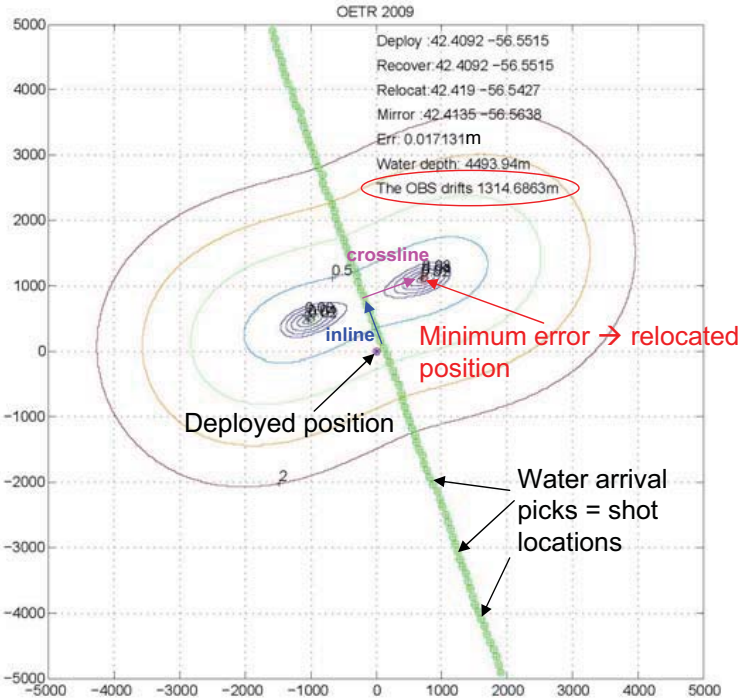

- Water velocities and depths = NovaSpan-2000 model
- Water depths = NovaSpan-2000 model or GEBCO_08
- The water arrival picks were inverted for a set of corresponding offset ranges through raytracing
- For any assumed OBS position, another set of offset ranges can be calcuated and compared with the inverted set
- The position within our search grid of 5x5 km which gives a minimum RMS difference (i.e. error) is our relocated position.
- Two minima are a result of shot profile being a straight line
- We found drift in both inline and crossline directions

Relocated geometry

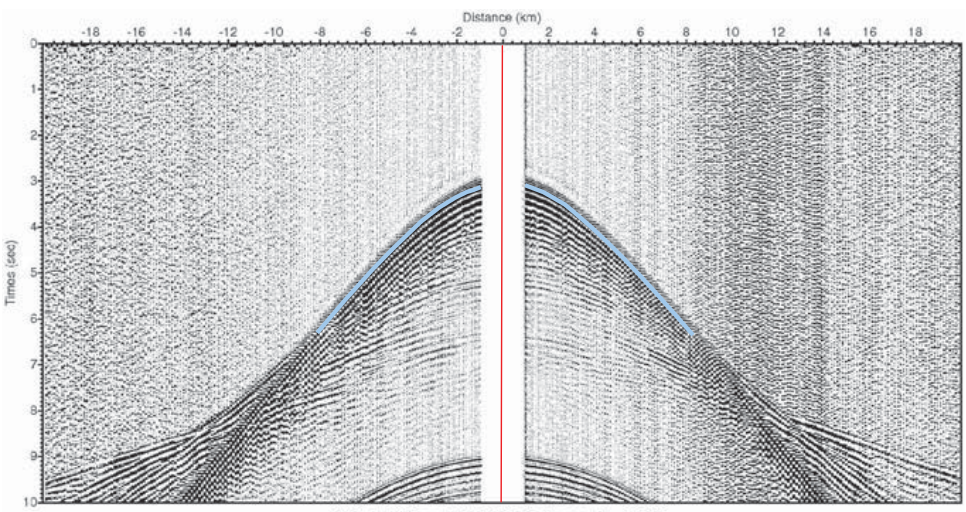

92.ch4 filtered 2-4-16-22 hz scale=0.001

- Corrected offsets were calculated using the relocated OBS position and the true shot positions.
- The corrections due to inline drift place the water arrival symmetrical about the time axis at zero distance (red line)
- The corrections due to the crossline drift produce a gap in observed data near zero distance. Such gaps are commonly seen in publications as OBSs often drift from deployment positions.
- This exercise is important in getting the near offsets right. Accurate modeling of area near the OBS would required correct offsets for near traces. Inaccuracy may translate into errors in depths of layer boundaries for other parts of the velocity model.

Variations in crustal structure across the Nova Scotia continental margin and its conjugate

Ka Wai Helen Lau (1); **Keith E. Louden** (2); **M. Nedimovic** (3)

(1) Dept. of Oceanography, Dalhousie University, Halifax, NS, B3H 4J1, Canada; kwhlau@dal.ca
(2) Dept. of Oceanography, Dalhousie University, Halifax, NS, B3H 4J1, Canada; Keith.Louden@dal.ca
(3) Dept. of Earth Sciences, Dalhousie University, Halifax, NS, B3H 4J1, Canada; mladen@dal.ca

ABSTRACT

The East Coast Magnetic Anomaly and associated seaward dipping reflectors, both suggesting volcanism, are observed on the south-western Nova Scotia margin but quickly reduce in magnitude to the northeast. A comparison of seismic observations across three previous refraction profiles (from NE to SW: SMART-1,2,3) also shows a parallel decrease in syn-rift volcanism as the margin becomes non-volcanic near the central line (SMART-2). A velocity model from a new profile northeast of SMART-1 suggests continuation of non-volcanic features, such as serpentinized mantle and thin oceanic crust, to the north-eastern end of the margin. Being conjugated to SISMAR-4 on the Moroccan margin, this new profile facilitates a better constrained kinematic reconstruction of the rifting and breakup of the complete Nova Scotia-Morocco conjugate margins.

KEYWORDS: Nova Scotia, Morocco, Atlantic, Conjugates.

1. Introduction

The Nova Scotia rifted continental margin lies in a transitional segment between the volcanic US East Coast margin to the south and the non-volcanic Newfoundland margin to the north. The East Coast Magnetic Anomaly (ECMA) and the associated seaward dipping reflectors (SDR), both well-known volcanic margin phenomena, are observed off Georges Bank on the south-western part of the margin, but they quickly reduce in magnitude to the northeast (FIG.1). A comparison of seismic observations across different parts of the margin also shows a parallel decrease in syn-rift volcanism as defined by three previous cross-margin refraction profiles (SMART-1,2,3). The margin changes from volcanic to non-volcanic between the southern line (SMART-3; Dehler *et al.*, 2004) and the central line (SMART-2; Wu *et al.*, 2006).

In addition to the lack of evidence for syn-rift volcanism, there is another feature that uniquely defines the non-volcanic part of the margin. Existing data between the central and the northern line (SMART-1; Funck *et al.*, 2004) show a wide continent-ocean-transition (COT) zone characterized by a pervasive layer with velocities of 7.3–7.9 km/s, intermediate between crust and mantle, that we interpret as partially serpentinized mantle (FIG.1, 2b & c). The nature of the crust overlying the partially serpentinized layer is, however, difficult to define as it was under-sampled due to sparse receiver spacing. Furthermore, there is a lack of a conjugate pair profile with the SISMAR-4 profile on the Moroccan margin. Therefore, new data acquisition was necessary to reduce the uncertainties in crustal interpretations and conjugate margin reconstructions.

In November 2009, a new refraction profile was acquired by the Offshore Energy and Technical Research (OETR) Association of Nova Scotia along a coincident deep reflection profile (ION/GXT NovaSPAN 2000) to the northeast of SMART-1 (FIG.1). The profile was obtained using 100 ocean-bottom seismometers and with particularly dense spacing (2.5 km) within the COT that gives greatly improved resolution in this region. It also extends 125 km seaward of the reflection profile to better constrain the oceanic crust. Please refer to Makris *et al.* (in section Nova Scotia, this conference) for details on data acquisition and velocity modelling. In this paper, we present our interpretation of this new velocity model and integration with other observed refraction and coincident multi-channel reflection profiles in the study area. This comparison clearly demonstrates a northeastward continuation of the non-

volcanic structures. A comparison of conjugate margin structures confirms a marked asymmetry with a much narrower COT off Morocco.

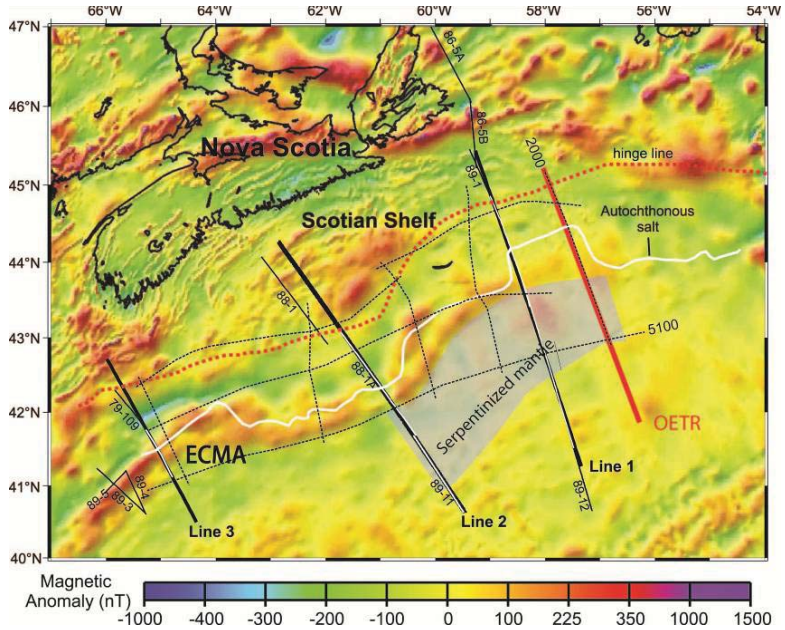

FIG.1 – Magnetic anomaly map of Nova Scotia margin. Red line – new refraction profile (OETR). Thick black lines – SMART profiles. Thin black lines – Lithoprobe profiles. Dashed black lines – ION/GXT NovaSPAN profiles.

2. Structural variations

FIG. 2a shows the velocity model of the OETR profile. This simple model shows structures very similar to those determined for SMART-1 (FIG.2a & b). This comparison indicates similar non-volcanic characteristics of the three major crustal zones, namely continental, transitional and oceanic. Firstly, the continental crust in the NW of profile OETR thins over a relatively wide zone (> 180 km). Even wider rifts are observed on the SMART-1 and SMART-2 profiles. Secondly, the oceanic crust composed of layers 2 and 3, is found to be thinner than average. In the SE of profile OETR, oceanic crust is 4–5 km thick, which is similar to SMART-1, while for SMART-2, it increases only slightly to ~ 6 km. Thirdly, there is a wide transitional zone (COT) on all profiles that cannot be explained by either a continental or oceanic crustal model. The COT is modeled on profiles OETR and SMART-1 as two layers above normal mantle. The lower layer, interpreted as partially serpentinized mantle, has velocities of 7.2–7.6 km/s and a thickness of ~ 6 km. A similar layer is observed on profile SMART-2 but with higher velocities (7.6–7.8 km/s) and smaller thicknesses, suggesting a lower degree of serpentinization.

The upper layer of the COT is the most variable crustal feature along the margin and its crustal origin is least constrained due to its small thickness and large depth. According to profile OETR, this layer has a velocity of ~ 5.3 km/s and an overall seaward decrease in thickness (from 4 to 2 km). It is best interpreted as oceanic layer 2 as it is continuous with this layer on the seaward end. On SMART-1, a thin layer, with similar velocities, is interpreted as exhumed mantle for the seaward half of the COT. Since we do not see evidence for exhumed mantle on profile OETR and SMART-2, we reinterpret this layer to be ultra-thin oceanic crust. As oceanic layers 2 and 3 are interpreted for the seaward part of the COT on SMART-2, we observe a southward trend of more fully developed oceanic crust above serpentinized mantle.

On the landward part of the COT, the upper layer is interpreted as continental crust on

SMART-1 and -2. On SMART-2, it is observed as rotated fault blocks with fanning syn-rift sediment layers in the reflection data. Therefore, on profile OETR, continental crust may possibly extend beyond the seemingly abrupt thinning at ~ 170 km.

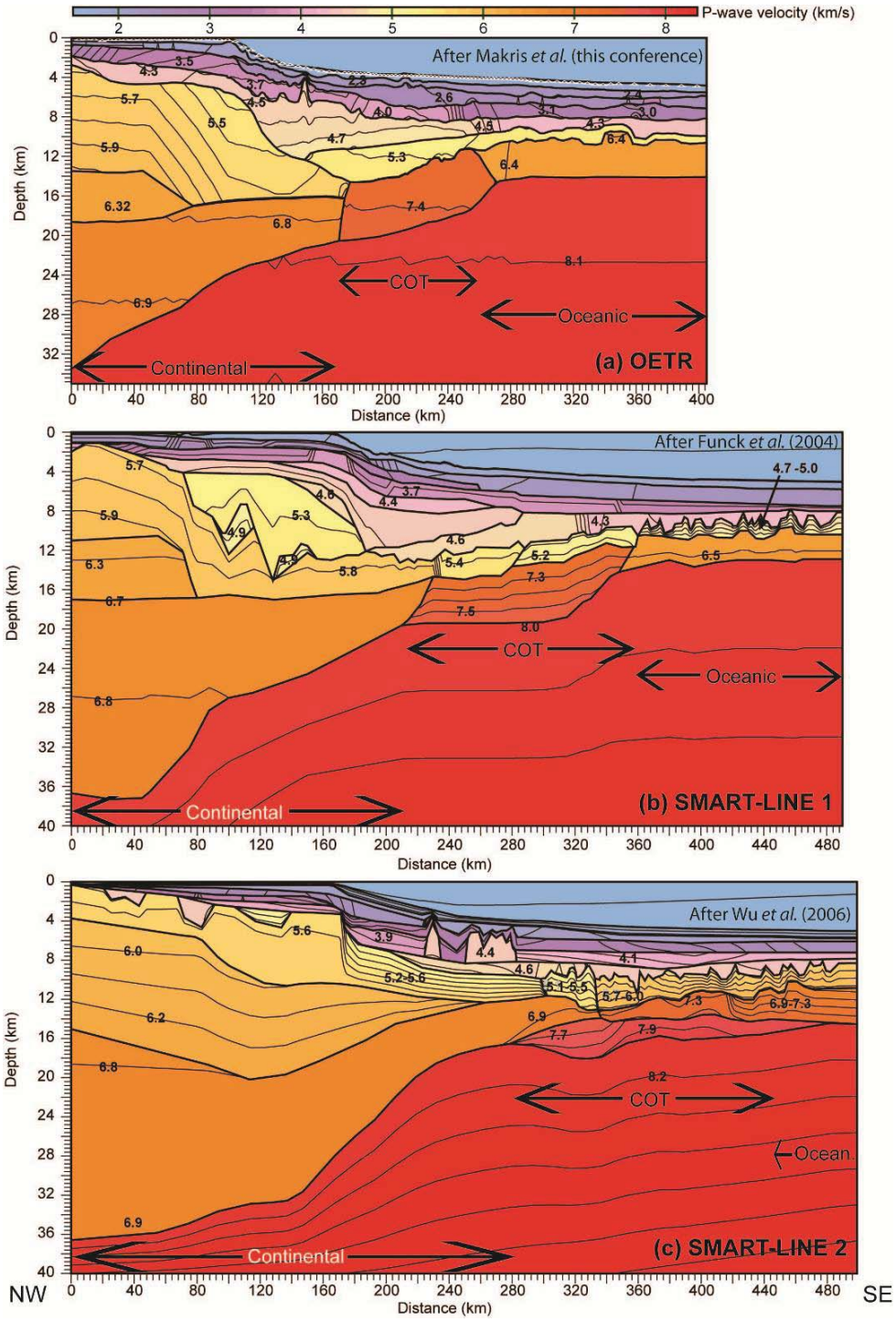

FIG.2 – P-wave velocity models across the NE Nova Scotia margin.

A mapping of the COT zone (FIG.1) shows close correlation with the hinge line of the

rift basin, implying a common regional scale forcing behind its formation. Within this zone, a strong crustal reflection (W) is observed on reflection profile NovaSPAN 5100 (FIG.3) at about the depth of the top of the interpreted serpentinized mantle, suggesting an abrupt velocity contrast across the boundary. Therefore, a mapping of the 3-D geometry of this reflection would help to discriminate between the different crustal models of the transitional upper crust.

A kinematic reconstruction of the rifting and breakup of the complete Nova Scotia-Morocco conjugate margins will be presented using these new results. After plate reconstruction, a dramatic asymmetry in all three crustal zones (i.e. width of continental thinning, nature of the COT and oceanic crustal thickness) is clearly observed on the Moroccan margin along profile SISMAR-4, which is nearly conjugate to NovaSPAN 2000 (Contrucci *et al.*, 2004). Either a ridge jump or post-spreading volcanism may be required to explain such asymmetry.

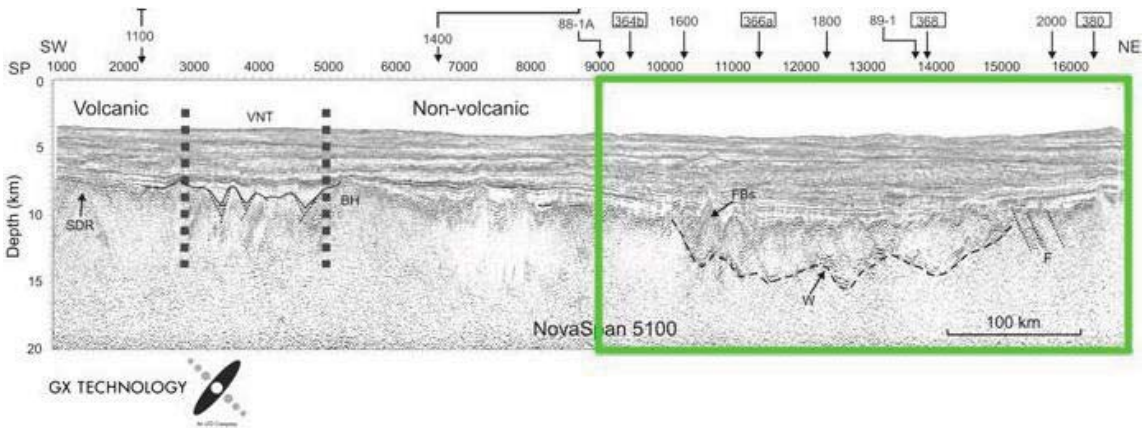

FIG.3 Prestack depth migrated section of NovaSpan 5100.

4. Future work

We will refine existing models targeting detailed velocity structures of the upper transitional crustal layer. For line OETR, the close spacing of OBS receivers should allow a refined model with unprecedented level of detail for the structures already identified. We will also map in 3-D the strong reflection within the OCT using newly reprocessed MCS data.

Acknowledgements

We would like to thank the Offshore Energy and Technical Research (OETR) Association of Nova Scotia, RPS Energy and Geopro for their support and cooperation. ION/GXT kindly allowed use of the NovaSPAN MCS reflection profiles.

References

Contrucci, I., Klingelhofer, F., Perrot, J., *et al.* (2004), The crustal structure of the NW Moroccan continental margin from wide-angle and reflection seismic data, *Geophysical Journal International,* 159, p.117–128.

Dehler, S. A., Keen, C. E., Funck, T., Jackson, H. R. and Louden, K. E. (2004). The limit of volcanic rifting: A structural model across the volcanic to non-volcanic transition off Nova Scotia. *Eos Trans. AGU, 85(17), Jt. Assem. Suppl.*, Abstract T31D-04.

Funck, T., Jackson, H.R., Louden, K.E., Dehler, S.A. & Wu, Y. (2004) – Crustal structure of the northern Nova Scotia rifted continental margin (eastern Canada). *Journal of Geophysical Research,* 109, B09102, doi:10.1029/2004JB003008.

Wu, Y., Louden, K.E., Funck, T., Jackson, H.R. & Dehler, S.A. (2006) – Crustal structure of the central Nova Scotia margin off Eastern Canada. *Geophysical Journal International,* 166, p.878–906.